Methodology for the Syntheses of Pharmaceutically Significant Functional Groups

by

Kelley E. Danahy

B. A. Chemistry, *summa cum laude*
Boston University, 2014

Submitted to the Department of Chemistry as Partial Fulfillment of the Requirements for the Degree of

DOCTOR OF PHILOSOPHY IN CHEMISTRY

at the

MASSACHUSETTS INSTITUTE OF TECHNOLOGY

June 2019

Signature of Author Signature redacted
Department of Chemistry
May 10, 2019

Certified by Signature redacted
Timothy F. Jamison
Department Head and Robert R. Taylor Professor of Chemistry
Thesis Supervisor

Accepted by Signature redacted
Robert W. Field
Haslam and Dewey Professor of Chemistry
Chairman, Departmental Committee on Graduate Studies

This doctoral thesis has been examined by a committee in the Department of Chemistry as follows:

Professor Timothy F. Jamison

Signature redacted

Thesis Advisor
Department Head and Robert R. Taylor Professor of Chemistry

Professor Mohammad Movassaghi

Signature redacted

Thesis Committee Chair
Professor of Chemistry

Professor Timothy M. Swager

Signature redacted

John D. MacArthur Professor of Chemistry

Methodology for the Syntheses of Pharmaceutically Significant Functional Groups

by

Kelley E. Danahy

Submitted to the Department of Chemistry on May 10, 2019
in partial fulfillment of the requirements for the degree of
Doctor of Philosophy in Chemistry

Abstract

Though pharmaceutical small molecules span a wide range of structures and functions, several common features emerge upon analysis. For example, many medicinal compounds contain combinations of nitrogen-containing heterocycles, polar functional groups such as fluorides or sulfoximines, and stereoisomers that are vital to their bioactivity. As a result, new methods to synthesize these important functional groups are continually in demand. Three main methods to synthesize common pharmacophores are discussed herein: the selective benzylic fluorinations of azaheterocycles via a nitrogen–fluorine halogen bond, the synthesis of sulfoxides and sulfenamides from highly reactive and unstable chloramine in continuous-flow, and partial translation of the process route to enantiopure (S)-naproxen from batch chemistry to continuous-flow.

Thesis Supervisor: Timothy F. Jamison

Title: Department Head and Robert R. Taylor Professor of Chemistry

to my father, Mark J. Danahy (1955–2018)

Acknowledgements

First and foremost, I would like to thank my advisors, Professor Timothy F. Jamison and Professor Jeffrey F. Van Humbeck, for supporting my research in organic chemistry through advice, knowledge, and funding. Special thanks to Tim for accepting a fourth-year student transferring into his lab. Thank you also to my committee members, Professor Mohammad Movassaghi and Professor Timothy M. Swager, for their suggestions and support.

In terms of research, there are many people to acknowledge, so first I'll say, in general, that I am grateful to my fellow members of both the Van Humbeck and Jamison research groups for their suggestions and support throughout my doctoral work. In the Van Humbeck group, special thanks are owed to Julian Cooper for his assistance in elucidating the mechanism of our fluorinations, and for being a good sport every time I drew a cat on his hood. And in the Jamison group, special thanks to Dr. Laurel Heckman and Dr. Evan Styduhar for their previous work on chloramine, and to Dr. Justin Lummiss, Dr. Jessica M. Weber, and Aria M. Fodness for their assistance with naproxen. Thank you, also, to Dr. Timothy M. Monos for helpful discussions on the potential mechanisms for the fluorination of azaheterocycles.

To my friends across the PhD program, especially Saki Ichikawa, Krysta Dummit, Soyoung Kim, Jessica Weber, Laurel Heckman, Elise Miner, Amanda Stubbs, Amanda Wicker, and Julian Cooper – I really appreciate your support and friendship. In particular, Jessica, thank you for living with me for a few years, and Saki, thank you for becoming my friend while helping me clean up after flooding the undergraduate research lab our first week of TA training. To the members of our 2018 Organic Retreat Committee – Bryan Ingoglia, Krysta Dummit, Saki

Ichikawa, Julian Cooper, Joey Dennis, and Julia Zhao – thanks for providing fun and camaraderie during a new experience for all of us.

To my friends outside the PhD program: Kate, thanks for being not only my identical twin, but also my friend. And for providing extreme confusion to anyone in chemistry who saw you working at MIT and thought that I just didn't recognize them anymore. Mei and Sarah and Jaymie: thank you for providing cat pictures and anime to keep me distracted, and for encouragement whenever I showed you my pretty colored reactions.

To my cats, of course I'll thank you; I have no shame. Thank you to Sushi for showing unconditional love, to Myshkin for not entirely hating me, and to both for providing me with copious chemistry puns. You might say...for *catalyzing* my pun production. Ahem, I'll wrap up these acknowledgements and see myself out to the thesis now.

Most importantly, to my supportive fiancé, Dr. Bryan Ingoglia – thank you for keeping me sane and working with me to overcome chemistry's endless trolling, and for those Friday night dinners where we scribbled potential mechanisms and our latest ideas on paper napkins, as one does during a normal date. And for all the afternoons you 'borrowed' my wallet to buy us coffee to fuel more hours of research. Your consistent encouragement and patience and thoughtfulness have been invaluable throughout grad school, even back when we were casual friends and you stopped to talk with me during my grief over our Synthesis II final.

To my mother Diane, brother Mark, and sister Kate, thank you for your patience and encouragement. And lastly, especially to my father, Mark Danahy, thank you for your love and belief in me. You told me you thought I would be a doctor when I was in 8th grade, and I don't think this is exactly what you meant, but close enough, right?

Abbreviations

Ac	acetyl
Ar	aryl
BPR	back pressure regulator
Bu	*n*-butyl
Bu_3N	tributylamine
CH_2Cl_2	dichloromethane
$CHCl_3$	chloroform
DMF	dimethylformamide
DMSO	dimethylsulfoxide
ee	enantiomeric excess
Et	ethyl
Et_2O	diethyl ether
equiv	equivalent(s)
GC	gas chromatography
GC–MS	gas chromatography mass spectrometry
Het	heterocycle
HRMS	high-resolution mass spectrometry
HPLC	high-performance liquid chromatography
KO*t*-Bu	potassium *tert*-butoxide
LDA	lithium diisopropylamide
Me	methyl
MeCN	acetonitrile
MeOH	methanol
NMR	nuclear magnetic resonance
Ph	phenyl
PFA	perfluoroalkoxy polymer
psi	pounds per square inch
Selectfluor®	1-chloromethyl-4-fluoro-diazabicyclo[2.2.2]octane bis(tetrafluoroborate)
t-Bu	*tert*-butyl
THF	tetrahydrofuran
t_R	retention time
UV-Vis	ultraviolet-visible spectroscopy

Chapter 1: Highly Selective Benzylic Fluorinations of Azaheterocycles via an N–F Halogen Bond

Chapter 2: Harnessing Chloramine as a Source of Electrophilic Nitrogen in Continuous-flow

Chapter 3: Synthesis and Purification of (*S*)-Naproxen in Continuous-flow

Portions of this thesis have been adapted with permission from the following publication, co-written by the author:

Danahy, K. E.; Cooper, J. C.; Van Humbeck, J. F. Benzylic Fluorination of Aza-heterocycles Induced by Single-Electron Transfer to Selectfluor. *Agnew. Chem. Int. Ed.* **2018**, *57*, 5134.

Chapter 1

Highly Selective Benzylic Fluorinations of Azaheterocycles via a N–F Halogen Bond

Abstract

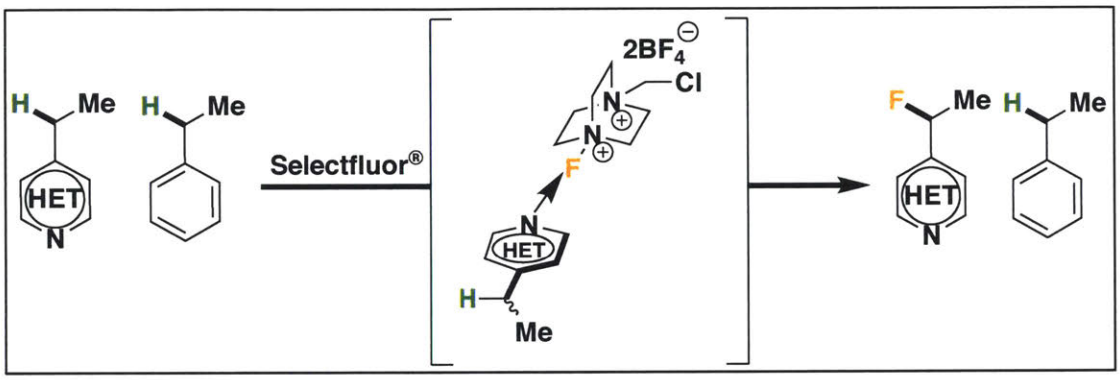

A selective and mild method for the benzylic fluorination of aromatic azaheterocycles with Selectfluor® has been investigated. These reactions take place by a previously unreported mechanism, in which an N–F interaction between the azaheterocycle and the electrophilic fluorinating reagent Selectfluor® eventually yields a benzylic radical, leading to benzylic C–F bond formation. This mechanism enables high intra- and intermolecular selectivity for azaheterocycles over other benzylic components with similar C–H bond-dissociation energies.

Thesis Supervisor: Jeffrey F. Van Humbeck

Kelley E. Danahy contributed the syntheses and optimization of substrates unless otherwise specified, and investigation of the reaction mechanism, including analysis of the kinetic isotope experiment. Julian C. Cooper developed an independent method to synthesize the benzylpyridine dimer, as well as the synthesis of substrate **14**. Jeffrey F. Van Humbeck completed syntheses and fluorination for substrates **10** and **18**, as well as the kinetic isotope experiment.

Introduction

Aromatic azaheterocycles and carbon–fluorine bonds are key building blocks in small molecules designed for medicinal chemistry. As of 2014, 84% of pharmaceuticals contained at least one nitrogen atom. Moreover, over 250 FDA approved medicines contained aromatic azaheterocycles (**Figure 1**).[1, 2] As a result, methods to selectively modify these substructures remain in demand.

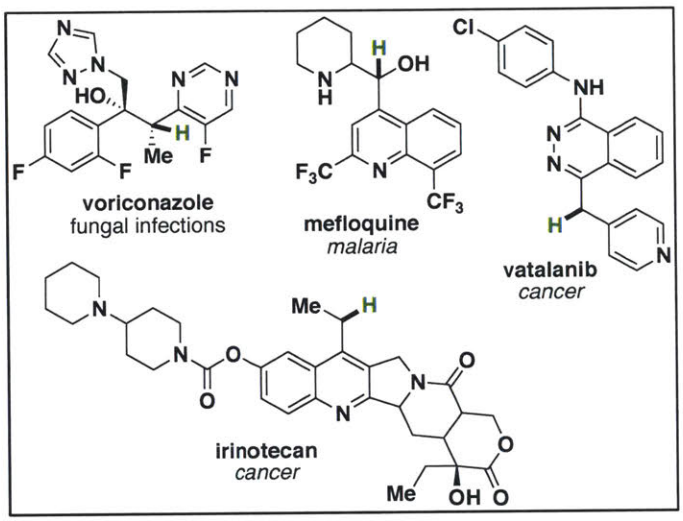

Figure 1. Examples of medicinally relevant aromatic 4-alkylazaheterocles.

Likewise, the unique properties and increasing prevalence of fluorine in pharmaceuticals and radiotracers have led to its inclusion in 20 % of pharmaceutical small molecules and 30–40 % of agrochemicals.[3, 4] Specifically, the unusual strength of the fluorine-carbon *sigma* bond (>110 kcal/mol) has led to fluorine's use as a bioisostere of hydrogen. The replacement of hydrogen with fluorine can result in increased metabolic stability and thus a longer lifetime *in vivo*, as the energy required to break a carbon-hydrogen bond is over 10 kcal/mol less than to break a carbon-fluorine bond.[5]

Additionally, fluorine's high electronegativity provides the paradoxical effect of both increased lipophilicity and decreased pKa. Many polar functional groups that decrease pka – carboxylic acids, amines, etc. – result in decreased solubility amongst hydrocarbons. However, the electronegativity of fluorine is so great that the atom does not engage in intermolecular forces as readily as other electronegative atoms, such as oxygen and nitrogen. Hence, despite their internal polarity, fluorinated compounds often remain soluble in nonpolar materials and solutions.

As a consequence of these unique features, the development of new fluorination methods for organic small molecules is an active area of research. While several notable methods to add difluoroalkyl[5] and trifluoromethyl[6] groups to heterocycles are known (**Figure 2**), direct addition of monofluoroalkyl groups has so far remained limited to α-fluorocarbonyl fragments.[7] Heterobenzylic monofluorination of an unactivated alkyl group has been rarely reported, most notably in the palladium-catalyzed fluorination of 8-methylquinoline by Sanford and co-workers, the ^{18}F manganese-salen-catalyzed fluorination of papaverine reported by Groves and coworkers, and recently the *N*-fluorobenzenesulfonamide (NFSI) promoted fluorinations of pyridines and pyrimidines by Britton and co-workers.[8c] Britton's work used NFSI to efficiently monofluorinate pyridines under mild reaction conditions (60 °C, MeCN). However, azaheterocycles less nucleophilic than pyridine proved challenging, as pyrimidine substrates required 120–150 °C to provide significant conversion.[8c]

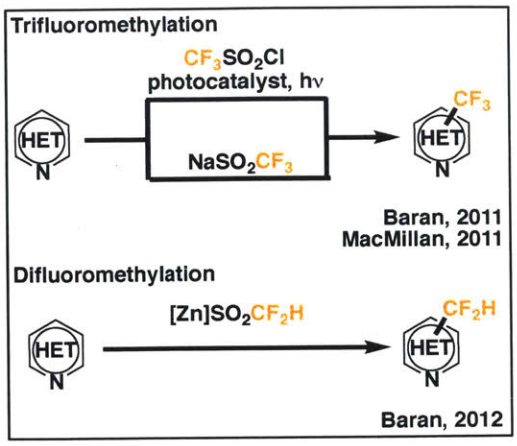

Figure 2. Heterocyclic trifluoromethylation and difluoromethylation examples.

We hypothesized that, analogous to the tri- and difluorination conditions, a radical mechanism may expand the scope of azaheterocyclic monofluorination substrates. C–F bond-forming methods are typically divided into three categories: electrophilic,[9] nucleophilic,[10] and radical.[11] The latter emerged recently with the demonstration, by Sammis and co-workers, that electrophilic fluorine sources, such as NFSI and Selectfluor®, can function as radical fluorine sources.[11a] Since their seminal report, numerous examples of radical fluorinations have been reported.[11] However, attempts to use radical mechanisms for C–H monofluorination adjacent to azaheterocycles face a significant challenge: even modestly complex molecules may feature multiple reactive C–H bonds (for example, benzylic methylenes). Thus, reactions selective for heterobenzylic C–H bonds over other weak bonds are needed to allow predictable fluorination in advanced intermediates.

The nitrogen lone pair provides a key means to differentiate between the reactivity of azaheterocycles and other similar aromatic compounds. Based on our recent studies on site-selective methylene oxidation[12a] and amination,[12b] we postulated that the coordinative ability of azaheterocyclic lone pairs could be harnessed to interact with a variety of transition metals, such

as copper, iron, or cobalt. This coordination may thereby facilitate a selective radical pathway that would lead to our desired reactivity and selectivity (**Scheme 1**).

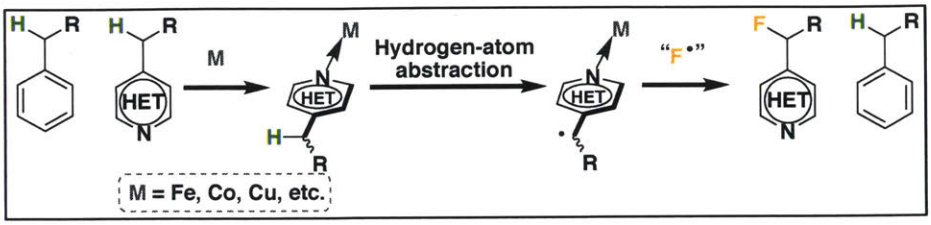

Scheme 1. Proposed plan for selective radical fluorination on azaheterocycles.

Optimization and Substrate Scope

Our initial investigations pitted 4-ethylpyridine (**1**) against ethylbenzene (**2**), and used known radical initiators (ACBN, NHPI; **Table 1**). We were excited to see selective fluorination with both copper(II) and iron(III) salts, albeit in low yield (entries 1 and 2). However, our control experiments revealed that the selective fluorination of pyridine was optimal with merely a slight excess of Selectfluor® (**5**) and no other additives, resulting in 67% monofluorinated product, 10 % or less of difluorinated pyridine, and protonated starting material. Addition of base, or modification of our fluorine source, proved detrimental to the yield (entries 4–8). We were pleased to find that these conditions delivered complimentary results to those reported using NFSI (**Figure 3**).

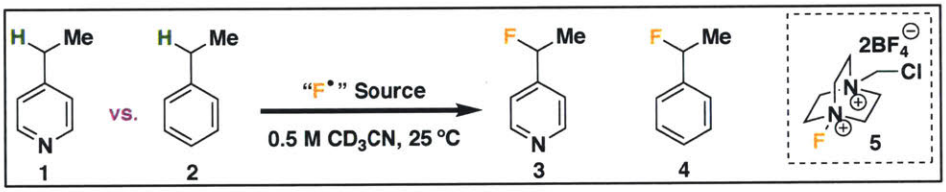

Entry	Additive	Solvent	"F⁺" Source	Yield (%)	3/4
1	$Cu(OTf)_2$[a]	CD_3CN	Selectfluor®	28	>99:1
2	$FeCl_3$[b]	CD_3CN	Selectfluor®	25	>99:1
3	none	DMF-d_7	Selectfluor®	20	>99:1
4	none	CD_3CN	Selectfluor®	67	>99:1
5	DABCO	CD_3CN	Selectfluor®	50	>99:1
6	Li_2CO_3[c]	CD_3CN	Selectfluor®	50	>99:1
7	none	CD_3CN	Selectfluor®[d]	53	>99:1
8	none	CD_3CN	NFSI	44	>99:1

Table 1. [a] Used 5 mol % copper and 5 mol % 1,1′-azobis(cyclohexanecarbonitrile) as a radical inititator. [b] Used 5 mol % iron and 5 mol % *N*-hydroxyphthalimide as a radical initiator. [c] Used 1 equiv of base. [d] Used 2 equivalents Selectfluor. All reactions were run at 25 °C. DABCO =1,4-diazabicyclo[2.2.2]octane, DMF = N,N-dimethyformamide, Tf = trifluoromethanesulfonyl.

Alkylpyridines are reactive towards Selectfluor® at room temperature, though they generally deliver slightly lower yields than those reported by Britton.[8] Importantly, we observe a different behavior in the case of diazines and fused heterocycles. Pyrimidines, quinazolines, and purines, including an electron-poor pyrimidine (**13**), proved to be reactive at only 40 °C. We found that the inclusion of catalytic amounts of the iron(III) complex $[FeCl_4][FeCl_2(dmf)_3]$ provided increased yields. Though the use of this complex over $FeCl_3$ can be attributed to the hygroscopic nature of $FeCl_3$, the exact role of iron is currently unknown. However, in all cases where another benzylic position was present (**10**, **14**, **18**), fluorination was completely selective for the 4-position of the azaheterocycle.

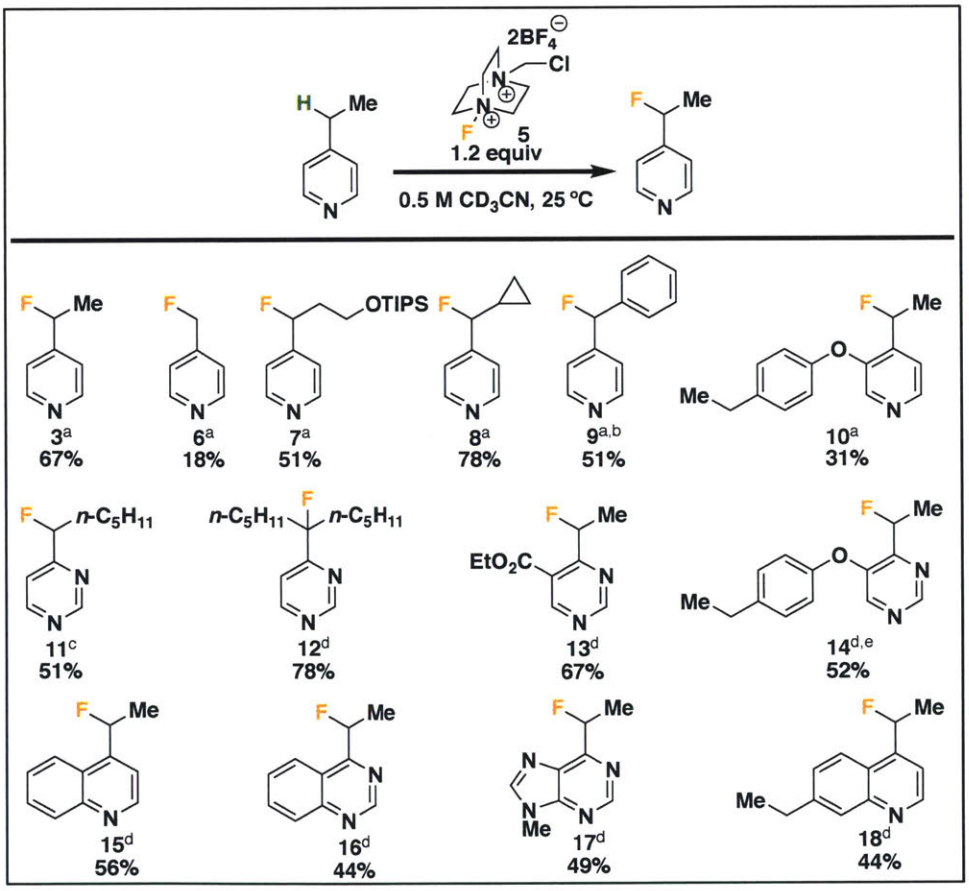

Figure 3. Substrate scope for benzylic fluorination. Reaction conditions: [a] Acetonitrile, 1.2 equiv Selectfluor®, 25 °C. [b] 5 % dimer observed (see **Scheme 3**). [c] DMF, 2.5 mol %

$[FeCl_4][FeCl_2(dmf)_3]$, 1.5 equiv Selectfluor®, 40 °C. [d] DMF, 2.5 mol % $[FeCl_4][FeCl_2(dmf)_3]$, 1.2 equiv Selectfluor®, 40 °C. [e] With 2 % starting material. TIPS=triisopropylsilyl.

Mechanistic Investigation

Given that transition metals and radical initiators were not needed to observe reactivity, we initially suspected an ionic mechanism. Drawing on precedent set by the Boekelheide Reaction[13] or, more closely, Briton's NFSI monofluorinations,[8c] a potential mechanism is shown in **Scheme 2**.

Acidification of the benzylic position resulting from pyridinium cation formation (**20**) would allow deprotonation and dearomatization (**21**). Then, attack by the now-nucleophilic benzylic position onto another equivalent of electrophilic fluorine would yield our desired C–F bond (**22**). Pyridinium **21** could then transfer fluorine to another equivalent of substrate, thus delivering the observed product and regenerating the pyridinium intermediate **20**.

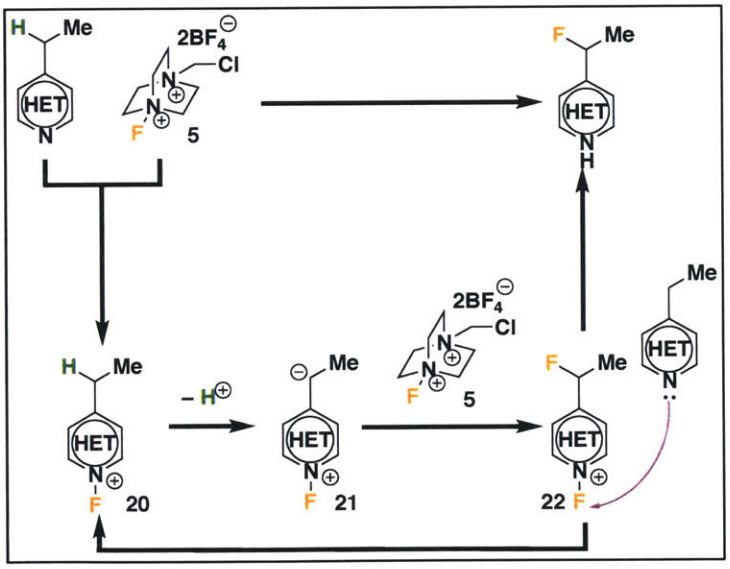

Scheme 2. Proposed ionic mechanism for azaheterocyclic fluorination with Selectfluor®.

However, several observations appeared inconsistent with this mechanism. During our optimization studies, we had observed the complete failure of both *N*-fluorocollidinium (**23**) and *N*-fluoropyridinum (**24**) to promote the desired transformation (**Scheme 3**), leading instead

to substrate decomposition. Given that an ionic mechanism using Selectfluor® requires fluorine transfer between *N*-fluoropyridiniums, the failure of these reagents strongly suggests that the presented ionic mechanism does not occur. Additionally, no pyridinium fluoride peaks (from **20** or **22**) were observed during the NMR studies. Furthermore, the successful fluorination of 4-alkylpyrimidines under mild reaction conditions would be unusual for an ionic mechanism, as the formation of pyrimidinium fluorides typically requires both harsh fluorinating reagents like hypofluorites, as well as oxidation to the pyrimidinone state.[14]

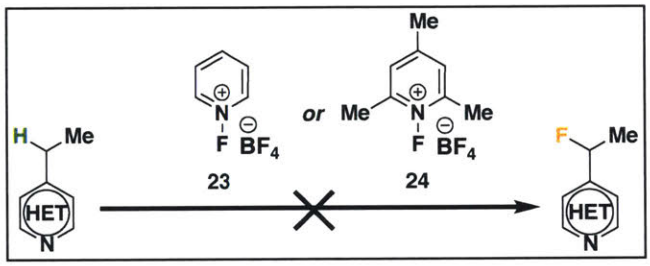

Scheme 3. Failure of *N*-fluoropyridinium reagents to yield product.

Fortunately, fluorination of 4-benzylpyridine provided an insight into the mechanism (**25**; **Scheme 4**). Though the primary product was the expected monofluorinated structure (**9**), dimeric byproduct **26** was observed by GC/MS, and confirmed by independent synthesis. The alkene stereochemistry was confirmed as *E* by hydrogenation to the known racemic dipyridyldiphenylethane **28**.[15] In our reaction, with only Selectfluor®, substrate, and acetonitrile present, it is difficult to explain the formation of this dimer without invoking the radical **27**. As radical dimerization would lead to the saturated **28**, we then confirmed that Selectfluor® is able to further oxidize the saturated intermediate to the observed product.

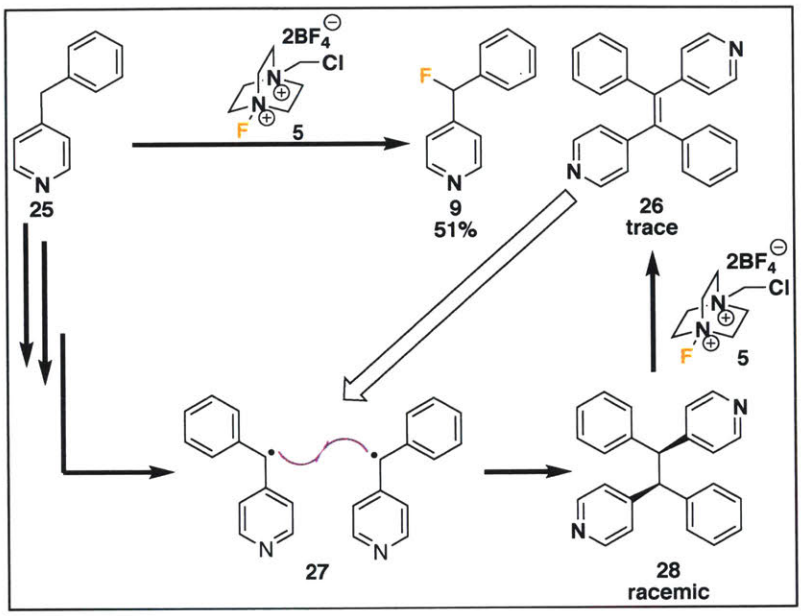

Scheme 4. Partial mechanism for the formation of radical dimer byproduct **26**.

To reconsider a radical mechanism, we investigated the failure of substrate **8** (**Figure 3**) to rearrange as a radical clock. However, lack of rearrangement does not *negate* the existence of a radical species; rather, lack of rearrangement merely indicates that no radical species exists within the rate of rearrangement. Indeed, radical clocks have often failed to provide evidence for radical intermediates in transformations with Selectfluor®, yet ESI-MS has shown radical cation intermediates that implicate a radical mechanism despite a lack of rearranged products.[16,17] Thus, regarding **8**, two possible explanations exist. First, the rate of radical fluorination may outcompete the rate of cyclopropane ring opening. Second, while cyclopropylmethyl radical clocks are known to yield rearranged products on orders of 10^{11} s^{-1}, the rate of ring *closure* for aryl cyclopropylmethyl radical clocks (k=5.4×10^{6} s^{-1}) is faster than the rate of opening (k=6.1×10^{4} s^{-1}).[18] This scenario suggests an equilibrium favoring the closed form of the cyclopropane ring if opening were to occur. As a result, the closed cyclopropane ring of **8** neither confirms nor opposes an ionic or a radical pathway.

Previous studies have suggested that fluorination with Selectfluor® proceeds by single-electron transfer (SET) following the formation of a charge-transfer complex. Calculations by Liu and co-workers predict that even simple electrophilic aromatic substitution with Selectfluor® should not follow the classic two-electron mechanism.[19] And, moving beyond theory, Ritter and co-workers recently found that charge-transfer complexes between aromatic groups and Selectfluor® allowed highly *para*-selective C–H functionalization by a radical pathway.[20]

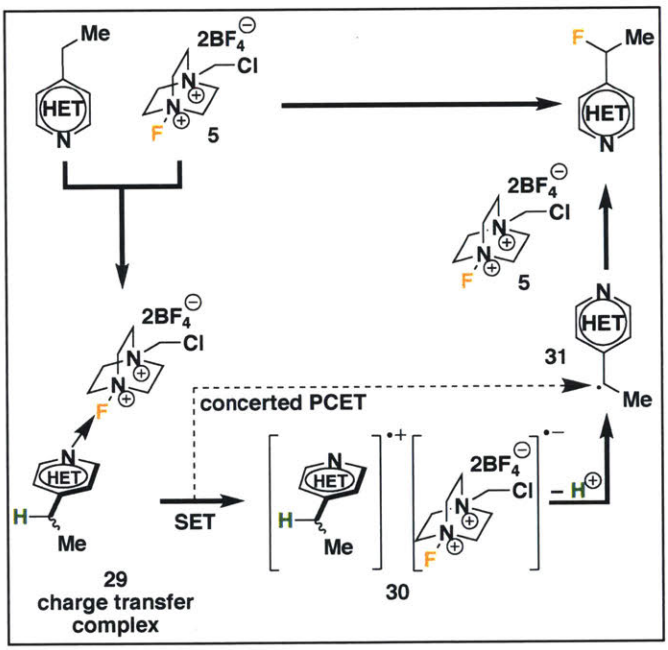

Scheme 5. Initially proposed radical mechanism for azaheterocyclic fluorination with Selectfluor®.

Our proposed radical mechanism for this transformation is shown in **Scheme 5**. Several scenarios could result in the high chemoselectivity observed. Pyridine itself is more easily oxidized in acetonitrile than benzene ($E_{1/2}$ vs. $Ag/AgNO_3$: 1.82 V for pyridine, 2.04 V for benzene),[21] and so selective electron transfer may be simply favored. However, substrates such as **10** (**Figure 3**) contain an anisole-type fragment that should be more easily oxidized in acetonitrile than pyridine ($E_{1/2}$ vs. $Ag/AgNO_3$: 1.40 V for anisole,[22] 1.30 V for diphenyl ether[22]), and yet these

substrates do not deliver C–F bond formation adjacent to the anisole-type ring. In these cases, we speculated that formation of a charge-transfer complex (**29**), isoelectronic to the aryl iodide-DABCO complexes studied by Garcia-Garibay and coworkers,[23] leads to the observed selectivity.

We evaluated the formation of a pyridine/Selectfluor® charge-transfer complex in solution using qualitative UV/Vis spectrophotometry (**Figure 4**). At identical concentrations, a 4-ethylpyridine solution shows a maximum absorbance at λ=255 nm, but an identically concentrated reaction sample showed an absorbance nearly two-and-a-half times as intense, although its wavelength (λ=252 nm) was nearly identical to the pyridine maximum. Furthermore, a broad shoulder began around λ=270 nm and tailed to over λ=350 nm. These spectra contain all three characteristics (intensity, overlap of pyridyl charge-transfer absorbances with the free pyridine absorbance, and tailing) also seen in the well-studied pyridine/I_2 and pyridine/Br_2 charge-transfer complexes.[24]

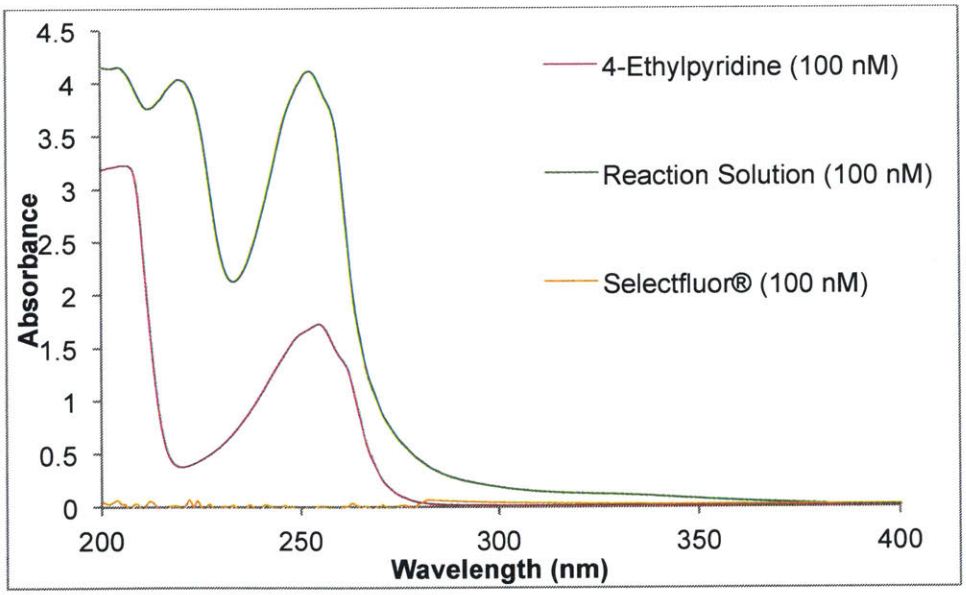

Figure 4. Qualitative UV-Vis spectra of reaction and starting materials.

An although a radical cation would be unusual for pyridines, the oxidation potentials of Selectfluor® and pyridine indicate that such a transfer is feasible.[25] In an attempt to distinguish between a PCET and a stepwise mechanism, we analyzed the kinetic isotope effect in an intermolecular competition between protonated and deuterated 4-ethylquinoline. ^{1}H NMR results indicated a substantial primary k_H/k_D of 5.2, consistent with breaking of the benzylic C–H benzyl as the rate-determining step. This is, however, consistent with both a concerted process and reversible SET, followed by irreversible deprotonation.[26]

Additionally, a third possibility exists: rate-determining loss of a proton preceding electron transfer, as shown in **Scheme 6**. In this mechanism, deprotonation of complex **29** would yield intermediate complex **32.** Subsequent SET yields benzylic radical complex **33**, in a process akin to the barrier-less fragmentation of *N*-methoxypyridine anions observed by Gould and coworkers.[27] In theory, this could occur in a concerted fashion, or stepwise through a Kochi-type intermediate pyridinium (**34** and **36**).[28]

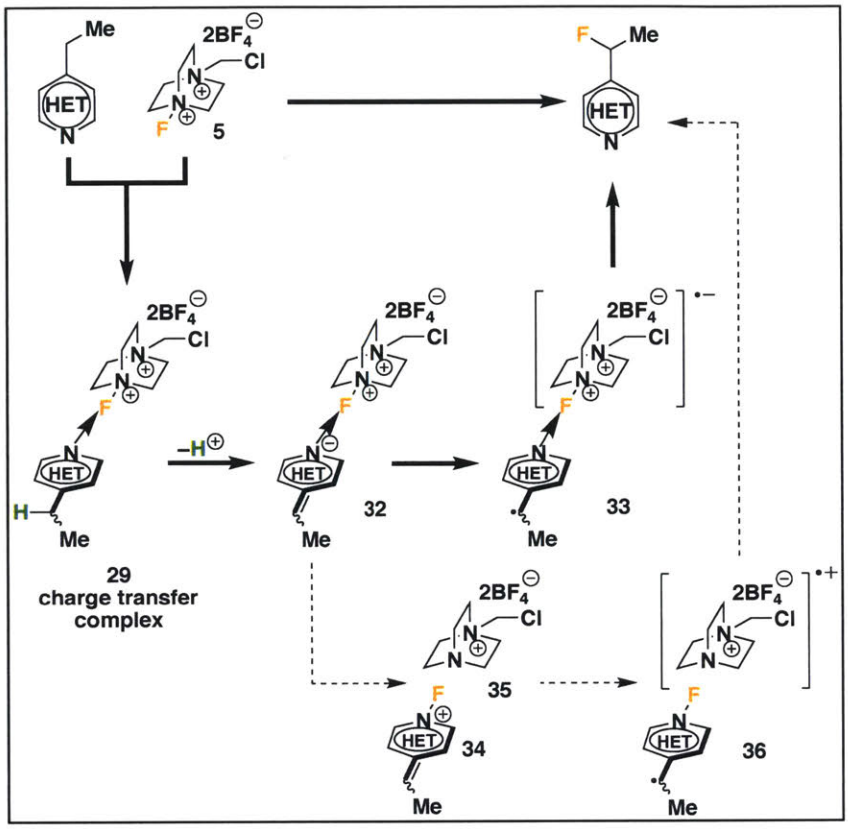

Scheme 6. Precedent for a potential fragmentation pathway yielding a benzylic radical.

Detailed studies, such as ESI–MS and electron paramagnetic resonance (EPR), would be required to differentiate between rate-determining deprotonation before electron transfer, PCET, or SET followed by irreversible deprotonation. Regardless, the evidence at the very least points towards a radical mechanism arising from an N–F halogen bond, which has been further supported by subsequent studies by the Hratchian, Baxter, and Lei groups.[29]

Conclusion

In summary, we have observed the ability of Selectfluor® to directly fluorinate benzylic C–H bonds in the 4-position of azaheterocycles. No additive is required for selectivity, though a catalytic amount of iron(III) may be added in some cases for optimum yield. This approach provides a diverse array of 4-alkyl azaheterocycles, including medically relevant pyrimidines and quinazolines. In regards to mechanism, our complete selectivity for azaheterocycles may be attributed to a charge-transfer complex arising from an N–F halogen bond, and the formation of dimer **25** suggests a radical intermediate. Further investigation is required to elucidate subsequent steps in this mechanism.

References

1. Vitaku, E.; Smith, D. T.; Njardarson, J. T. *J. Med. Chem.* **2014**, *57*, 10257.
2. a) Kullberg, B.J.; Sobel, J. D.; Ruhnke, M.; Pappas, P. G.; Viscoli, C.; Rex, J. H.; Cleary, J. D.; Rubinstein, E.; Church, L. W. P.; Brown, J. M.; Schlamm, H. T.; Oborska, I. T.; Hilton, F.; Hodges, M. R. *Lancet* **2005**, *366*, 1435. b) Petti, F.; Thelemann, A.; Kahler, J.; McCormack, S.; Castaldo, L.; Hunt, T.; Nuwaysir, L.; Zeiske, L.; Haack, H.; Sullivan, L.; Garton, A.; Haley, J. D. *Mol. Cancer. Ther.* **2005**, *4*, 1186-1197. c) Maguire, J. D.; Krisin, M. H.; Richie, L.; Fryauff, D. J.; Baird, J. K. *Clin. Infect. Dis.* **2006**, *42*, 1067. d) Ramesh, M.; Ahlawat, P.; Srinivas, N. R. *Biomed. Chromatogr.* **2010**, *24*, 104. e) Jost, L. M.; Gschwind, H.; Jalava, T.; Wang, Y.; Guenther, C.; Souppart, C.; Rottmann, A.; Denner, K.; Waldmeier, F.; Gross, G.; Masson, E.; Laurent, D. *Drug. Metab. Dispos.* **2006**, *34*, 1817.
3. a) Wang, J.; Sánchez-Roselló, M.; Aceña, J. L.; del Pozo, C.; Sorochinsky, A. E.; Fustero, S.; Soloshonok, V. A.; Liu, H. *Chem. Rev.* **2014**, *114*, 2432. b) Liang, T.; Neumann, C. N.; Ritter, T. *Angew. Chem. Int. Ed.* **2013**, *52*, 8214-8264. c) Champagne, P. A.; Desroches, J.-D.; Hamel, J.; Vandamme, M.; Paquin, J.-F. *Chem. Rev.* **2015**, *115*, 9073-9174.
4. Fujiwara, Y.; Dixon, J. A.; Rodriguez, R. A.; Baxter, R. D.; Dixon, D. D.; Collins, M. R.; Blackmond, D. G.; Baran, P. S. *J. Am. Chem. Soc.* **2012**, *134*, 1494.
5. Luo, Y. *Handbook of Bond Dissociation Energies in Organic Compounds*, CRC Press, Boca Raton, FL, 2003, pp 11, pp 140.
6. a) Ji, Y.; Brueckl, T.; Baxter, R. D.; Fujiwara, Y.; Seiple, I. B.; Su, S.; Blackmond, D G.; Baran, P. S. *Proc. Natl. Acad. Sci.* **2011**, *108*, 14411. b) Nagib, D. A.; MacMillan, D. W. C. *Nature* **2011**, *480*, 224.
7. a) Brandt, J. R.; Lee, E.; Boursalian, G. B.; Ritter, T. *Chem. Sci.* **2014**, *5*, 169. b) Kwiatkowski, P.; Beeson, T. D.; Conrad, J. C.; MacMillan, D. W. C. *J. Am. Chem. Soc.* **2011**, *133*, 1738. c) Howard, J. K.; Müller, M.; Berry, A.; Nelson, A. *Angew. Chem. Int. Ed.* **2016**, *55*, 6767.
8. a) Hull, K. L.; Anani, W. Q.; Sanford, M. S. *J. Am Chem. Soc.* **2006**, *128*, 7134. b) Huang, X.; Liu, W.; Ren, H.; Neelamegam, R.; Hooker, J. M.; Groves, J. T. *J. Am. Chem. Soc.* **2014**, *136*, 6842. c) Meanwell, M.; Nodwell, M. B.; Martin, R. E.; Britton, R. *Angew. Chem. Int. Ed.* **2016**, *55*, 13244.
9. For select examples of electrophilic fluorination, see the following and references therein: a) Lal, G. S.; Pez, G. P.; Syvret, R. G. *Chem. Rev.* **1996**, *96*, 1737. b) Beeson, T. D.; MacMillan, D. W. C. *J. Am. Chem. Soc.* **2005**, *127*, 8826. c) Rauniyar, V.; Lackner, A. D.; Hamilton, G. L.; Toste, F. D. *Science* **2011**, *334*, 1681. d) Yamada, S.; Gavryushin, A.; Knochel, P. *Angew. Chem. Int. Ed.* **2010**, *49*, 2215. e) Anbarasan, P.; Neumann, H.; Beller, M. *Angew. Chem. Int. Ed.* **2010**, *49*, 2219. f) Wolstenhulme, J. R.; Rosenqvist, J.; Lozano, O.; Ilupeju, J.; Wurz, N.; Engle, K. M.; Pidgeon, G. W.; Moore, P. R.; Sandford, G.; Gouverneur, V. *Angew. Chem., Int. Ed.* **2013**, *52*, 9796.
10. For select examples of nucleophilic fluorination, see the following and references therein: a) Lee, H. G.; Milner, P. J.; Buchwald, S. L. *J. Am. Chem. Soc.* **2014**, *136*, 3792. b) Woerly, E. M.; Banik, S. M.; Jacobsen, E. N. *J. Am. Chem. Soc.* **2016**, *138*, 13858. c) Katcher, M. H.; Sha, A.; Doyle, A. G. *J. Am. Chem. Soc.* **2011**, *133*, 15902. d) Hollingworth, C.; Gouverneur, V. *Chem. Commun.* **2012**, *48*, 2929. e) Nielsen, M. K.; Ugaz, C. R.; Li, W.; Doyle, A. G. *J. Am.*

Chem. Soc. **2015**, *137*, 9571. f) Graham, T. J. A.; Lambert, R. F.; Ploessl, K.; Kung, H. F.; Doyle, A. G. *J. Am. Chem. Soc.* **2014**, *136*, 5291.

11. For select examples of radical fluorination, see the following and references therein: a) Rueda-Becerril, M.; Sazepin, C. C.; Leung, J. C. T.; Okbinoglu, T.; Kennepohl, P.; Paquin, J.-F.; Sammis, G. M. *J. Am. Chem. Soc.* **2012**, *134*, 4026. b) Amaoka, Y.; Nagatomo, M.; Inoue, M. *Org. Lett.* **2013**, *15*, 2160. c) Bloom, S.; Pitts, C. R.; Miller, D. C.; Haselton, N.; Holl, M. G.; Urheim, E.; Lectka, T. *Angew. Chem. Int. Ed.* **2012**, *51*, 10580. d) Ventre, S.; Petronijevic, F. R.; MacMillan, D. W. C. *J. Am. Chem. Soc.* **2015**, *137*, 5654. e) Hua, A. M.; Mai, D. N.; Martinez, R.; Baxter, R. D. *Org. Lett.* **2017**, *19*, 2949. f) Ma, J.-J.; Yi, W.-B.; Lu, G.-P.; Cai, C. *Org. Biomol. Chem.* **2015**, *13*, 2890. g) Nodwell, M. B.; Bagai, A.; Halperin, S. D.; Martin, R. E.; Knust, H.; Britton, R. *Chem. Commun.* **2015**, *51*, 11783. h) Halperin, S. D.; Fan, H.; Chang, S.; Martin, R. E.; Britton, R. *Angew. Chem. Int. Ed.* **2014**, *53*, 4690. i) Rueda-Becerril, M.; Mahé, O.; Drouin, M.; Majewski, M. B.; West, J. G.; M. Wolf, O.; Sammis, G. M.; Paquin, J.-F. *J. Am. Chem. Soc.* **2014**, *136*, 2637. j) Leung, J. C. T.; Chatalova-Sazepin, C.; West, J. G.; Rueda-Becerril, M.; Paquin, J.-F.; Sammis, G. M. *Angew. Chem. Int. Ed.* **2012**, *51*, 10804. k) Bume, D. D.; Pitts, C. R.; Ghorbani, F.; Harry, S. A.; Capilato, J. N.; Siegler, M. A.; Lectka, T. *Chem. Sci.* **2017**, *8*, 6918. l) Pitts, C. R.; Bume, D. D.; Harry, S. A.; Siegler, M. A.; Lectka, T. *J. Am. Chem. Soc.* **2017**, *139*, 2208. m) Bloom, S.; McCann, M.; Lectka, T. *Org. Lett.* **2014**, *16*, 6338. n) Bloom, S.; Pitts, C. R.; Woltornist, R.; Griswold, A.; M. Holl, M. G.; Lectka, T. *Org. Lett.* **2013**, *15*, 1722.
12. a) Cooper, J. C.; Luo, C.; Kameyama, R.; Van Humbeck, J. F. *J. Am. Chem. Soc.* **2018**, *140*, 1243. b) Bentley, K. W.; Dummit, K. A.; Van Humbeck, J. F. *Chem. Sci.* **2018**, *9*, 6440.
13. Boekelheide, V.; Linn, W. J. "Rearrangements of N-Oxides. A Novel Synthesis of Pyridyl Carbinols and Aldehydes". *Journal of the American Chemical Society.1954.* *76*, 1286.
14. a) Stavber, S.; Zupan, M. *J. Chem. Soc.. Chem. Commun.* **1983**, 563. b) Katritzky, A. R.; *Advances in Heterocyclic Chemistry*, Vol. 57. Elsevier: Amsterdam, Netherlands, 1993, pp 300.
15. Itoh, M. Hirano, K.; Satoh, T.; Miura, M. *Org. Lett.* **2014.** *16*, 2050.
16. Nyffeler, P. T.; Durón, S. G.; Burkart, M. D.; Vincent, S. P.; Wong, C.-H. *Angew. Chem. Int. Ed.* **2004**, *44*, 192.
17. Zhang, X.; Liao, Y.; Qian, R.; Wang, H.; Guo, Y. *Org. Lett.* **2005**, *7*, 3877.
18. Newcomb, M. Radical Kinetics and Clocks. *Encyclopedia of Radicals in Chemistry, Biology, and Materials.* John Wiley & Sons, Ltd: Hoboken, NJ, 2012.
19. Geng, C.; Du, L.; Liu, F.; Zhu, R.; Liu, C. *RSC Adv.* **2015**, *5*, 33385.
20. Boursalian, G. B.; Ham, W. S.; Mazzotti, A. R.; Ritter, T. *Nat. Chem.* **2016**, *8*, 810.
21. Miller, L. L.; Nordblom, G. D.; Mayeda, E. A. *J. Org. Chem.* **1972**, *37*, 916.
22. Janissek, P. R.; Pardini, V. L.; Viertler, H. *J. Chem. Soc., Chem. Commun.* **1987**, 576-577. Measurement was made using Ag/AgI reference electrode, which was adjusted to $Ag/AgNO_3$ using known half-cell values of Ag/Ag^+ (0.799 V vs. NHE) and Ag/AgI (-0.152 V vs. NHE).
23. Catalano, L.; Pérez-Estrada, S.; Terraneo, G.; Pilati, T.; Resnati, G.; Metrangolo, P.; Garcia-Garibay, M. A. *J. Am. Chem. Soc.* **2015**. *137*, 15386.
24. a) Rao, N. S.; Rao, G. B.; Ziessow, D. *Spectrochim. Acta A* **1990**, *46*, 1107. b) Daisey, J. M.; Sonnessa, A. J. *J. Phys. Chem.* **1972**, *76*, 1895. c) Ray, A. *J. Am. Chem. Soc.* **1971**, *93*, 7146.
25. For the oxidation potential of pyridine and related azaheterocycles, see: Sviatenko, L. K.; Gorb, L.; Hill, F. C.; Leszczynska, J.L. *Chem. Heterocycl. Compd.* **2014**, *50*, 311. For the

reduction potential of Selectfluor®, see: a) Toullec, P. Y.; Bonaccorsi, C.; Mezzetti, A., Togni, A. *Proc. Nat. Acad. Sci.* **2004**, *101*, 5810; b) Oliver, E. W.; Evans, D. H. *J. Electroanal. Chem.* **1999**, *464*, 1.

26. a) Dongare, P.; Maji, S.; Hammarström, L. *J. Am. Chem. Soc.* **2016**, *138*, 2194; b) Hammes-Schiffer, S.; Stuchebrukhov, A. A. *Chem Rev.* **2010**, *110*, 6939.
27. Lorance, E. D.; Kramer, W. H.; Gould, I. R. *J. Am. Chem. Soc.* **2004**, *126*, 14071.
28. Zhu, D.; Kochi, J. K. *Organometallics*. **1999**, *18*, 161.
29. a) Hua, A. M.; Bidwell, S. L.; Baker, S. I.; Hratchian, H. P.; Baxter, R. D. *ACS Catal.* **2019**, *9*, 3322; b) Liang, X.-A.; Niu, L.; Wang, S.; Liu, J.; Lei, A. *Org. Lett.* **2019**, *21*, 2441.

Chapter 1
Supporting Information

General Considerations

All reactions were performed with commercial reagents and solvents that were used as received, unless otherwise specified. Reagents and starting materials were purchased from Sigma Aldrich, Alfa Aesar, Combi-Blocks, TCI America, and/or Ark Pharm; solvents were purchased from Fischer or Sigma-Aldrich. Concentration and removal of solvents was performed using a Heidolph Instruments Hei-VAP rotary evaporator with a dry ice/acetone condenser. Column chromatography was carried out using silica gel purchased from Silicycle® or neutral alumina purchased from Sigma Aldrich.

Nuclear magnetic resonance (NMR) spectra were recorded on a JEOL 500 (500 MHz), Bruker 400 (400 MHz), or Varian 300 (300 MHz), using chloroform-d ($CDCl_3$), dimethylsulfoxide-d_6 (DMSO-d_6), dichloromethane-d_2 (CD_2Cl_2) or acetonitrile-d_3 (CD_3CN). Chemical shifts are given in parts per million (ppm) from trimethylsilane (0.00) and measured relative to the solvent signal (^{1}H NMR: δ 7.26 for $CDCl_3$, δ 2.50 for DMSO-d_6, or δ 1.94 for CD_3CN; ^{13}C NMR: δ 77.16 for $CDCl_3$, δ 54.00 for CD_2Cl_2). Coupling constants (*J* values) are reported in Hertz (Hz) to the nearest 0.1 Hz. ^{1}H NMR spectra are given in the following order: multiplicity (s, singlet; d, doublet; t, triplet; m, multiplet), coupling constants, number of protons.

HRMS was performed using a Bruker Daltonics APEXIV 4.7 Tesla Fourier Transform Ion Cyclotron Resonance Mass Spectrometer. GC/MS was run on an Agilent Technologies 7963 Gas Chromatography Automatic Liquid Sampler, and UV/Vis spectra were recorded with an Agilent Cary 4000 spectrophotometer.

Syntheses of Starting Materials

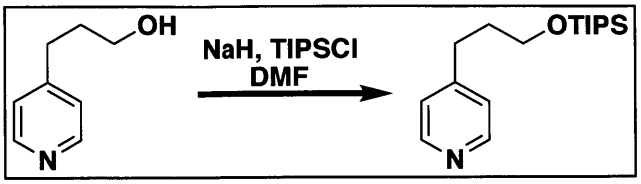

4-(3-((triisopropylsilyl)oxy)propyl)pyridine: 274 mg (2.0 mmol) of 4-(3-hydroxypropyl)pyridine were dissolved in 4 mL DMF. 80 mg (2.0 mmol) of sodium hydride (60% dispersion in mineral oil) was added, and the reaction was stirred at room temperature for 20 minutes. 0.43 mL (2.0 mmol) of triisopropylsilyl chloride were added, and the reaction was further stirred at room temperature for 12 hours. After quenching with water, the crude product was extracted with ethyl acetate, and dried over magnesium sulfate. The solvent was removed via a rotary evaporator, and the product purified by flushing through a silica gel plug with pure ethyl acetate. Evaporation via a rotary evaporator delivered the desired product as a light yellow oil (439 mg, 75%).

^{1}H NMR (300 MHz, $CDCl_3$) δ 8.48 (d, *J* = 5.5 Hz, 2H), 7.13 (d, *J* = 5.7 Hz, 2H), 3.70 (t, *J* = 6.1 Hz, 2H), 2.71 (t, *J* = 7.8 Hz, 2H), 1.92 - 1.77 (m, 2H), 1.05 (d, *J* = 3.1 Hz, 21H); ^{13}C NMR (75 MHz, $CDCl_3$) δ 151.5, 149.8, 124.2, 62.3, 33.6, 31.6, 18.3, 12.1; HRMS (ESI/Q-TOF) $[M + H]^+$ m/z: Calcd for ($C_{17}H_{30}NOSi$) 294.2248; Found 294.2237.

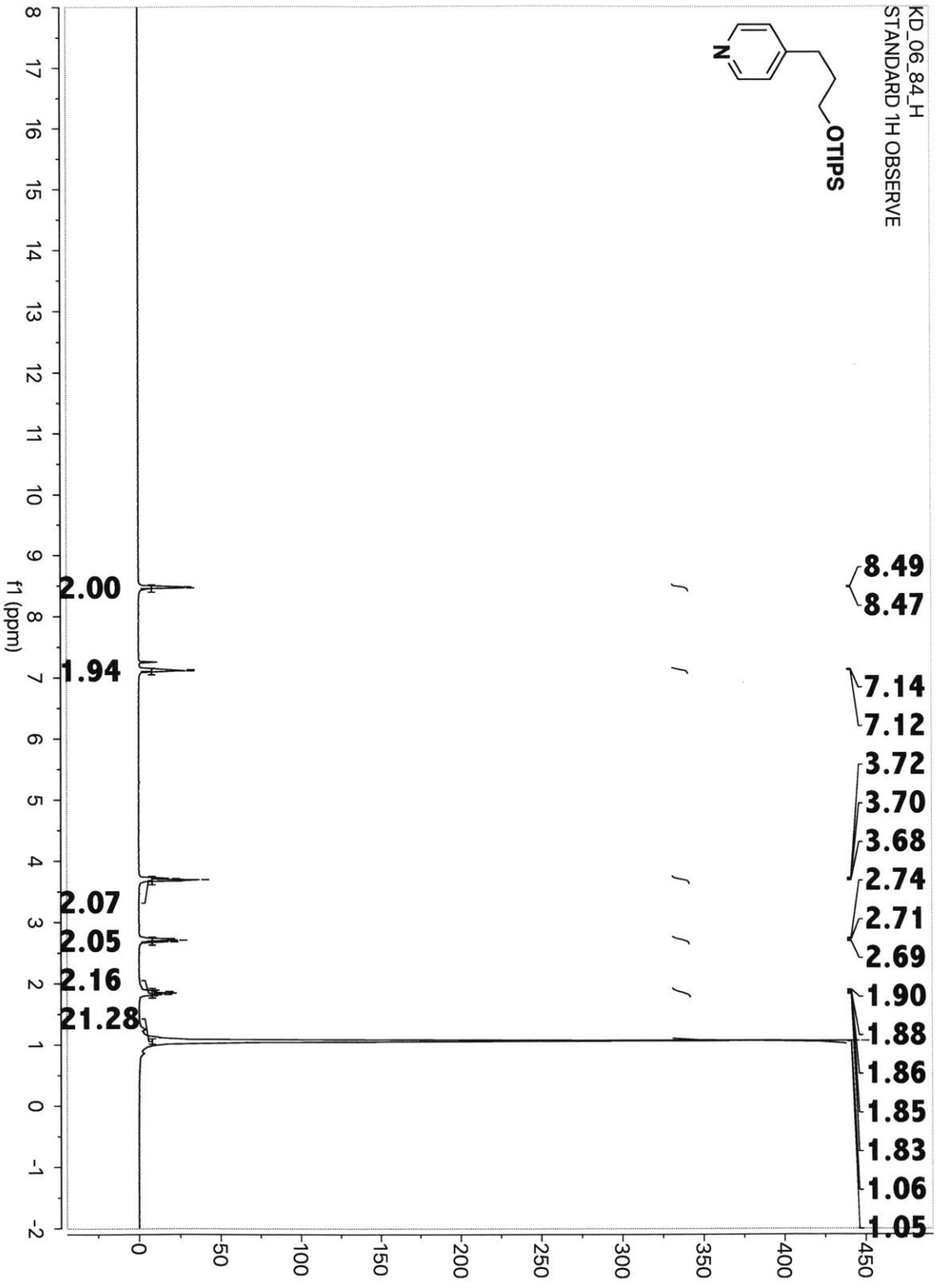

Figure S1. ^{1}H NMR spectrum of 4-(3-((triisopropylsilyl)oxy)propyl)pyridine

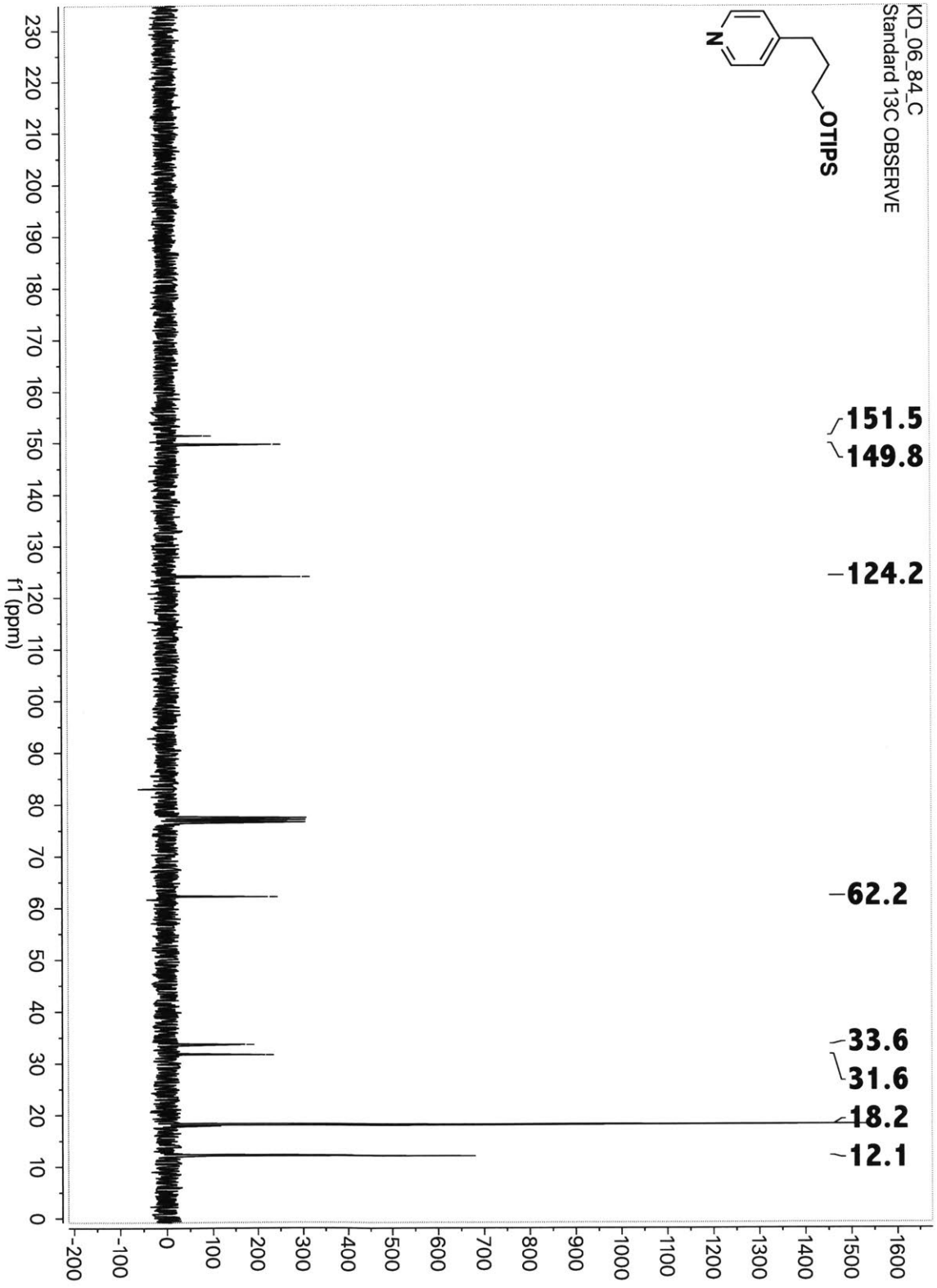

Figure S2. ^{13}C NMR spectrum of 4-(3-((triisopropylsilyl)oxy)propyl)pyridine

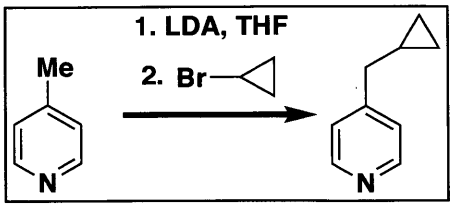

4-(cyclopropylmethyl)pyridine: Adapted from a procedure by Steves and Oestreich.[1] In an oven-dried round-bottom flask, 1.8 mL (13 mmol) diisopropylamine were dissolved in anhydrous THF (13 mL), and the resulting solution cooled to -78°C under N_2. 7.5 mL (6 mmol) of an *n*-butyllithium solution (1.6 M in hexanes) were added slowly, and the reaction was warmed to room temperature and stirred for 30 minutes at room temperature before being re-cooled to -78 °C. A solution of 4-picoline in 12.5 mL THF was added in one portion and stirred a further 30 minutes at -78 °C, upon which 0.4 mL (5 mmol) of 1-bromocyclopropane were added. The reaction was again warmed to room temperature, quenched with 13 mL H_2O and diluted with ethyl acetate. 1 M HCl was added to pH 7-8, and the organic phase was thrice extracted with . After drying over magnesium sulfate and removing volatiles with a rotary evaporator, the products were purified on silica gel, eluting with ethyl acetate to yield 120 mg (0.9 mmol, 18%) 4-(cyclopropylmethyl)pyridine. Spectra were consistent with those previously reported.[2]

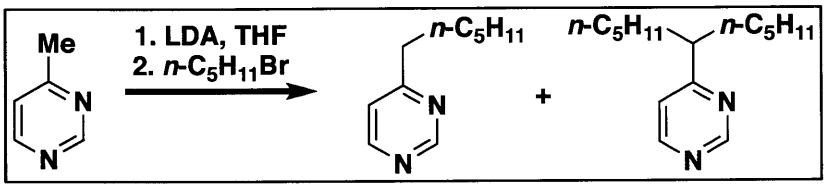

4-hexylpyrimidine and 4-(undecan-6-yl)pyrimidine: Adapted from a procedure by Steves and Oestreich.[1] An oven-dried 2-neck flask under N_2 was charged with 4-methylpyrimidine

(0.9 mL, 10 mmol) and 12 mL anhydrous THF, and the mixture was cooled to -78 °C. Freshly prepared LDA (12 mmol in 13 mL anhydrous THF: 4 mL hexanes) was added dropwise, and the reaction mixture was stirred at -78 °C for 30 min. 1-Bromopentane (1.2 mL, 10 mmol) was slowly added, and the reaction was warmed to room temperature and stirred for 10 minutes. The reaction was quenched with 1 M HCl to pH 7.5 and extracted with dichloromethane. After drying over magnesium sulfate and removing volatiles with a rotary evaporator, the products were purified on silica gel, eluting with a 10-20% ethyl acetate/hexanes solution to yield 590 mg (3.6 mmol, 36%) of 4-hexylpyrimidine (consistent with known spectra) and 370 mg (1.6 mmol, 16%) 4-(undecan-6-yl)pyrimidine. Both were light yellow oils.

4-hexylpyrimidine: ^{1}H NMR ($CDCl_3$) δ 8.99 (d, *J* = 1.4 Hz, 1H), 8.46 (d, *J* = 5.2 Hz, 1H), 7.05 (dd, *J* = 5.3, 1.4 Hz, 1H), 2.64 - 2.61 (m, 2H), 1.63 - 1.57 (m, 2H), 1.25 - 1.16 (m, 6H), 0.76 - 0.72 (m, 3H).). ^{13}C NMR ($CDCl_3$) δ 170.9, 158.6, 156.6, 120.4, 37.8, 31.6, 28.9, 28.8, 22.5, 14.0. HRMS m/z calcd. for $C_{10}H_{16}N_2$ $[M+H]^+$ 165.1386, found 165.1384.

4-(undecan-6-yl)pyrimidine: ^{1}H NMR (300 MHz, $CDCl_3$) δ 9.13 (s, 1H), 8.58 (d, *J* = 5.2 Hz, 1H), 7.11 (dd, *J* = 5.2, 1.4 Hz, 1H), 2.64 (tt, *J* = 8.5, 6.0 Hz, 1H), 1.75 - 1.53 (m, 4H), 1.30 - 0.94 (m, 13H), 0.83 (d, *J* = 6.4 Hz, 6H).^{13}C NMR (75 MHz, $CDCl_3$) δ 174.5, 159.0, 156.6, 120.6, 47.9, 35.2, 32.00, 27.2, 22.6, 14.1; HRMS (ESI/Q-TOF) $[M + H]^+$ m/z: Calcd for ($C_{15}H_{36}N_2$) 235.2169; Found 235.2163.

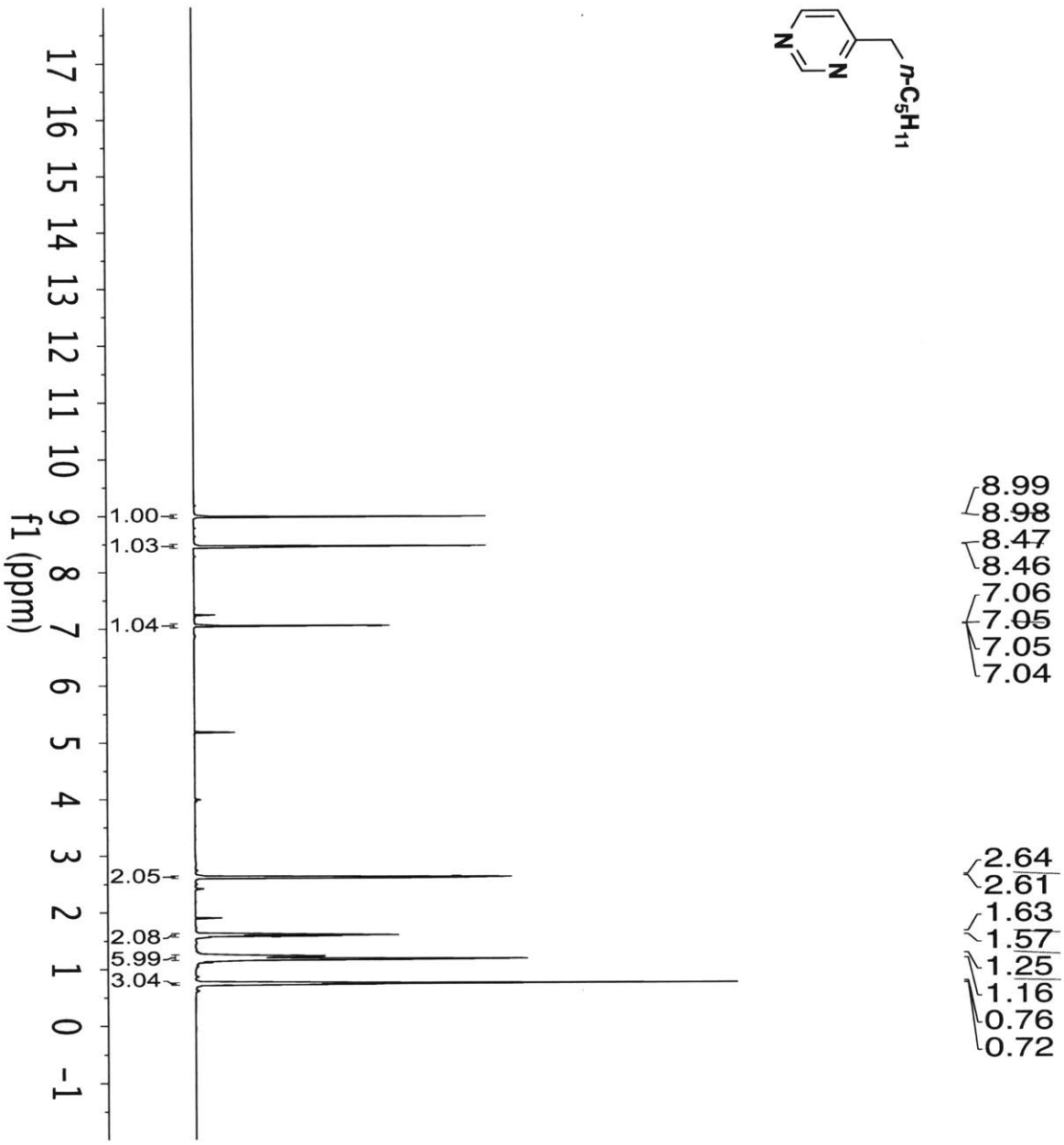

Figure S3. ^{1}H NMR spectrum of 4-hexylpyrimidine

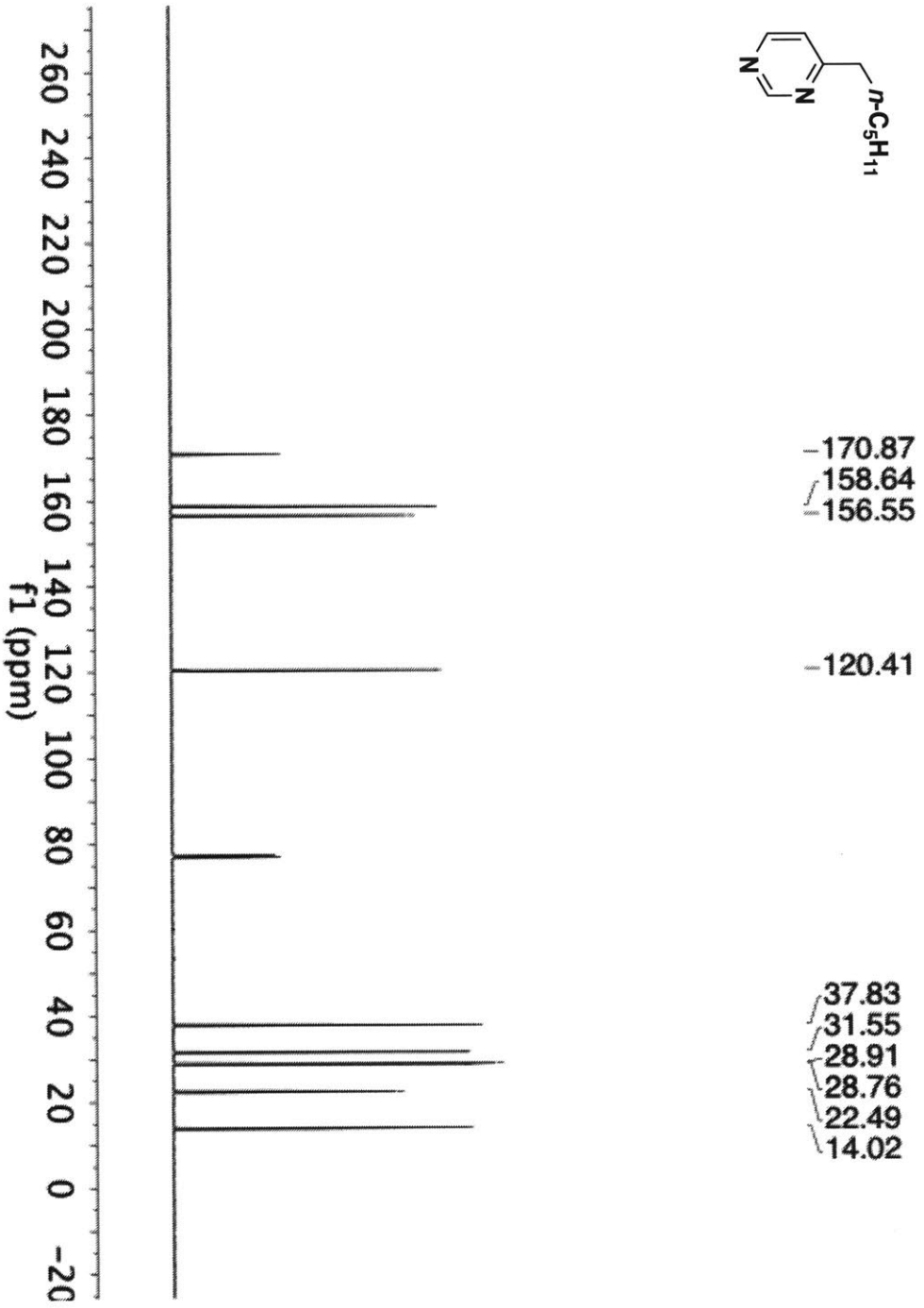

Figure S4. ^{13}C NMR spectrum of 4-hexylpyrimidine

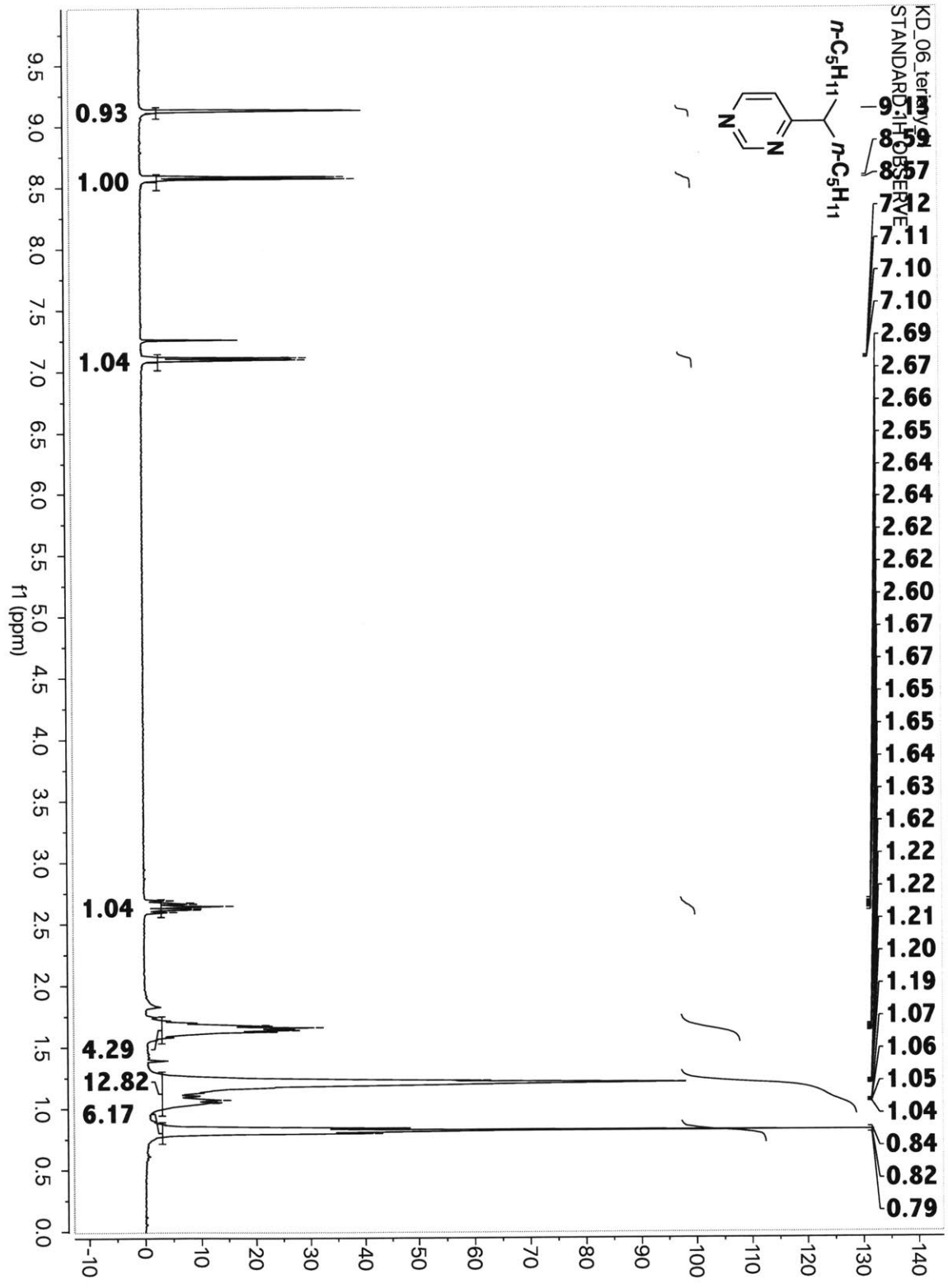

Figure S5. ^{1}H NMR spectrum of 4-(undecan-6-yl)pyrimidine

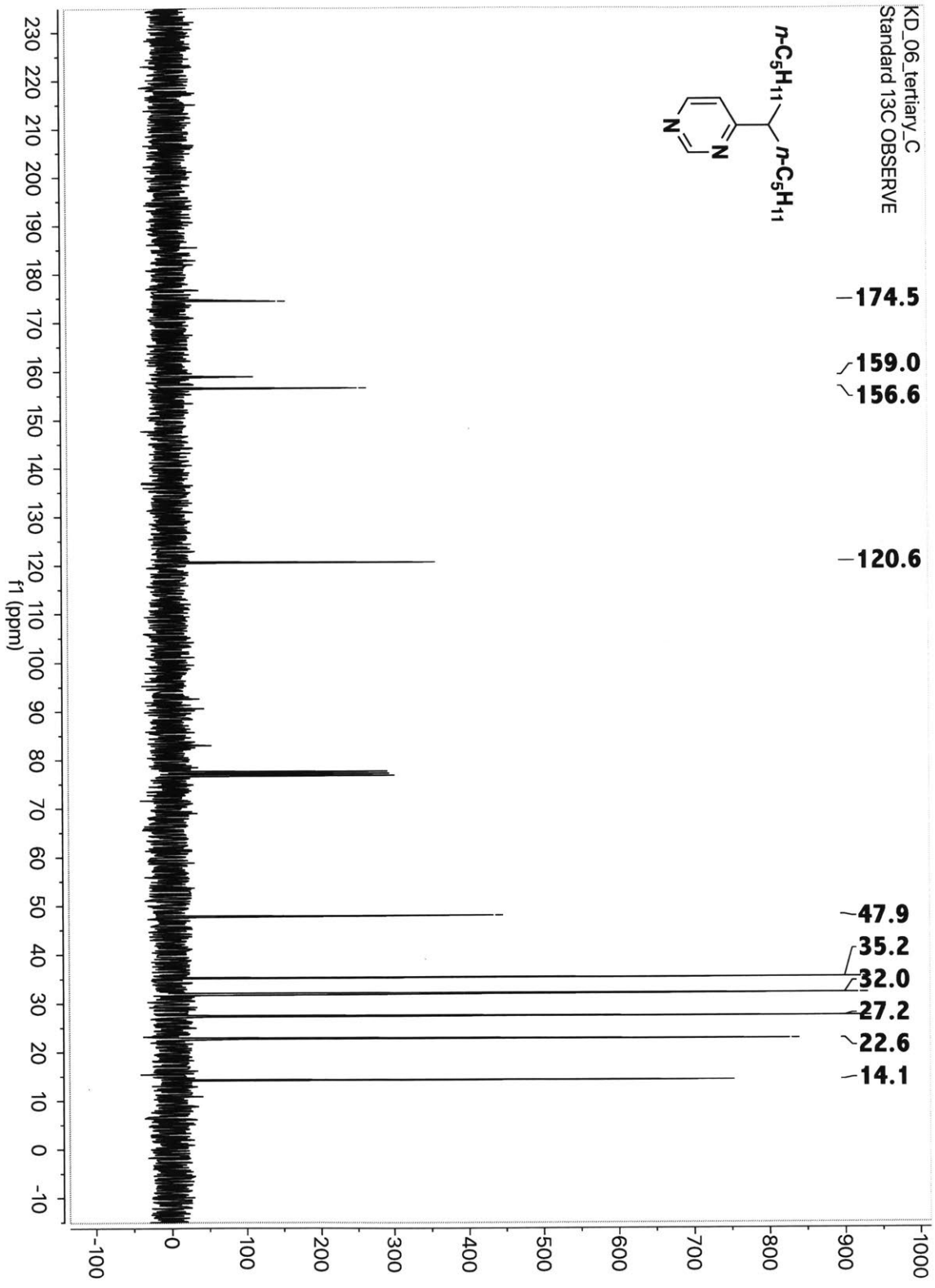

Figure S6. ^{13}C NMR spectrum of 4-(undecan-6-yl)pyrimidine

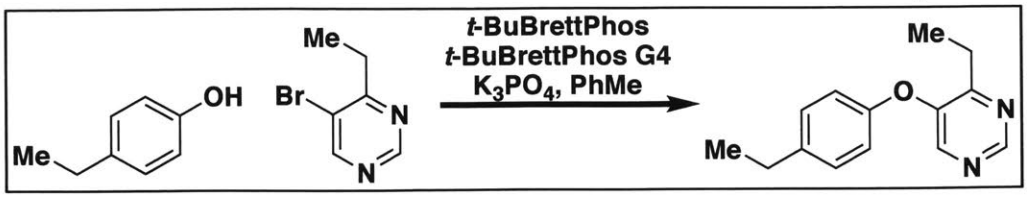

4-ethyl-5-(4-ethylphenoxy)pyrimidine: 2.27 g (10.6 mmol) anhydrous tribasic potassium phosphate were added to an oven-dried Schlenk flask equipped with a stir bar under N_2. 50 mL of dry toluene were added, followed by 78 mg (3 mol%) *tert*-butylBrettPhos and 137 mg (3 mol%) *tert*-butylBrettPhos third generation palladium catalyst (Buchwald type). The mixture was then heated to 100 °C for 15 hours. After cooling to room temperature, the reaction was diluted with ethyl acetate and water was added. The product was extracted three times with ethyl acetate, dried over magnesium sulfate and passed through Celite. After concentration via rotary evaporation, the product was purified on silica gel, eluting with a gradient of 10 - 20% ethyl acetate/hexanes. Removal of the solvent via rotary evaporation yielded 463 mg of the desired product (2.0 mmol, 38%).

^{1}H NMR (400 MHz, $CDCl_3$) δ 8.88 (s, 1H), 8.19 (s, 1H), 7.24 - 7.15 (m, 2H), 6.95 - 6.85 (m, 2H), 2.88 (q, *J* = 7.6 Hz, 2H), 2.65 (q, *J* = 7.6 Hz, 2H), 1.31 (t, *J* = 7.6 Hz, 3H), 1.24 (t, *J* = 7.6, 0Hz, 3H); ^{13}C NMR (101 MHz, $CDCl_3$) δ 163.2, 154.0, 153.2, 150.1, 145.8, 140.3, 129.4, 118.1, 77.2, 28.1, 25.3, 15.7, 11.6; HRMS: m/z calcd. for $C_{14}H_{16}N_2O$ $[M+H]^+$ 229.1335, found 229.1332.

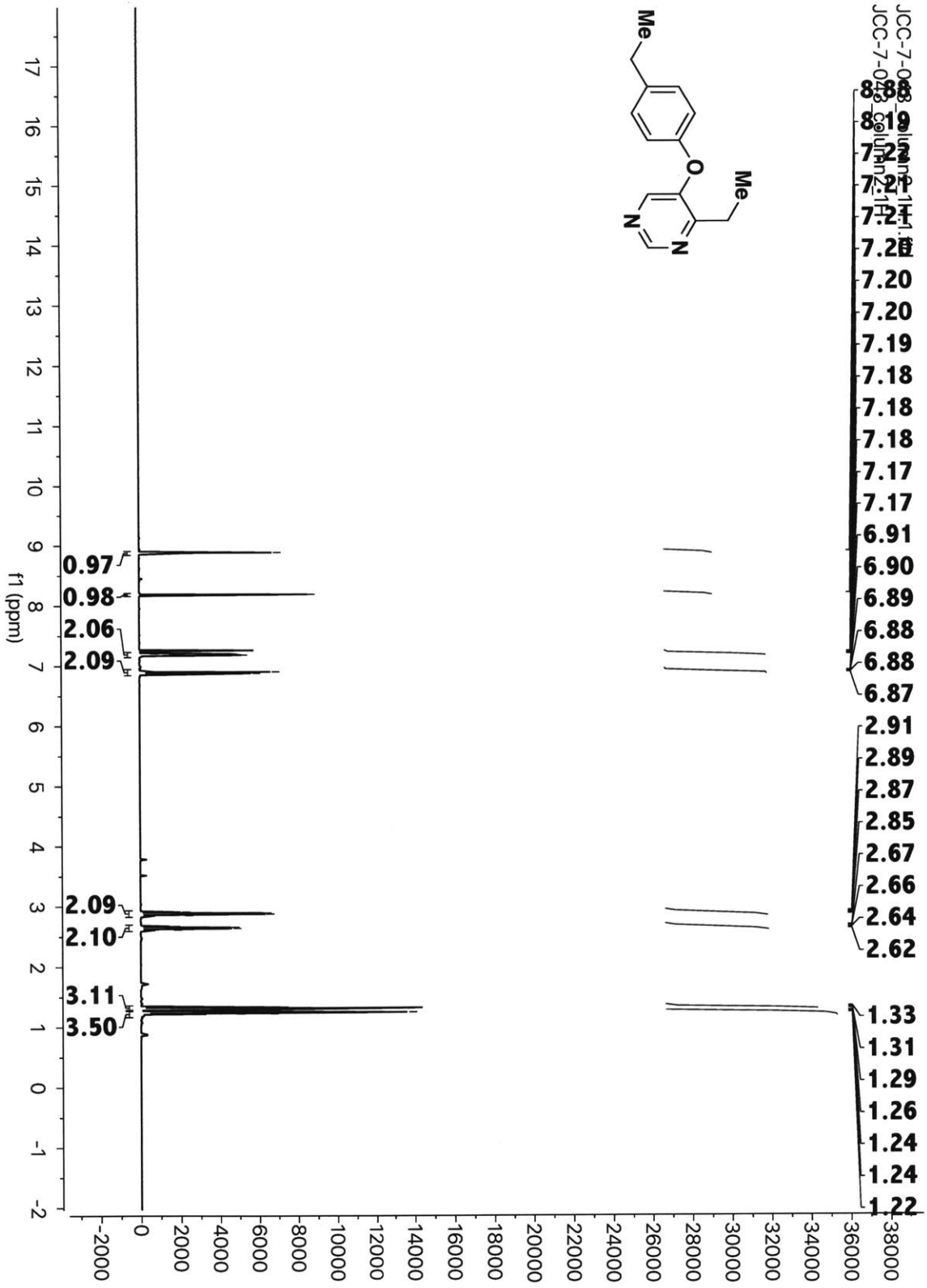

Figure S7. ^{1}H NMR spectrum of 4-ethyl-5-(4-ethylphenoxy)pyrimidine

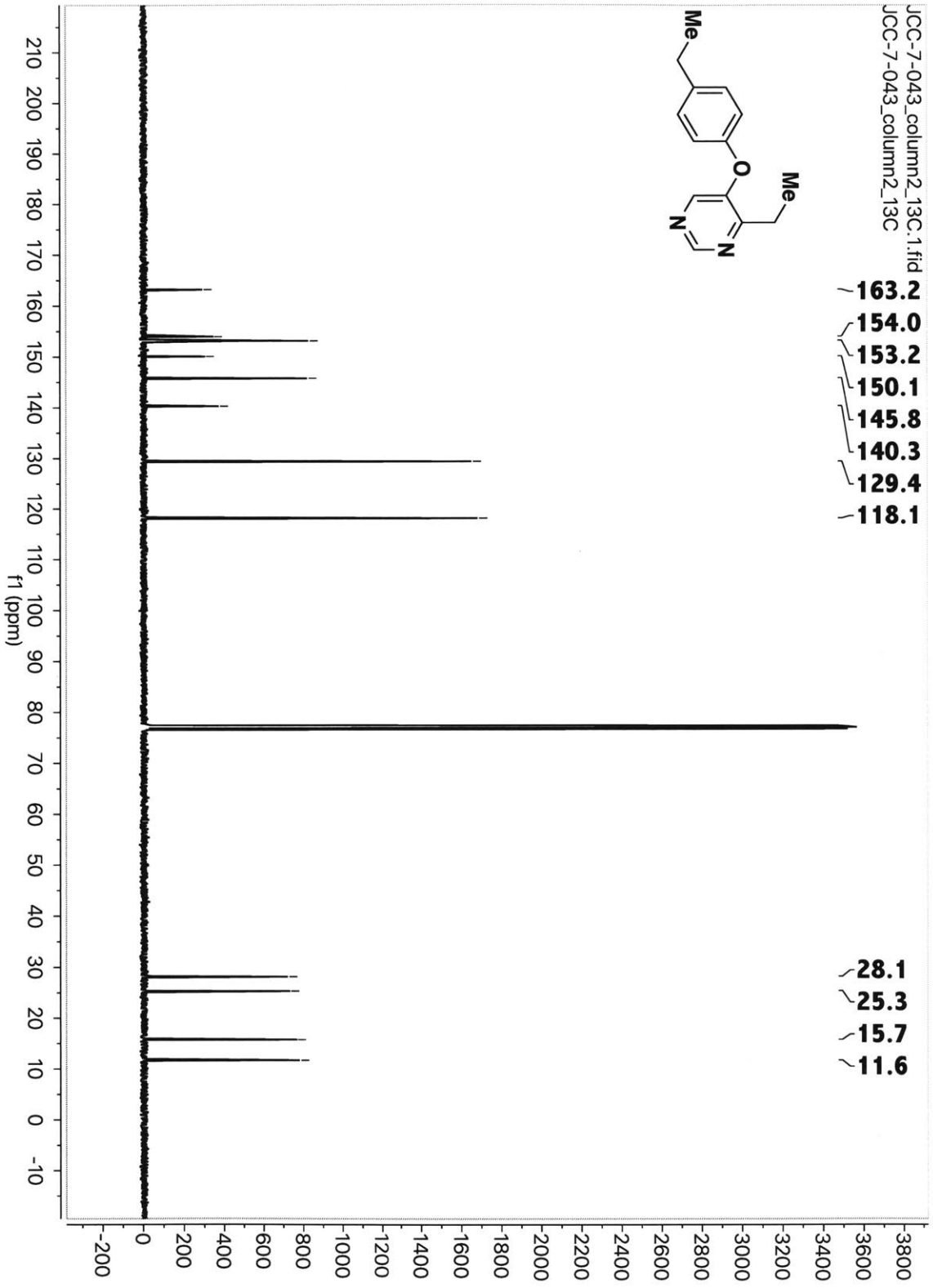

Figure S8. ^{13}C NMR spectrum 4-ethyl-5-(4-ethylphenoxy)pyrimidine

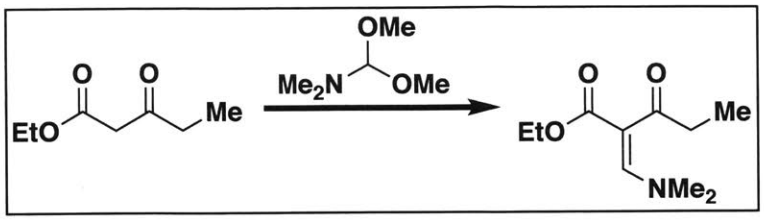

Ethyl (*E*)-2-((Dimethylamino)methylene)-3-oxopentanoate: Following the procedure of Antonsson and coworkers[3], 1.1 mL (8.4 mmol) of dimethylformamide dimethyl acetal was added dropwise to a stirring round bottom flask charged with 1 mL (7.0 mmol) of ethyl-3-oxopentanoate. The reaction was stirred at room temperature for 18 hours, upon which residual DMF was azeotroped off with 2 x 10 mL toluene to yield the desired product as a yellow oil (7.0 mmol, quantitative). NMR spectra matched those previously reported.[3]

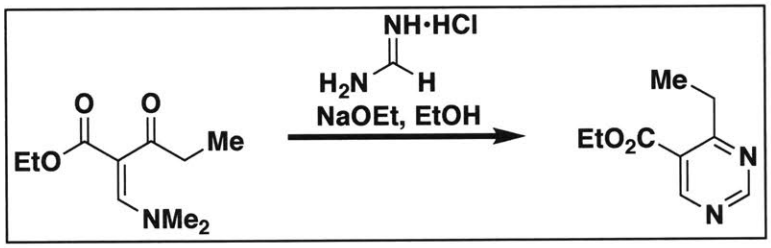

Ethyl 4-ethylpyrimidine-5-carboxylate: Ethyl (*E*)-2-((Dimethylamino)methylene)-3-oxopentanoate (500 mg, 2.5 mmol) was dissolved in 5 mL anhydrous ethanol. 202 mg (2.5 mmol mmol) formamidine hydrochloride were added to the solution, followed by 170 mg (2.6 mmol) of sodium ethoxide. The reaction was refluxed at 95 °C for 12 hours. After cooling, the reaction was diluted with ethyl acetate, washed with water, and dried over magnesium sulfate. After concentration, the product was purified on silica gel, eluting with 40% ethyl acetate/hexanes to yield a yellow oil (202 mg, 1.1 mmol, 45%), whose NMR spectra was consistent with spectra previously reported.[4]

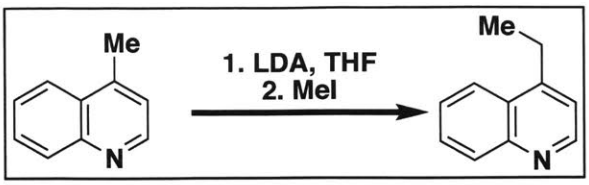

4-ethylquinoline: In an oven-dried 2-neck round bottom flask, 30 mL THF and 1.1 mL (7.5 mmol) diisopropylamine were added under N_2. The solution was cooled to -78 °C, and 3.4 mL (8.4 mmol) of an *n*-butyllithium solution (2.5 M in hexanes) were added dropwise. The mixture was stirred at -78 °C for 10 minutes, then warmed to 0 °C. In a separate round-bottomed flask, 0.92 mL (7 mmol) of lepidine was dissolved in 20 mL THF and cooled to -78 °C. The LDA solution was then transferred slowly via canula, and the reaction was stirred at -78 °C for 30 minutes. 0.61 mL (9.8 mmol) methyl iodide were added, and the reaction was stirred for 10 minutes before warming to room temperature. After quenching with H_2O and diluting with ethyl acetate, 1 M HCl was added to pH 7 - 8, and the organic phase was thrice extracted with dicholoromethane. After drying over magnesium sulfate and removing volatiles with a rotary evaporator, the products were purified on silica gel to yield 950 mg (6 mmol) of 4-ethylquinoline (87%). Spectra were consistent with those previously reported.[5]

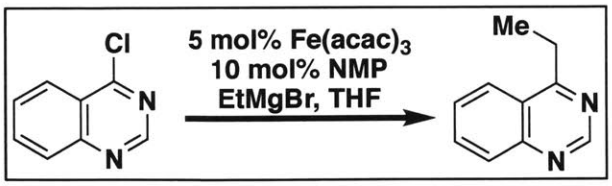

4-ethylquinazoline: Following the procedure of Fürstner and coworkers[6], 500 mg (3.0 mmol) of 4-chloro-quinazoline and 53 mg (0.15 mmol) $Fe(acac)_3$ were combined in an oven-dried round bottom flask and purged under nitrogen. 20 mL THF and 2.0 mL NMP

were added, followed by dropwise addition of 1.2 mL (3.6 mmol) of a 3.0 M ethylmagnesium bromide solution in diethyl ether. After stirring at room temperature for 10 minutes, the reaction was quenched with water and extracted with ethyl acetate, dried over magnesium sulfate, and the solvent removed via 20% ethyl acetate in hexanes as the eluent to yield a yellow oil (318 mg, 67%). Spectra were consistent with those preciously reported.[7]

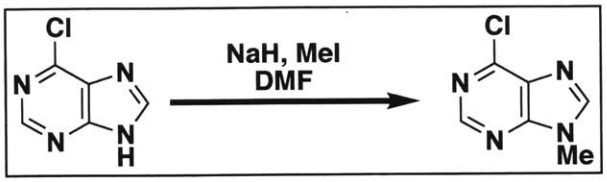

6-chloro-9-methyl-9*H*-purine: 500 mg (3.2 mmol) 6-Chloro-9*H*-purine were dissolved in 7 mL DMF. 128 mg (3.2 mmol) NaH (60% dispersion in mineral oil) were added at room temperature and the reaction was stirred for 5 minutes. 200 µL (3.2 mmol) methyl iodide was added drop wise, and the reaction stirred at room temperature for 12 hours. For workup, the reaction was diluted with dichloromethane, washed with saturated sodium bicarbonate solution, and dried over magnesium sulfate. Removal of the solvent via rotary evaporation gave the crude product, which was subsequently purified via column chromatography on silica gel, eluting with pure ethyl acetate. After removing the solvent via rotary evaporation to yield 334 mg (2.0 mmol, 62%) of an off-white solid, NMR spectra were determined to be consistent with spectra previously reported.[8]

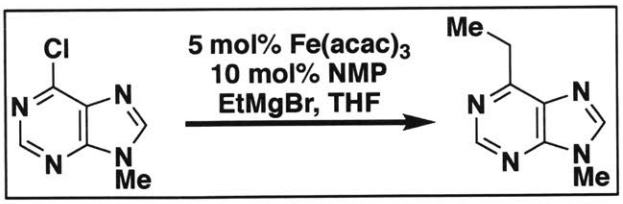

6-ethyl-9-methyl-9*H*-purine: Following the procedure of Fürstner and coworkers[6], 200 mg (1.19 mmol) of 6-chloro-9-methyl-9*H*-purine and 21 mg (0.06 mmol) $Fe(acac)_3$ were combined in an oven-dried round bottom flask and purged under nitrogen. 8.0 mL THF and 0.8 mL NMP were added, followed by 0.48 mL (1.4 mmol) of a ethylmagnesium bromide solution (3.0 M in THF) dropwise. After stirring at room temperature for 10

minutes, the reaction was quenched with water and extracted with ethyl acetate, dried over magnesium sulfate, and the solvent removed via 10% methanol in dichloromethane as the eluent to yield the desired products as a pale yellow, oily solid (112 mg, 46%).

^{1}H NMR (300 MHz, $CDCl_3$) δ 8.90 (s, 1H), 8.00 (s, 1H), 3.90 (s, 3H), 3.23 (q, J = 7.6 Hz, 2H), 1.44 (t, J = 7.6 Hz, 3H); ^{13}C NMR (125 MHz, $CDCl_3$) δ 164.0, 152.7, 151.2, 144.3, 132.3, 29.9, 26.6, 12.7; HRMS (ESI/Q-TOF) $[M + H]^+$ m/z: Calcd for ($C_8H_{10}N_4$) 163.0978; Found 163.0978.

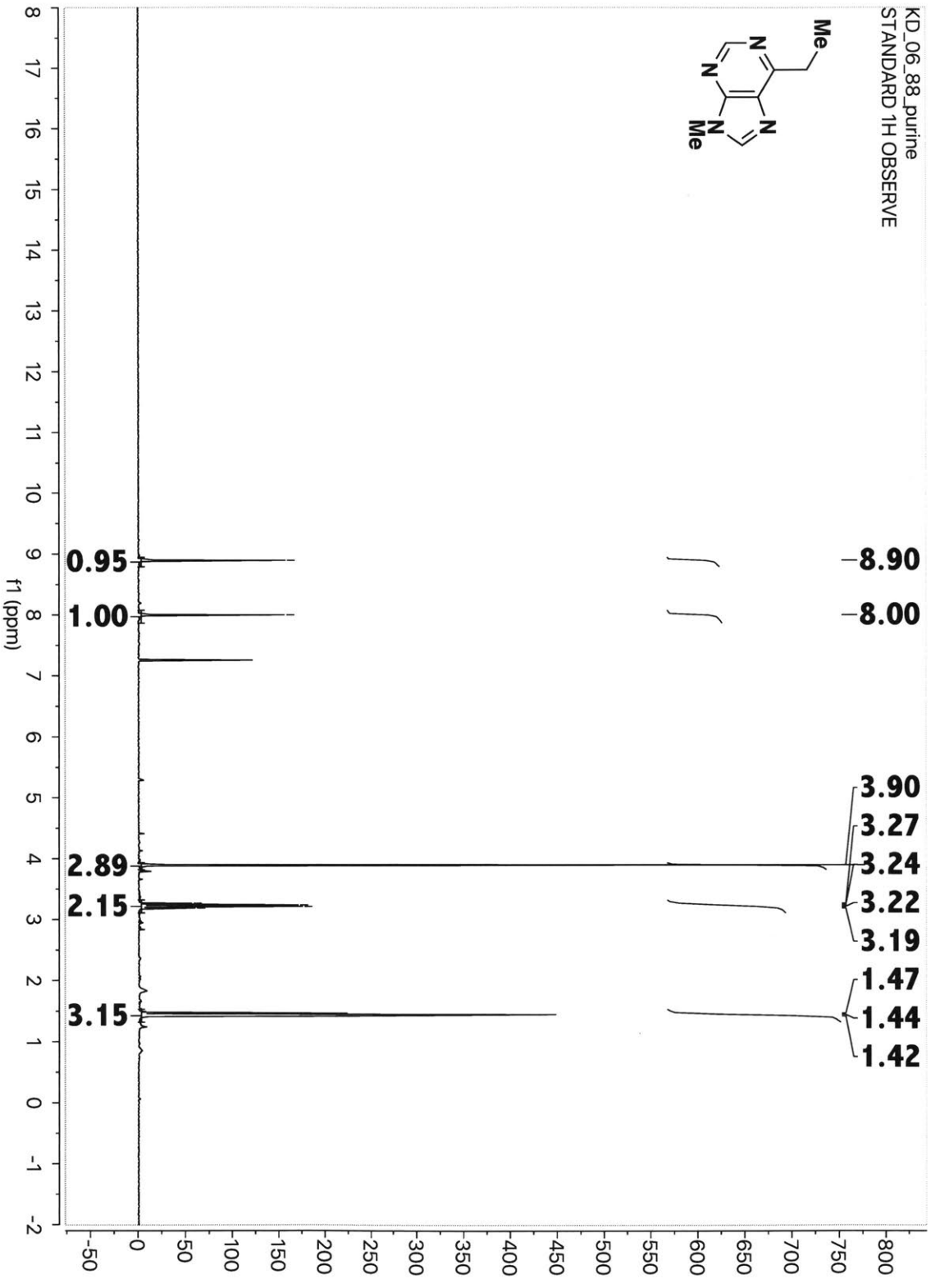

Figure S9. ^{1}H NMR spectrum of 6-ethyl-9-methyl-9*H*-purine

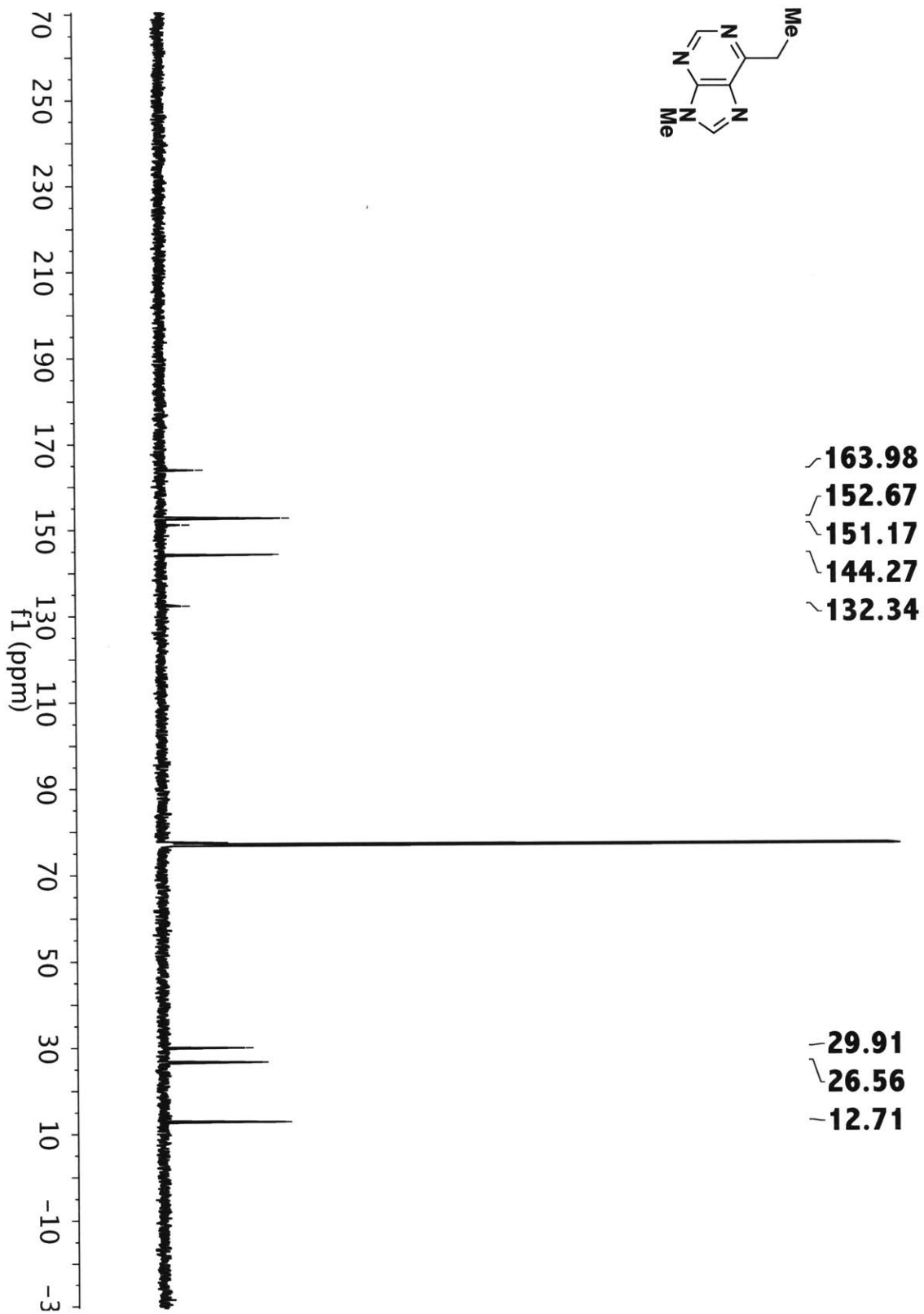

Figure S10. ^{13}C NMR spectrum of 6-ethyl-9-methyl-9*H*-purine

Benzylic Fluorination of Volatile Pyridines (Yield by ^{19}F NMR)

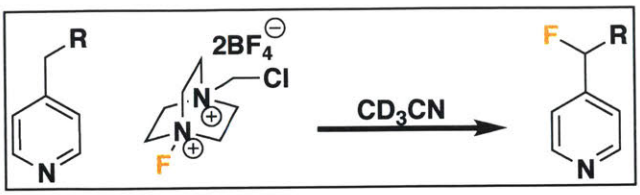

General Procedure: Under nitrogen, the pyridine (0.5 mmol) was added to an oven-dried 8 mL scintillation vial that had been purged with N_2 via a Teflon-faced septum. MeCN-d_3 (1 mL, stored over molecular sieves) was added, followed by 212 mg (0.6 mmol, 1.2 equivalents) Selectfluor®. The nitrogen needle was removed, and the cap sealed with melted parafilm. The suspension was stirred for 20 hours at 25 °C, gradually forming a pale yellow mixture. A saturated sodium bicarbonate solution was added to the reaction, and the product was extracted with 2 mL $CDCl_3$. 57 µL (0.5 mmol) of 4-fluoroanisole as an internal standard were added to the organic extract, and the yield analyzed via ^{19}F NMR. After removal of the solvent via rotary evaporation, the crude product was purified on silica or alumina to acquire clean NMR spectra. Besides the desired products, these reactions typically contained small amounts of remaining starting material and small amounts of difluorinated products.

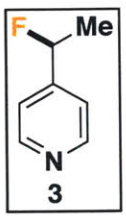

4-(1-fluoroethyl)pyridine: 68%, yellow oil. Purified by silica preparatory thin-layer chromatography by eluting first with pentane, followed by ethyl acetate. ^1H and ^{19}F NMRs were consistent with previously reported spectra.[9]

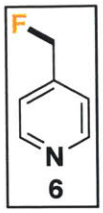

6

4-(1-fluoromethyl)pyridine: 18%, yellow oil. Purified by eluting with ethyl acetate on preparatory thin-layer chromatography. ^{1}H and ^{19}F NMRs were consistent with previously reported spectra.[10]

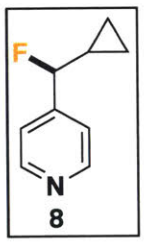

8

4-(cyclopropylfluoromethyl)pyridine: 78%, yellow oil. Purified by eluting in ethyl acetate on silica gel. ^{1}H and ^{19}F NMRs were consistent with previously reported spectra.[9]

Benzylic Fluorination of Non-Volatile Pyridines (Isolated Yields)

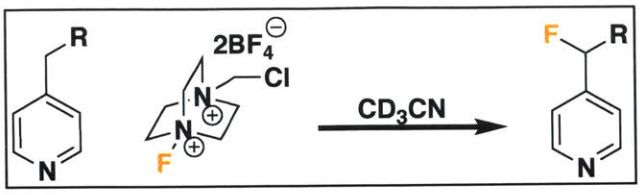

General Procedure: Under nitrogen, the pyridine (0.5 mmol) was added to an oven-dried 8 mL scintillation vial that had been purged with N_2 via a Teflon-faced septum. MeCN-d_3 (1 mL, stored over molecular sieves) was added, followed by 212 mg (0.6 mmol, 1.2 equivalents) Selectfluor®. The nitrogen needle was removed and the cap sealed with melted parafilm. The suspension was stirred for 20 hours at 25 °C, gradually forming a pale yellow mixture. The reaction mixture was transferred with the aid of ethyl acetate into a separator funnel. The organic layer was washed with a saturated sodium bicarbonate solution, which was then back-extracted with additional ethyl acetate three times. The combined organic layers were then dried with magnesium sulfate, filtered, and concentrated on rotary evaporator to provide the crude product mixture. The desired products were isolated by silica gel chromatography. Besides the desired products, these reactions typically contained small amounts of remaining starting material and small amounts of difluorinated products. In all cases, the desired monofluorinated product could be easily separated from these trace byproducts.

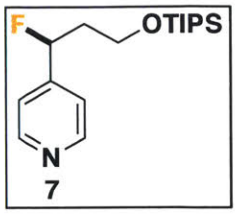

7

4-(1-fluoro-3-((triisopropylsilyl)oxy)propyl)pyridine: 51%, pale yellow oil. Purified on silica gel using 20 – 50% ethyl acetate/pentane as an eluent.

^{1}H NMR (500 MHz, $CDCl_3$) δ 8.64 - 8.60 (m, 2H), 7.28 (d, *J* = 6.0 Hz, 2H), 5.74 (ddd, *J* = 48.1 Hz, *J* = 9.1 Hz, *J* = 3.8 Hz, 1H), 3.95 (ddd, *J* = 10.2 Hz, *J* = 8.8 Hz, *J* = 4.4 Hz, 1H), 3.78 (dt, *J* = 10.1, 5.1 Hz, 1H), 2.15 - 1.92 (m, 2H), 1.16 – 1.04 (m, 21H);^{13}C NMR (126 MHz, $CDCl_3$) δ 151.0, 120.0 (d, *J* = 8.5 Hz), 89.7 (d, *J* = 171.9 Hz), 58.7 (d, *J* = 4.4 Hz), 40.6 (d, *J* = 21.9 Hz), 18.1, 12.0; ^{19}F NMR (471 MHz, $CDCl_3$): δ -188.0 (ddd, *J* = 49.2, *J* = 33.1 Hz, *J* = 16.9 Hz); HRMS (ESI/Q-TOF) $[M + H]^+$ m/z: Calcd for ($C_{17}H_{30}FNOSi$) 312.2153; Found 312.2140.

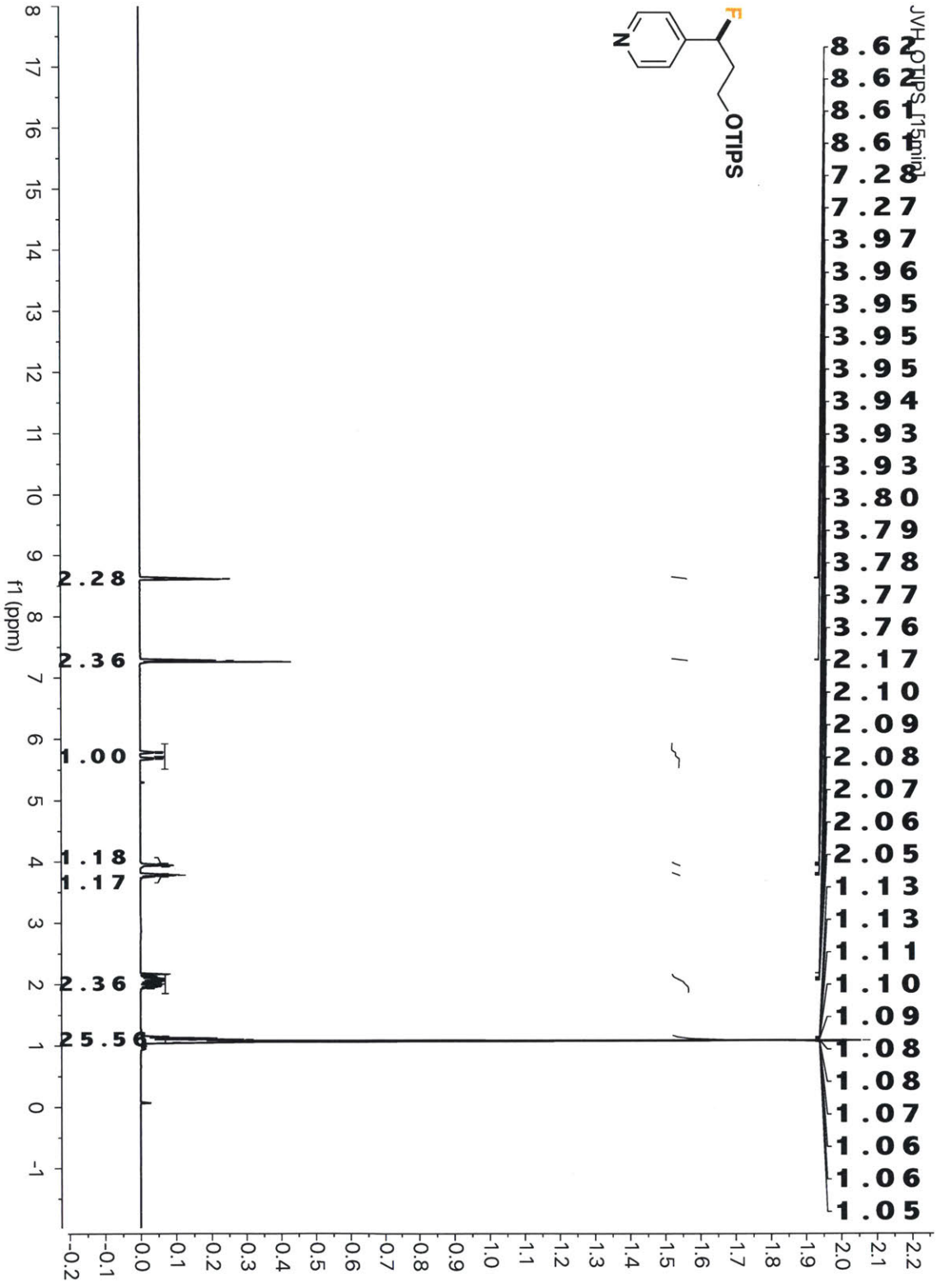

Figure S11. ^{1}H NMR spectrum of 4-(1-fluoro-3-((triisopropylsilyl)oxy)propyl)pyridine

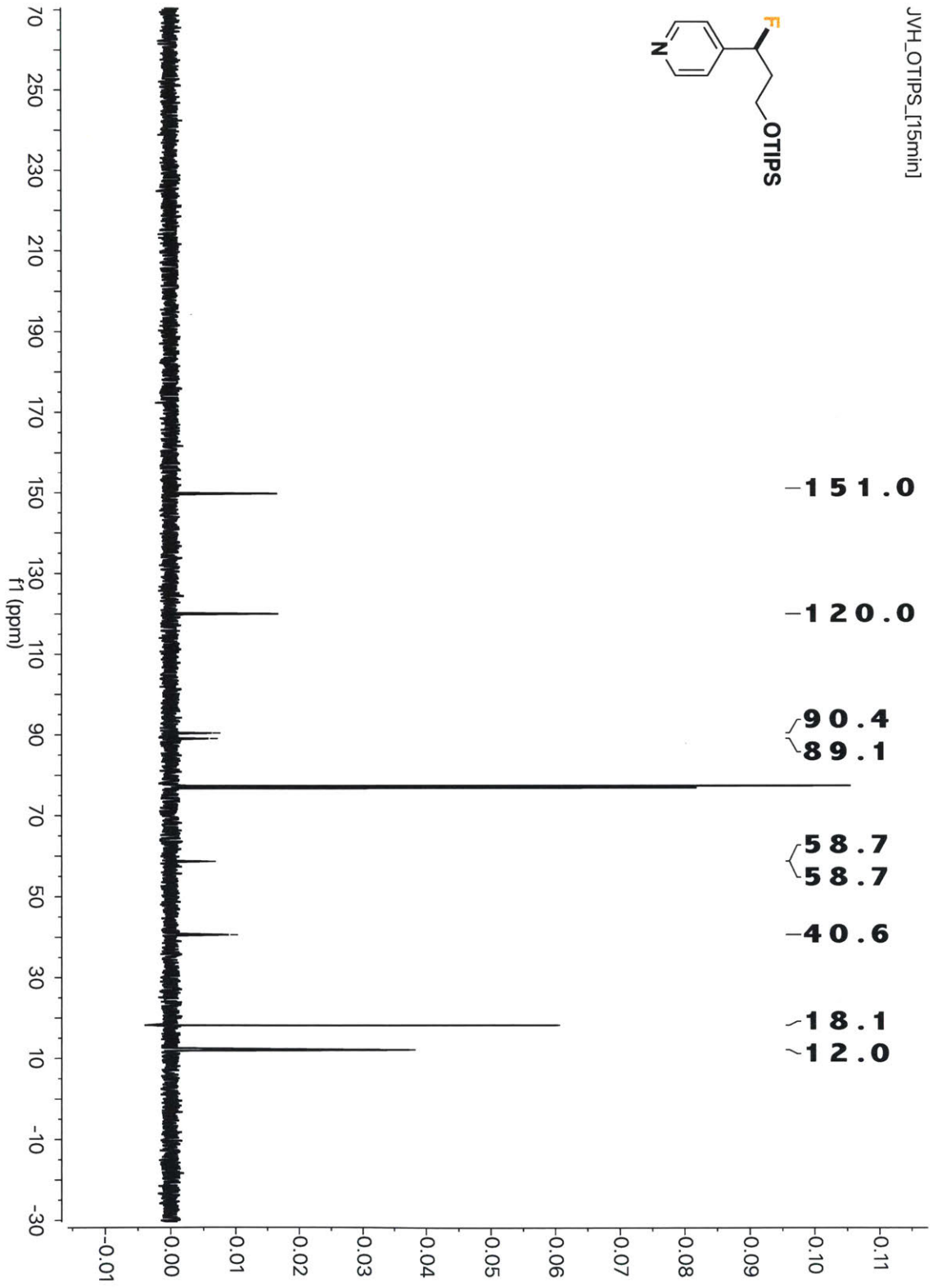

Figure S12. ^{13}C NMR spectrum of 4-(1-fluoro-3-((triisopropylsilyl)oxy)propyl)pyridine

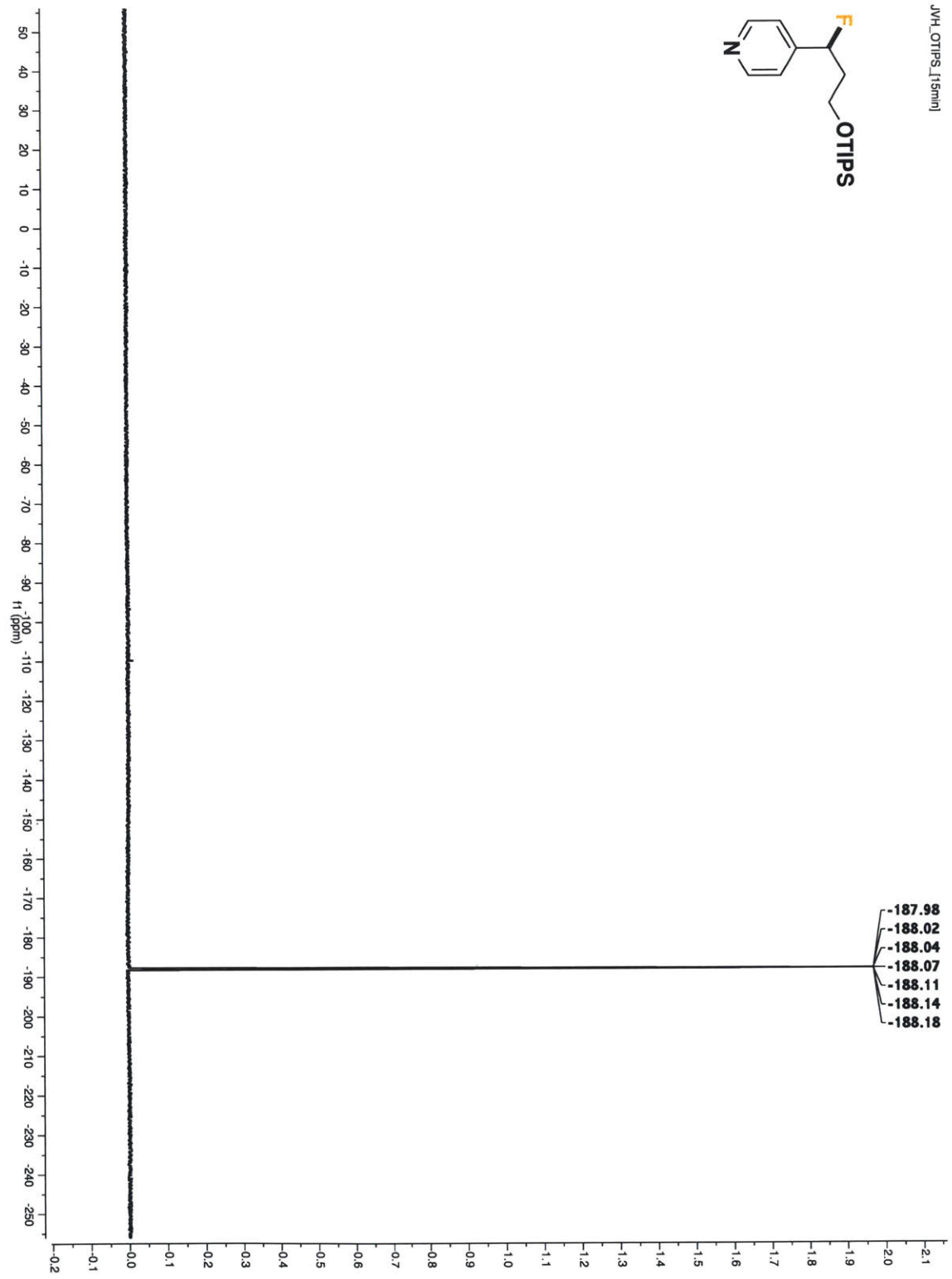

Figure S13. ^{19}F NMR spectrum of 4-(1-fluoro-3-((triisopropylsilyl)oxy)propyl)pyridine

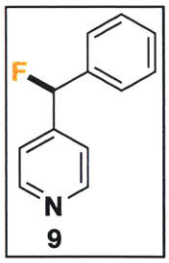

9

4-(1-fluoro(phenyl)methyl)pyridine: 56% total yield including dimer impurity **25**, yellow oil. Purified via column chromatography on silica gel using 15-30% ethyl acetate/hexanes gradient elution.

^{1}H NMR (500 MHz, $CDCl_3$) δ 8.61 (d, *J* = 6.0 Hz, 2H), 7.43 - 7.35 (m, 3H), 7.34 - 7.28 (m, 2H), 7.28 - 7.22 (m, 2H), 6.41 (d, *J* = 47.1 Hz, 1H); ^{13}C NMR (126 MHz, $CDCl_3$) δ 150.1, 129.4, 129.0, 127.2 (d, J = 5.3 Hz), 120.7 (d, *J* = 7.5 Hz), 93.0 (d, *J* = 175.5); ^{19}F NMR (471 MHz, $CDCl_3$) δ -172.2 (dt, *J* = 50.9 Hz, *J* = 21.6 Hz); HRMS (ESI/Q-TOF) [M + H]$^{+}$ m/z: Calcd for ($C_{12}H_{10}FN$) 188.0870; Found 188.0869.

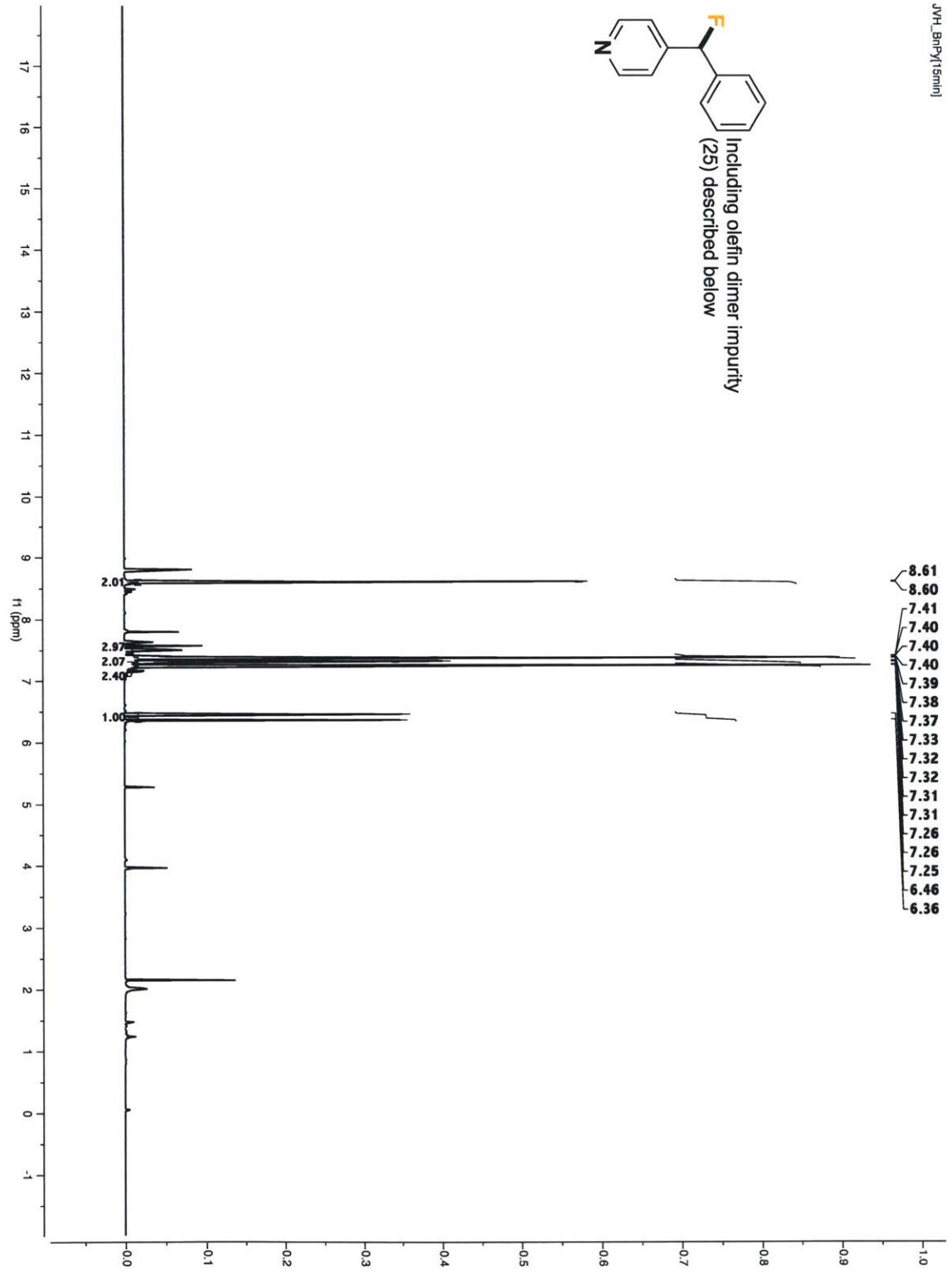

Figure S14. ^{1}H NMR spectrum of 4-(1-fluoro(phenyl)methyl)pyridine

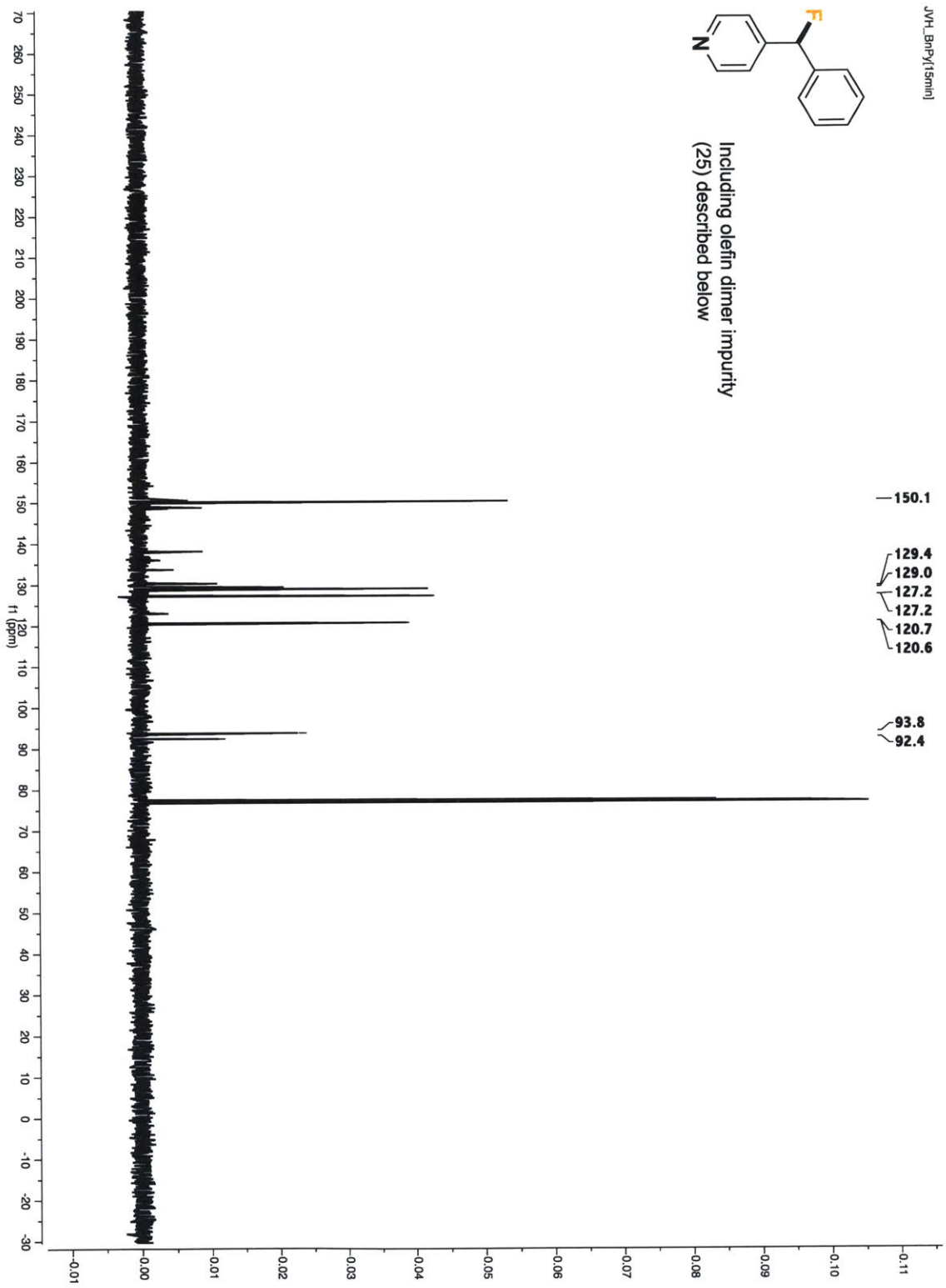

Figure S15. ^{13}C NMR spectrum of 4-(1-fluoro(phenyl)methyl)pyridine

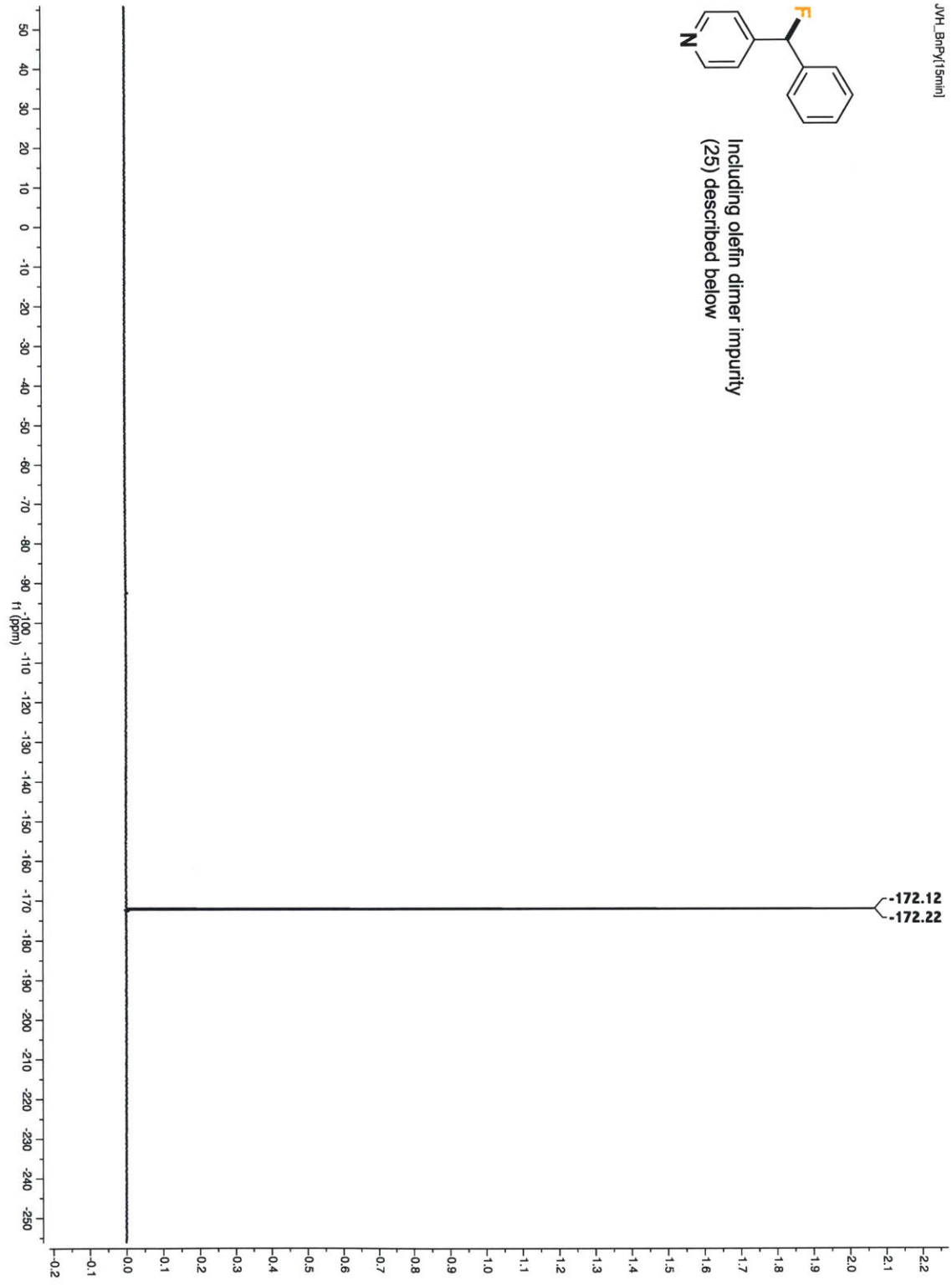

Figure S16. ^{19}F NMR spectrum of 4-(1-fluoro(phenyl)methyl)pyridine

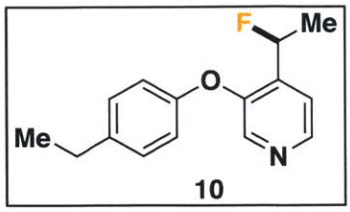

10

3-(4-ethylphenoxy)-4-(1-fluoroethyl)pyridine: 31% (with 2% staring material, 33% total), yellow oil. Purified via column chromatography on silica gel using 15%-30% ethyl acetate/hexanes gradient elution.

^{1}H NMR (500 MHz, $CDCl_3$) δ 8.40 (d, *J* = 4.9 Hz, 1H), 8.15 (s, 1H), 7.46 (d, *J* = 4.9 Hz, 1H), 7.22 - 7.15 (m, 3H), 6.94-6.87 (m, 2H), 5.94 (dq, *J* = 47.4 Hz, *J* = 6.4 Hz, 1H), 2.64 (q, *J* = 7.6 Hz, 2H), 1.64 (dd, *J* = 24.4 Hz, *J* = 6.4 Hz, 3H), 1.24 (t, *J* = 7.6 Hz, 3H). ^{13}C NMR (126 MHz, $CDCl_3$) δ 154.3, 149.7, 145.0, 141.2 (d, *J* = 22.3 Hz), 140.4, 129.5, 119.89, 119.8, 118.4, 85.8 (d, *J* = 170.5 Hz), 28.3, 22.0, 21.8, 15.8. ^{19}F NMR (471 MHz, $CDCl_3$) δ -181.9 (dq, *J* = 48.6 Hz, *J* = 24.4 Hz); HRMS (ESI/Q-TOF) $[M + H]^+$ m/z: Calcd for ($C_{15}H_{16}FNO$) 246.1289; Found 246.1284.

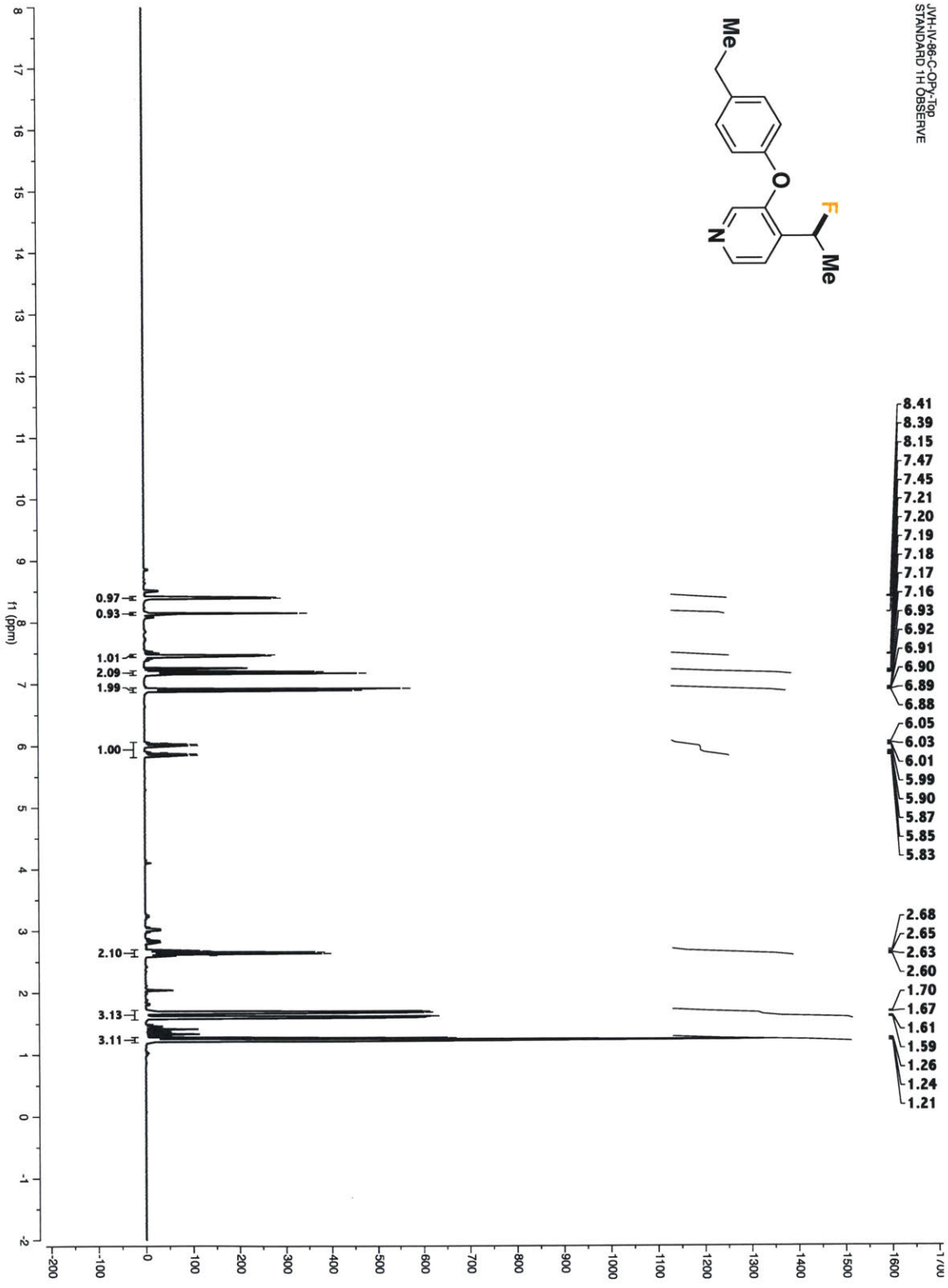

Figure S17. ^{1}H NMR spectrum of 3-(4-ethylphenoxy)-4-(1-fluoroethyl)pyridine

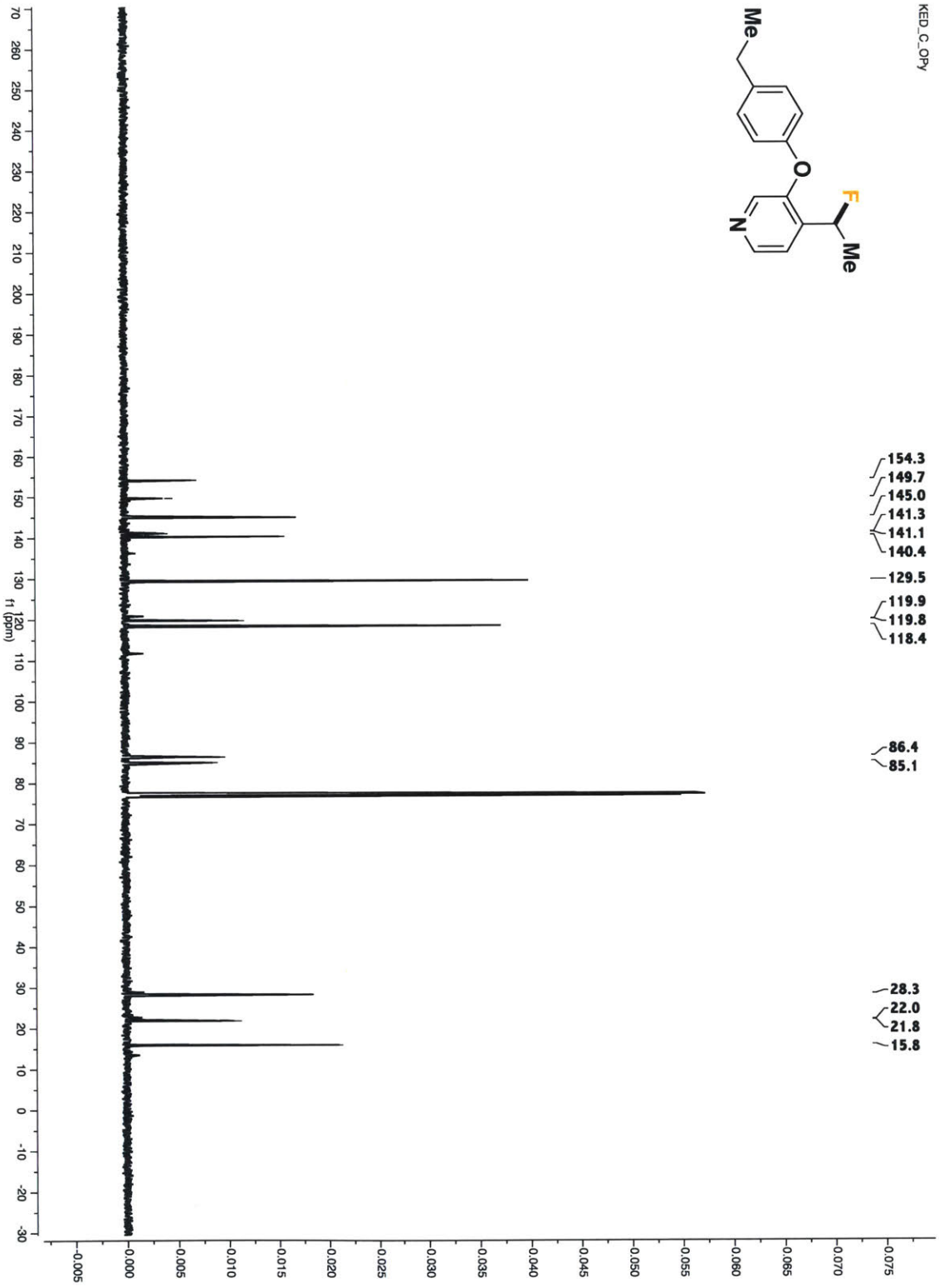

Figure S18. ^{13}C NMR spectrum of 3-(4-ethylphenoxy)-4-(1-fluoroethyl)pyridine

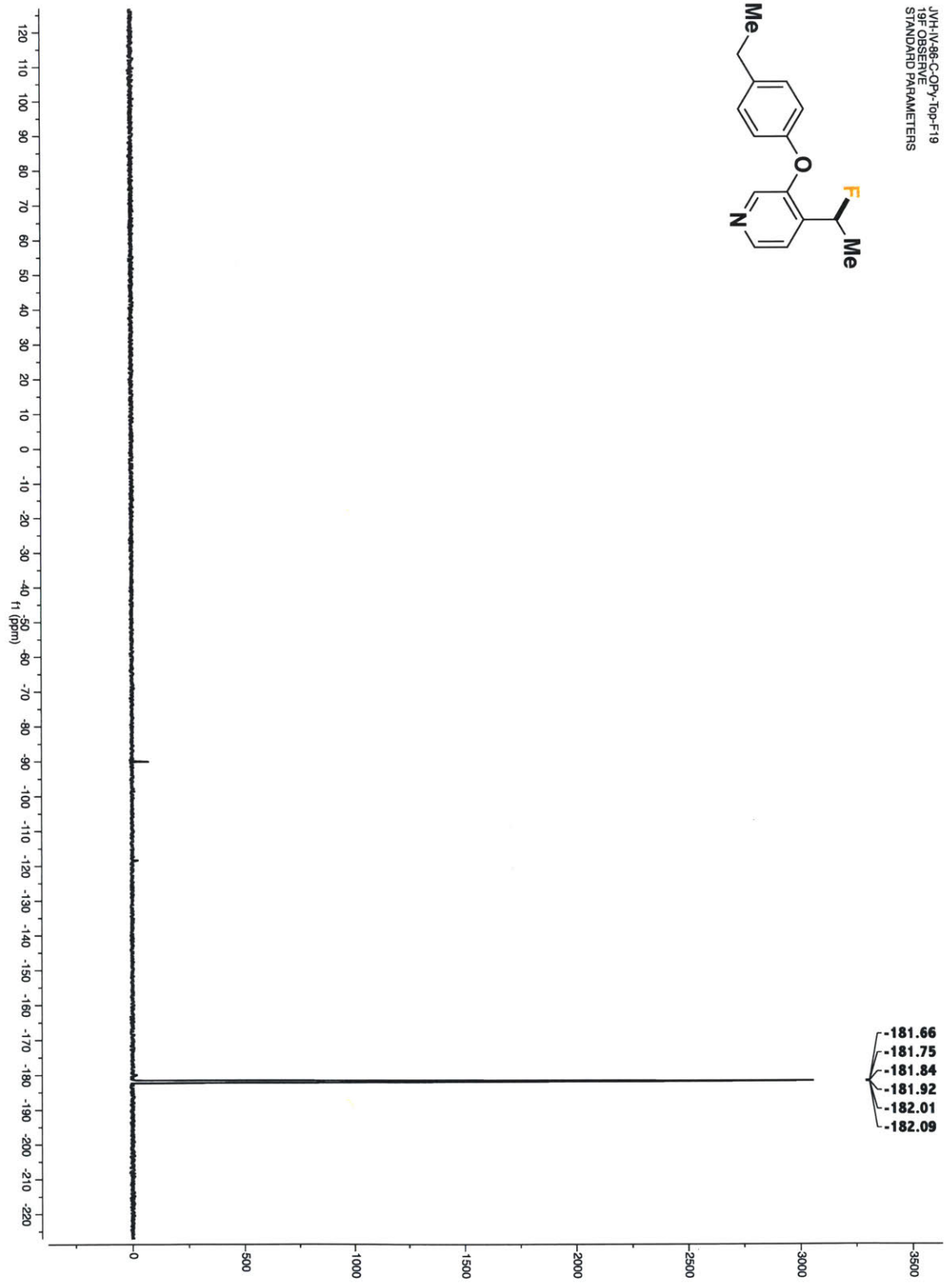

Figure S19. ^{19}F NMR spectrum of 3-(4-ethylphenoxy)-4-(1-fluoroethyl)pyridine

Benzylic Fluorination of Non-Pyridine Azaheterocycles

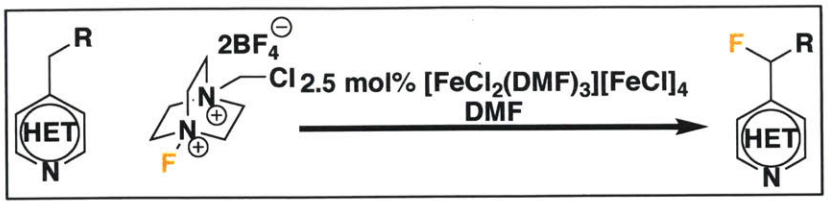

General Procedure: Under nitrogen, the *N*-heterocycle (0.5 mmol) was added to an oven-dried 8 mL scintillation vial. DMF (1 mL, degassed via bubbling nitrogen through the solvent for fifteen minutes and stored over molecular sieves) was added, followed by 6.7 mg (2.5 mol%) of $[FeCl_2(DMF)_3][FeCl_4]$ and 212 mg (0.6 mmol, 1.2 equivalents) Selectfluor®. The nitrogen needle was removed, and the cap sealed with melted parafilm. The solution was stirred for 20 hours at 40 °C, gradually forming a pale yellow solution. The reaction was transferred into a separatory funnel with the aid of ethyl acetate. The organic layer was washed with a 1 M sodium L-ascorbic acid solution to remove the iron, which was then back extracted three times with ethyl acetate. The combined organic layers were dried with $MgSO_4$, filtered and concentrated *in vacuo*. The crude product was purified on silica gel using the eluent systems described below. In general, most of the reactions also delivered small amounts of starting material and difluorinated byproducts, but which could be separated by column chromatography.

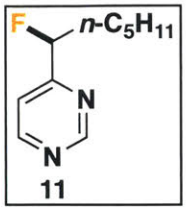

11

4-(1-fluorohexyl)pyrimidine: 51%, clear oil. Run with 1.5 equivalents of Selectfluor® instead of 1.2. Purified via column chromatography on silica gel using 15% – 30% ethyl acetate/hexanes gradient elution.

^{1}H NMR (500 MHz, $CDCl_3$) δ 9.16 (s, 1H), 8.77 (d, *J* = 5.0 Hz, 1H), 7.50 (d, *J* = 4.9 Hz, 1H), 5.47 (ddd, *J* = 48.5 Hz, *J* = 8.1 Hz, *J* = 3.5 Hz, 1H), 2.15 – 1.75 (m, 2H), 1.55 – 1.41 (m, 2H), 1.32 (s, 4H), 0.88 (t, *J* = 6.4 Hz, 3H); ^{13}C NMR (126 MHz, $CDCl_3$) δ 168.9 (d, *J* = 26.4 Hz), 158.2, 157.7, 116.9, 93.5 (d, *J* = 174.2 Hz), 35.4 (d, *J* = 21.1 Hz), 31.5, 24.4, 22.6, 14.1 ^{19}F NMR (471 MHz, $CDCl_3$) δ -192.1 (ddd, *J* = 48.7 Hz, *J* = 31.5 Hz, *J* = 21.9 Hz); HRMS (ESI/Q-TOF) $[M + H]^+$ m/z: Calcd for ($C_{10}H_{15}FN_2$) 183.1292; Found 183.1291.

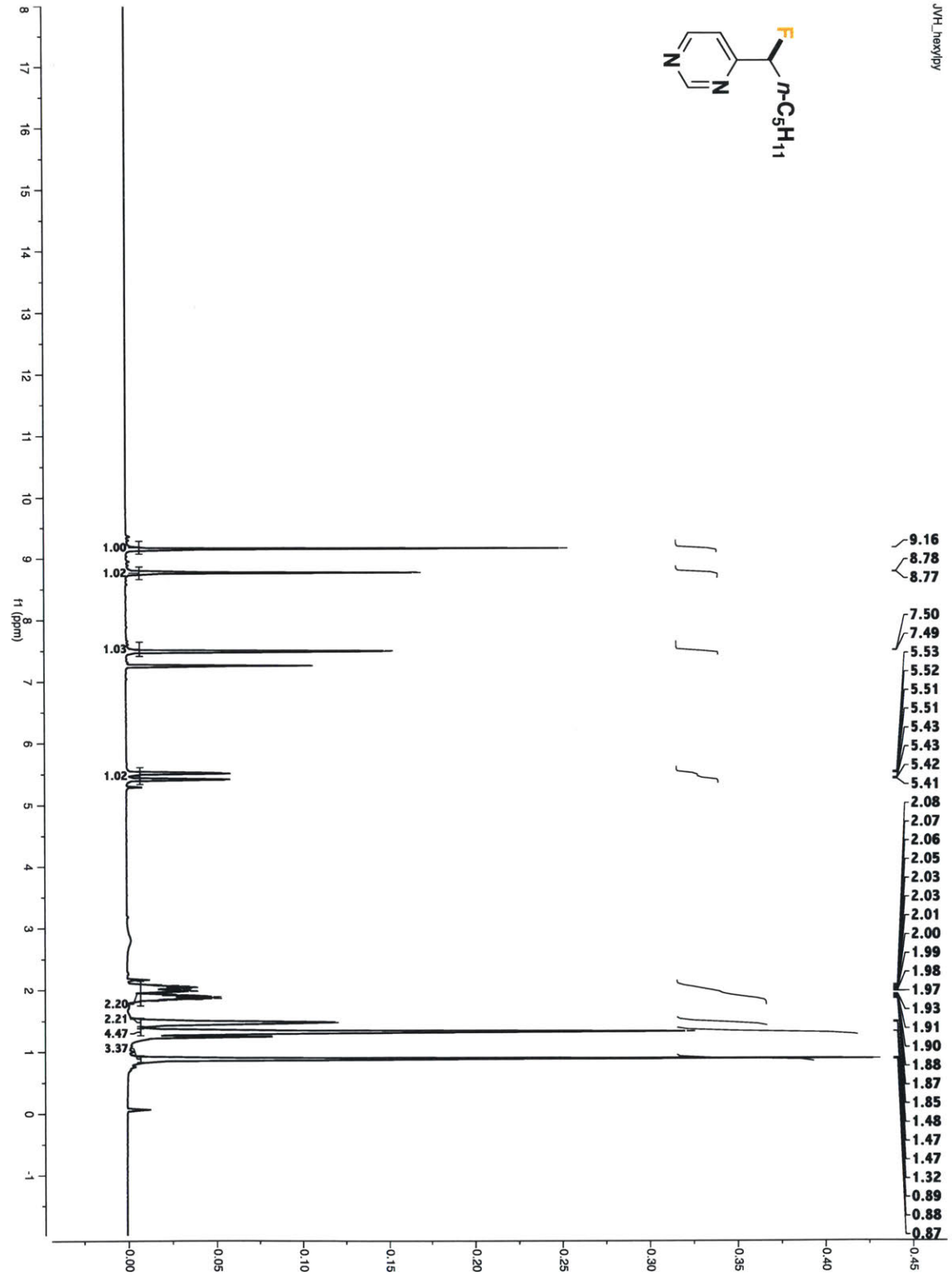

Figure S20. ^{1}H NMR spectrum of 4-(1-fluorohexyl)pyrimidine

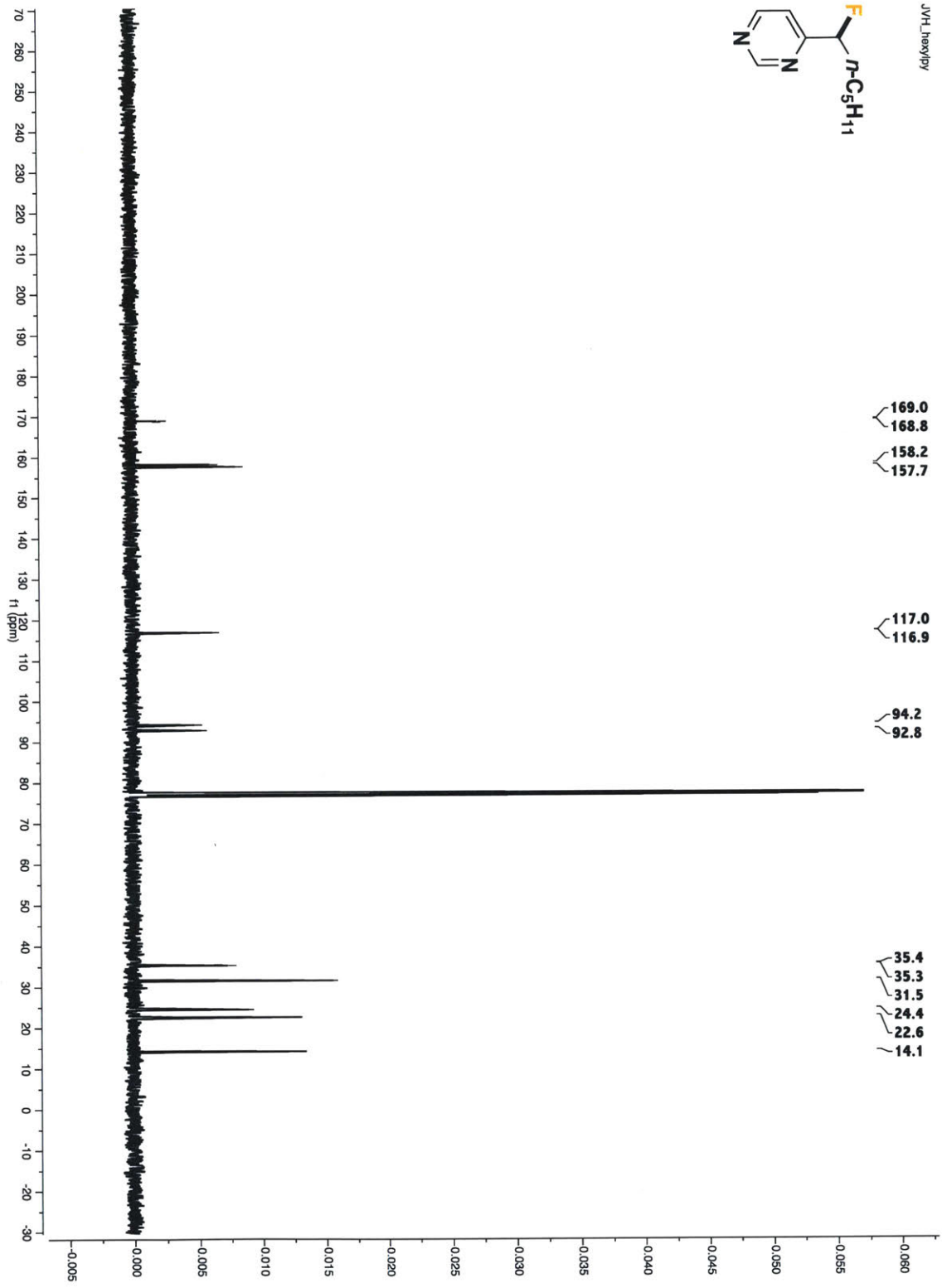

Figure S21. ^{13}C NMR spectrum of 4-(1-fluorohexyl)pyrimidine

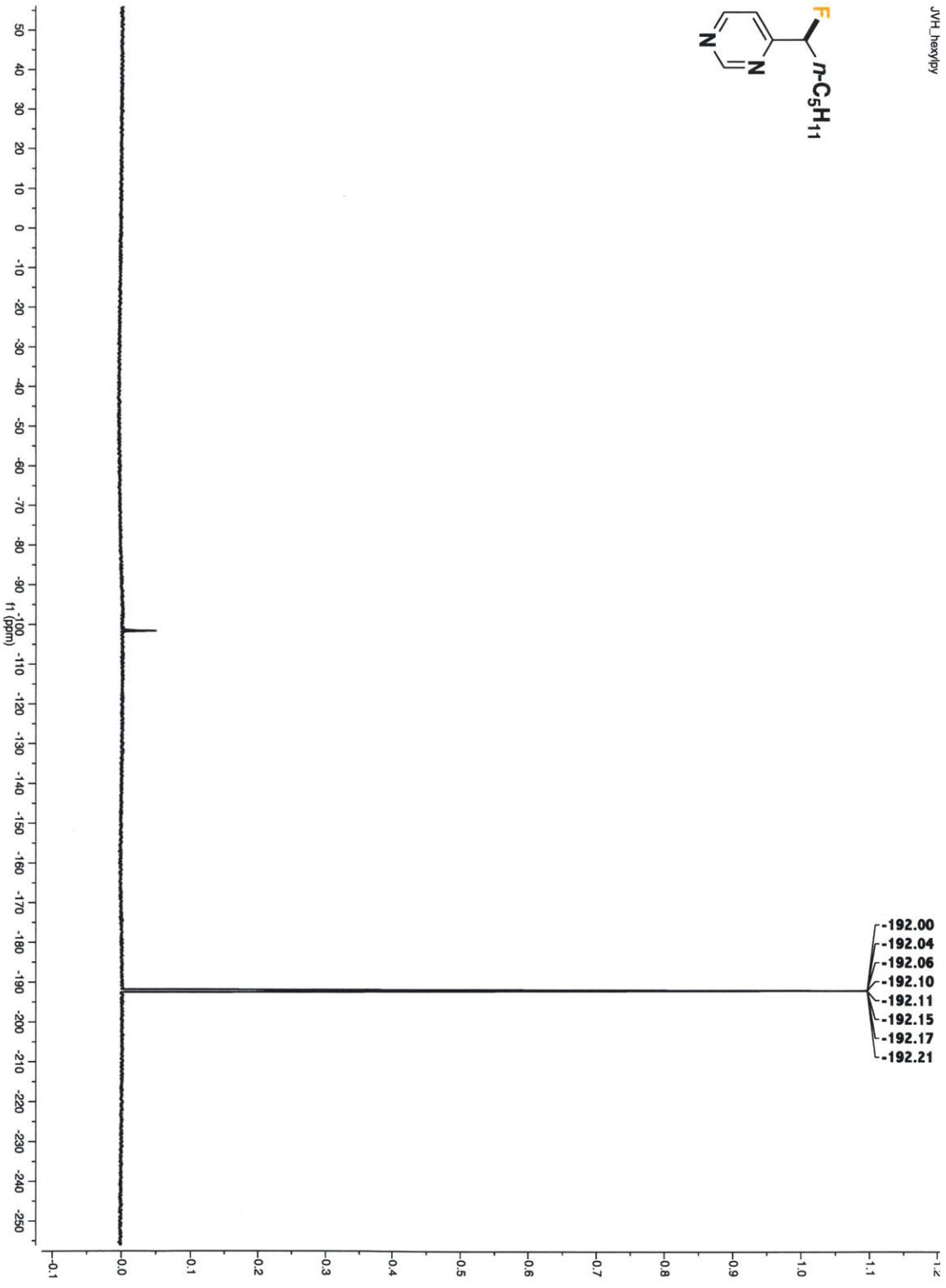

Figure S22. ^{19}F NMR spectrum of 4-(1-fluorohexyl)pyrimidine

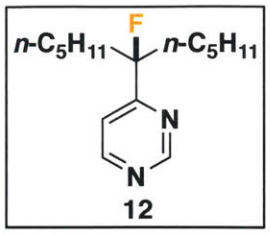

12

4-(6-fluoroundecan-6-yl)pyrimidine: 52%, clear oil. Purified via column chromatography on silica gel using 2-6% ethyl acetate/hexanes gradient elution.

^{1}H NMR (500 MHz, $CDCl_3$) δ 9.17 (s, 1H), 8.73 (d, *J* = 5.2 Hz, 1H), 7.52 (dt, *J* = 5.2 Hz, *J* = 1.5 Hz, 1H), 2.12 - 1.86 (m, 4H), 1.37 (dddd, *J* = 16.9 Hz, *J* = 8.2 Hz, *J* = 7.5 Hz, *J* = 5.0 Hz, 2H), 1.30 - 1.12 (m, 9H), 0.91 (ddd, *J* = 21.4 Hz, *J* = 10.9 Hz, *J* = 4.6 Hz, 2H), 0.86 - 0.76 (m, 7H); ^{13}C NMR (126 MHz, $CDCl_3$) δ 171.4 (d, *J* = 28.7 Hz), 158.4 (d, *J* = 2.5 Hz), 157.3, 117.7 (d, *J* = 11.3 Hz), 39.2 (d, *J* = 21.9 Hz), 32.0, 24.2, 22.7 (d, *J* = 27.5 Hz), 22.5, 14.1; ^{19}F NMR (471 MHz, $CDCl_3$) δ -168.8 (td, *J* = 31.3 Hz, *J* = 15.4 Hz). HRMS (ESI/Q-TOF) $[M + H]^+$ m/z: Calcd for ($C_{15}H_{25}FN_2$) 181.0884; Found 181.0879.

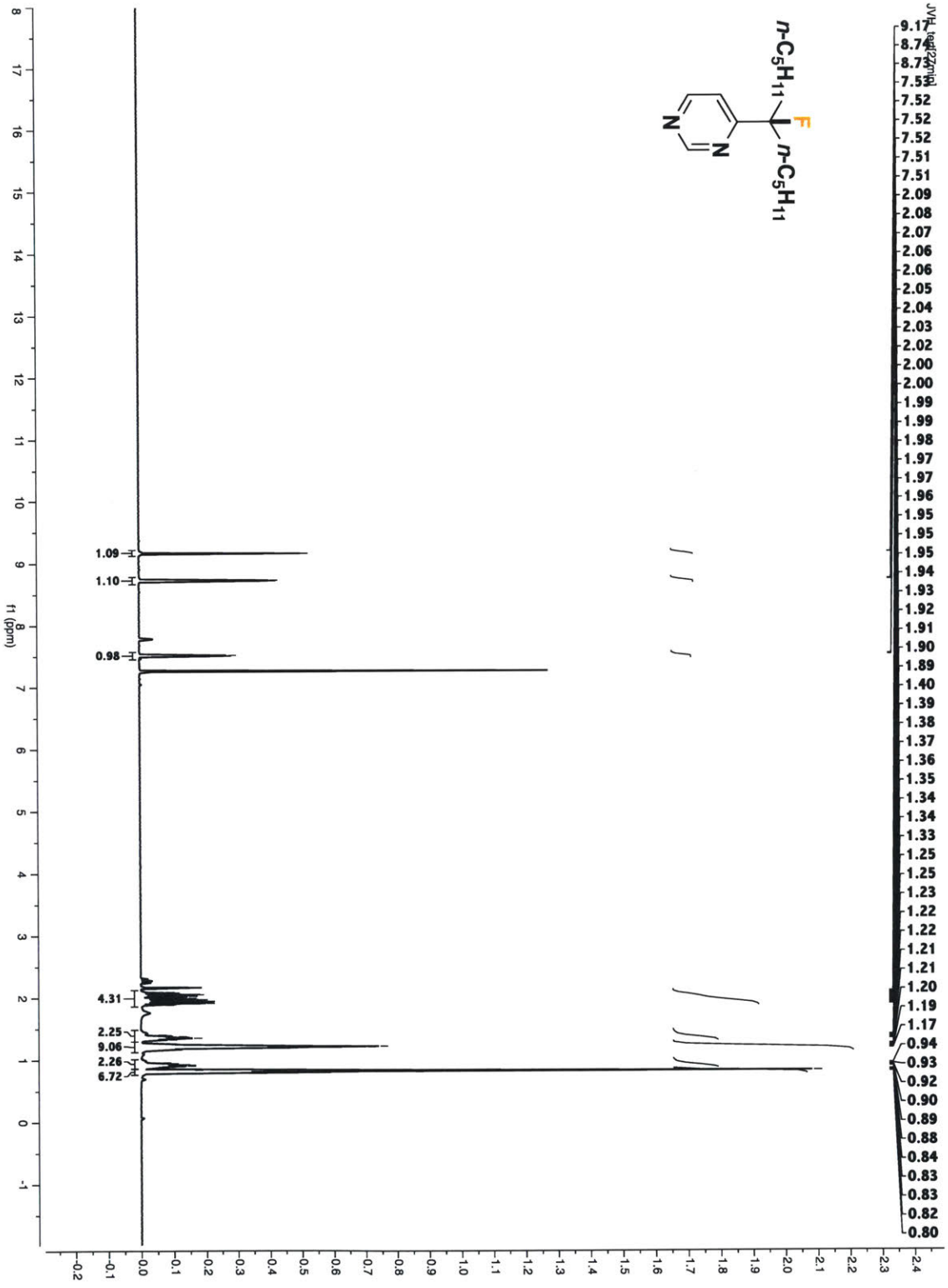

Figure S23. ^{1}H NMR spectrum of 4-(6-fluoroundecan-6-yl)pyrimidine

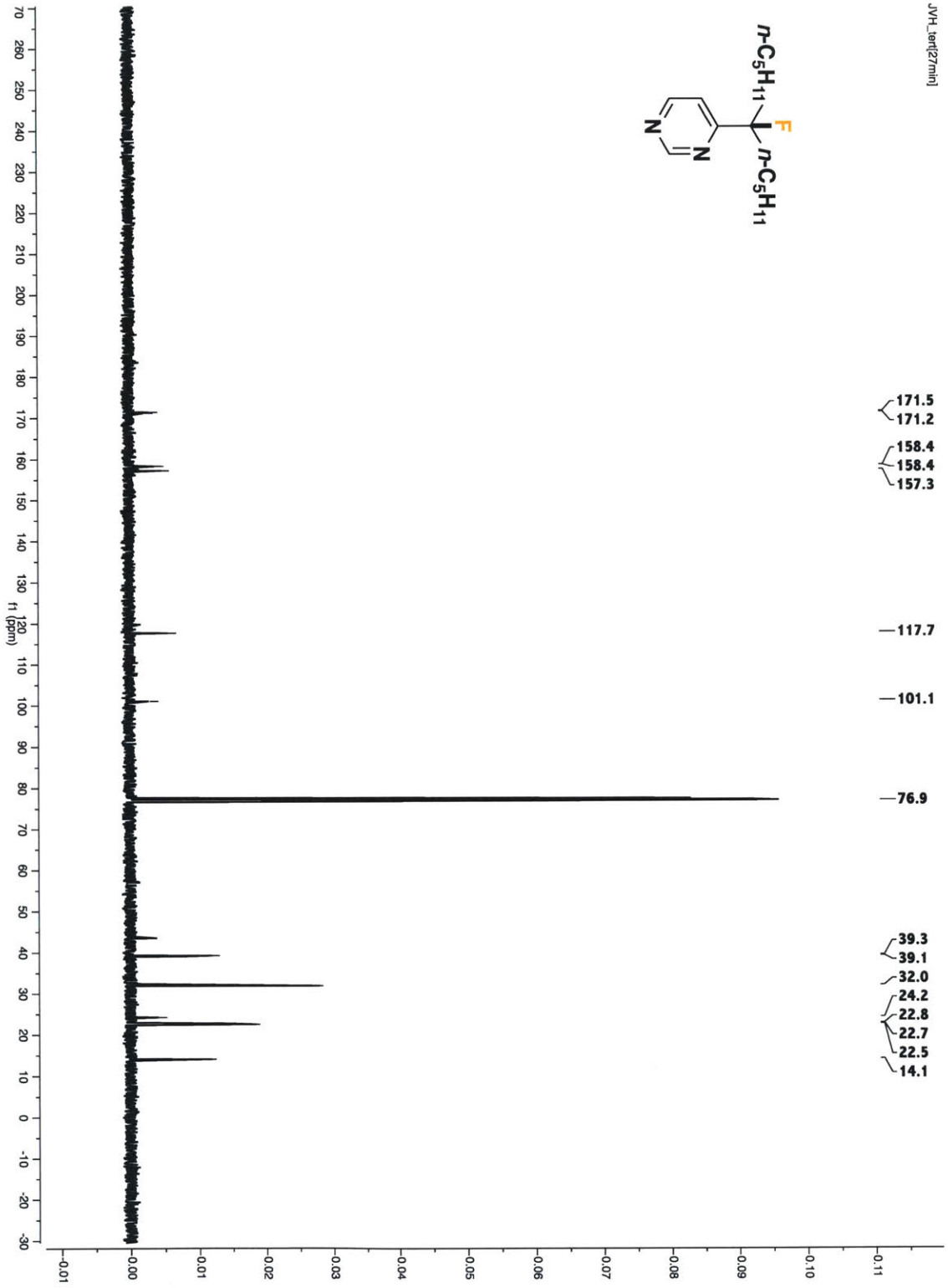

Figure S24. ^{13}C NMR spectrum of 4-(6-fluoroundecan-6-yl)pyrimidine

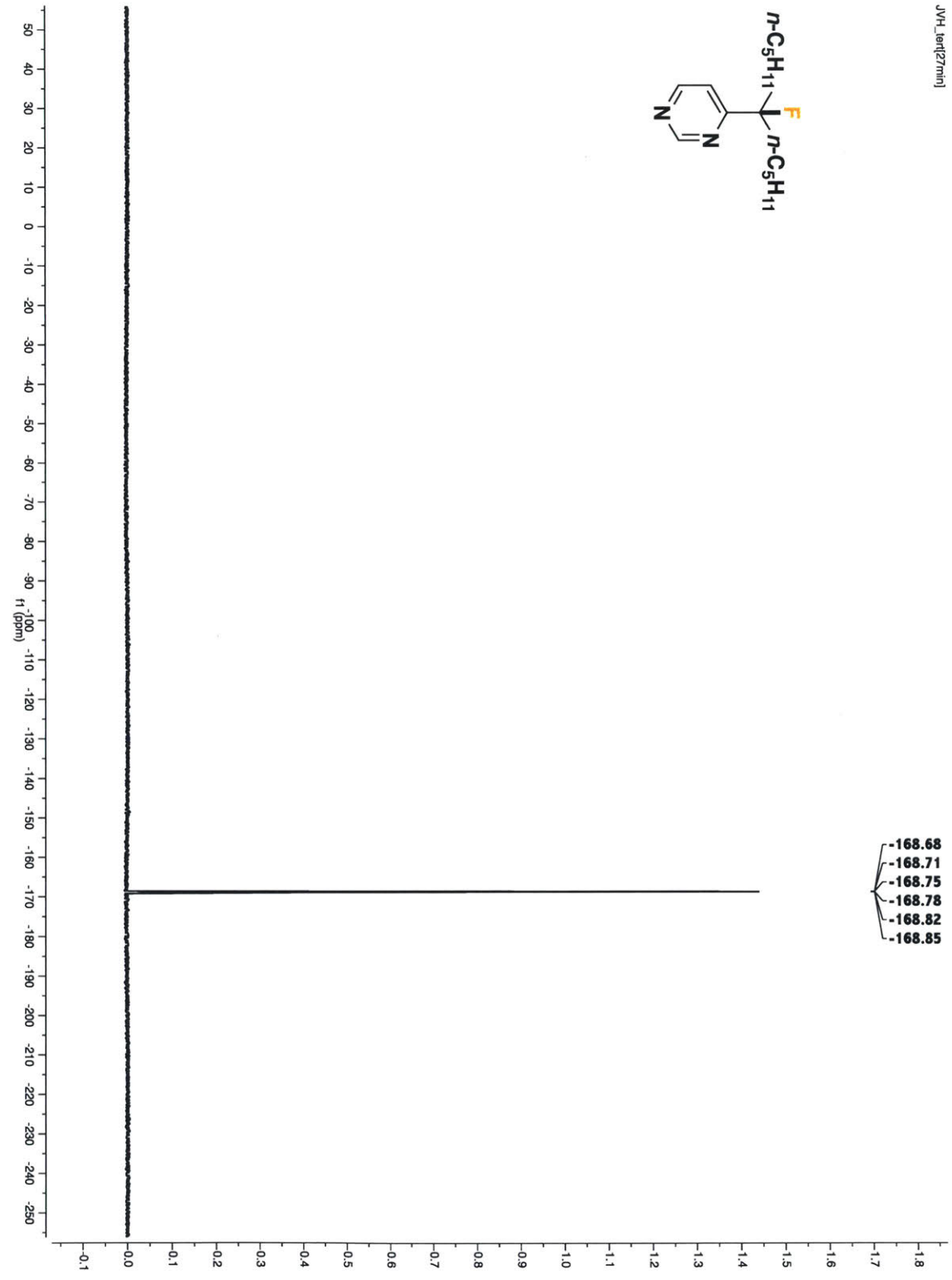

Figure S25. ^{19}F NMR spectrum of 4-(6-fluoroundecan-6-yl)pyrimidine

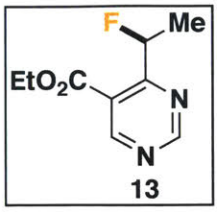

13

Ethyl 4-(1-fluoroethyl)pyridine-5-carboxylate: 67%, pale yellow oil. Purified via column chromatography on silica gel using 10-15% ethyl acetate/hexanes gradient elution.

^{1}H NMR (500 MHz, $CDCl_3$) δ 9.36 (s, 1H), 9.19 (s, 1H), 6.35 (dqd, J = 48.4 Hz, J = 6.5 Hz, J = 1.5 Hz, 1H), 4.44 (q, J = 7.2 Hz, 2H), 1.73 (dd, J = 24.0 Hz, J = 6.4 Hz, 4H), 1.43 (t, J = 7.2 Hz, 3H); ^{13}C NMR (126 MHz, $CDCl_3$) δ 167.1, 163.2, 159.7, 158.0, 121.3, 86.5 (d, J = 173.2 Hz), 61.5, 19.7 (d, J = 23.3 Hz), 13.3; ^{19}F NMR (471 MHz, $CDCl_3$) δ 180.4 (dq, J = 47.8 Hz, J = 24.6 Hz); HRMS (ESI/Q-TOF) $[M + H]^+$ m/z: Calcd for ($C_9H_{11}FN_2O_2$) 199.0877; Found 199.0879.

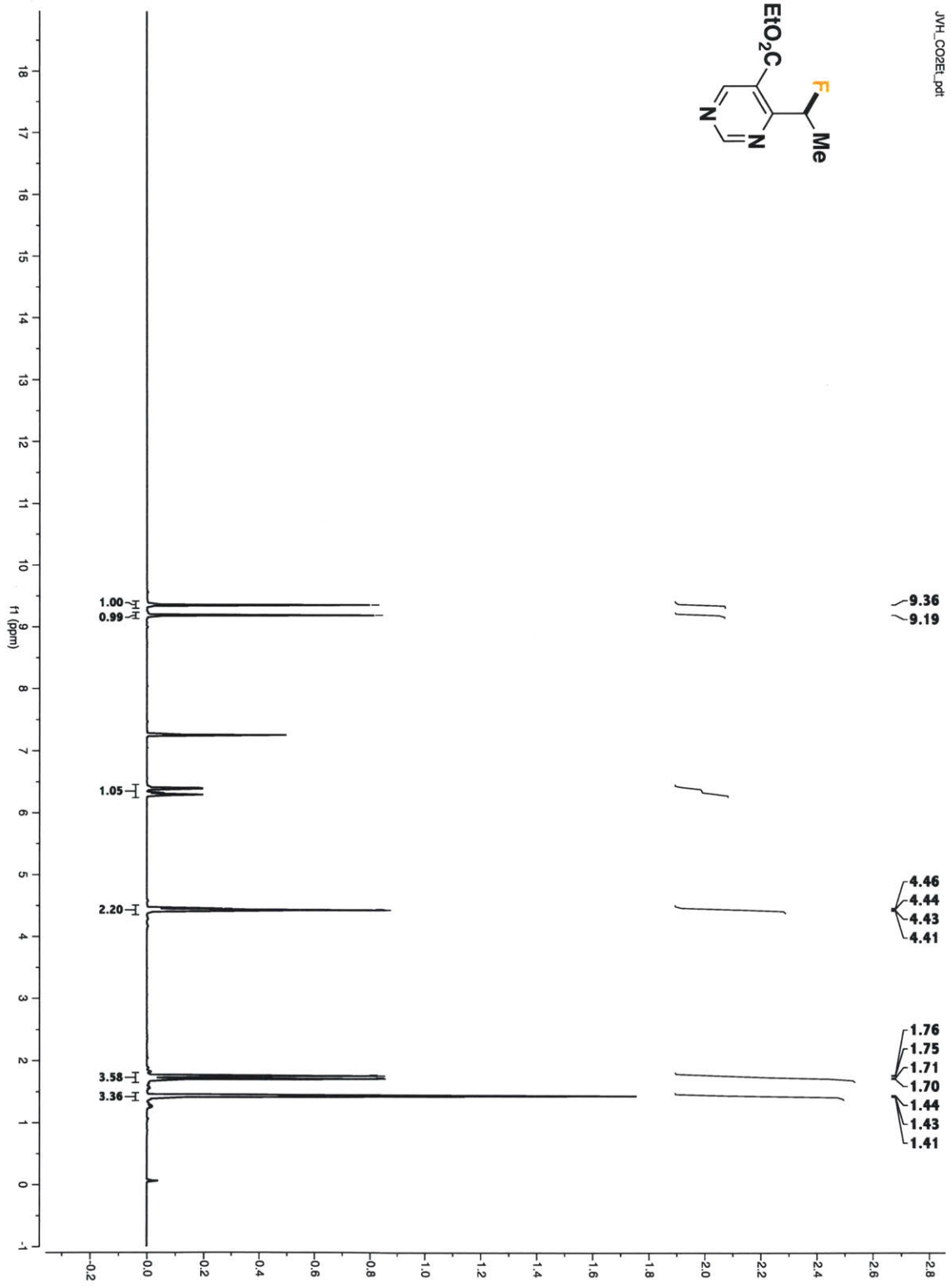

Figure S26. ^{1}H NMR spectrum of ethyl 4-(1-fluoroethyl)pyridine-5-carboxylate

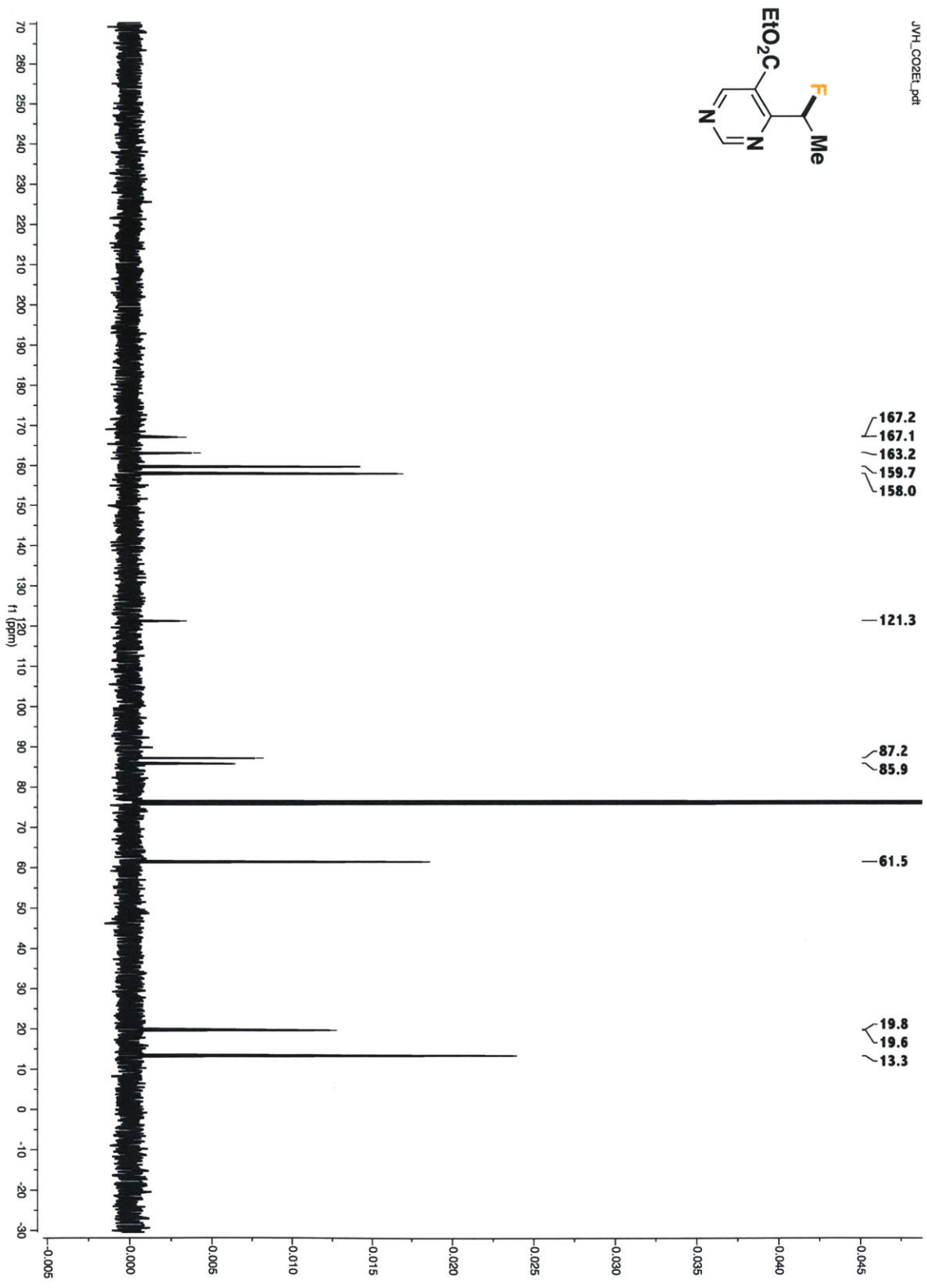

Figure S27. ^{13}C NMR spectrum of ethyl 4-(1-fluoroethyl)pyridine-5-carboxylate

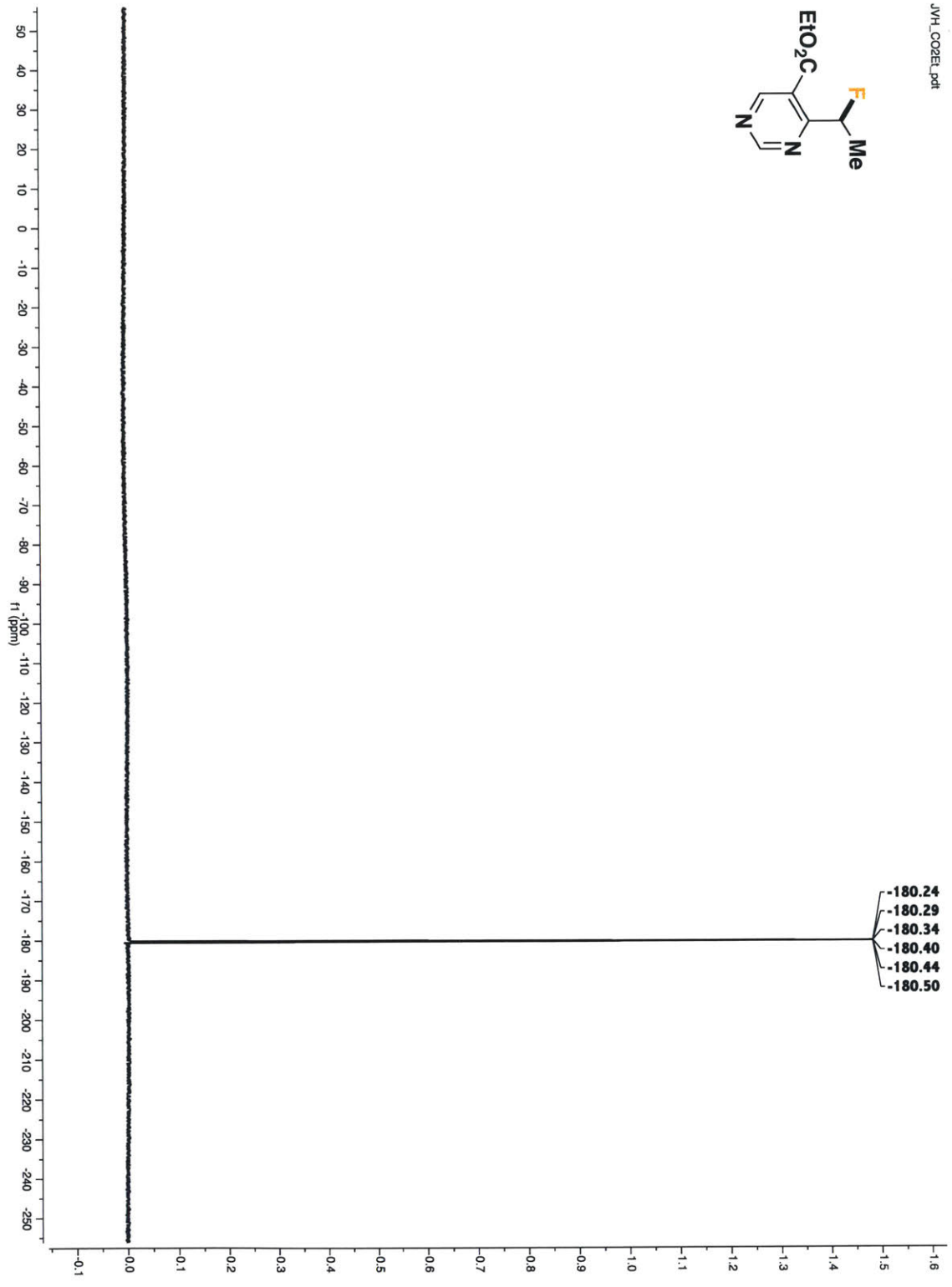

Figure S28. ^{19}F NMR spectrum of ethyl 4-(1-fluoroethyl)pyridine-5-carboxylate

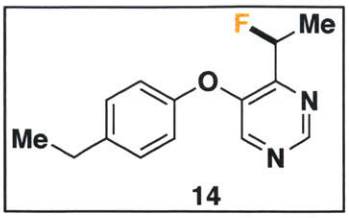

14

5-(4-ethylphenoxy)-4-(1-fluoroethyl)pyrimidine: 78% yield (on 0.2 mmol scale), clear oil. Purified via column chromatography on silica gel using 2 – 10% ethyl acetate/dichloromethane gradient elution.

^{1}H NMR (500 MHz, $CDCl_3$) δ 8.99 (s, 1H), 8.28 (s, 2H), 7.23 (d, *J* = 8.4 Hz, 2H), 6.97 – 6.92 (m, 3H), 6.05 (dq, *J* = 47.3 Hz, *J* = 6.5 Hz, 1H), 2.66 (q, *J* = 7.6 Hz, 2H), 1.75 (dd, *J* = 24.1 Hz, *J* = 6.5 Hz, 3H), 1.25 (t, *J* = 7.6 Hz, 3H); ^{13}C NMR (126 MHz, $CDCl_3$) δ 157.2, 153.3, 153.1, 149.5, 146.6, 141.4, 129.8, 119.0, 85.4 (d, *J* = 173.3 Hz), 28.3, 19.7, 15.8. ^{19}F NMR (471 MHz, $CDCl_3$) δ -180.8 (dq, *J* = 47.1 Hz, *J* = 18.8 Hz). HRMS (ESI/Q-TOF) [M + H]$^+$ m/z: Calcd for ($C_{14}H_{15}FN_2O$) 247.1241; Found 247.1237.

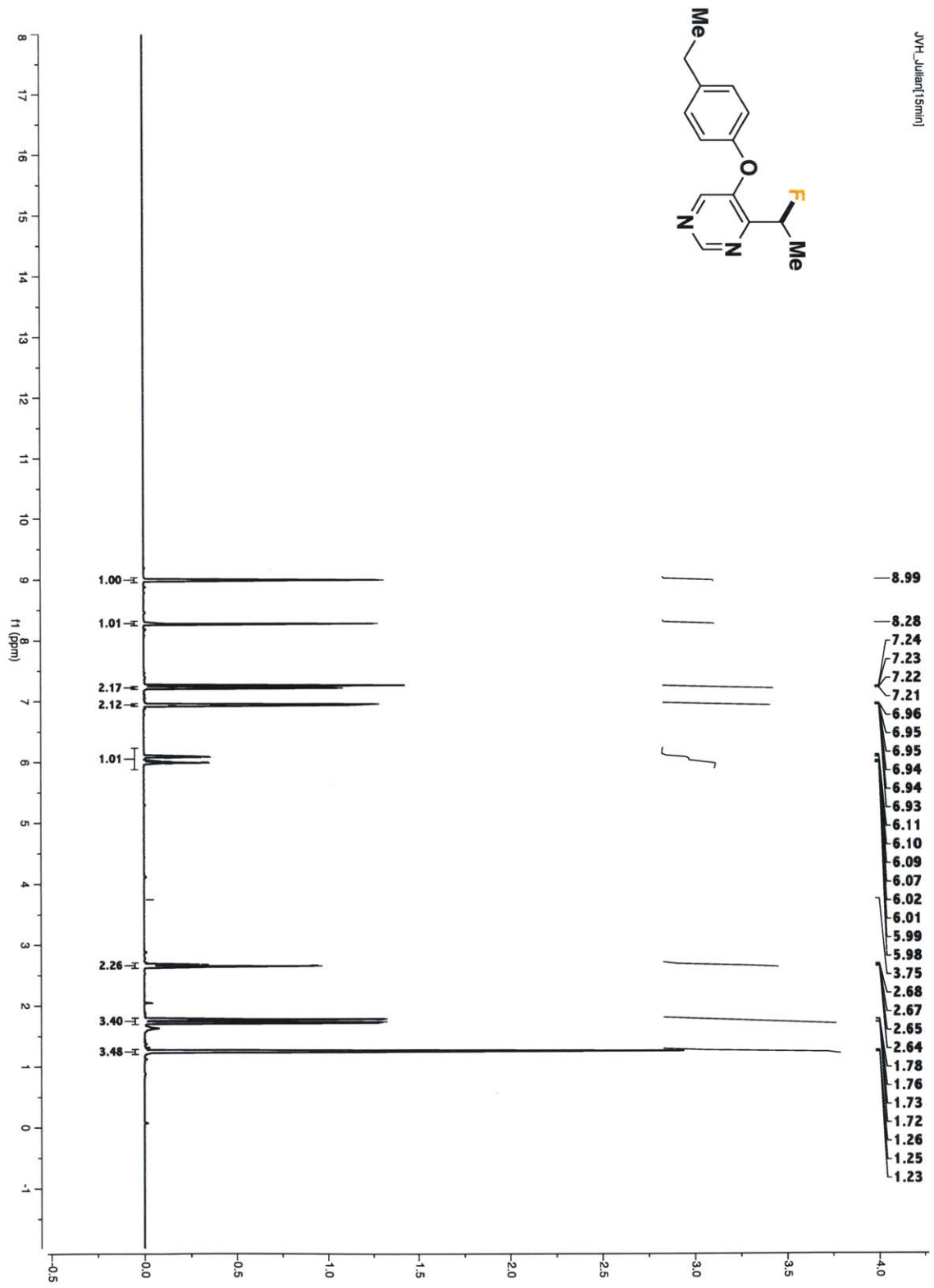

Figure S29. ^{1}H NMR spectrum of 5-(4-ethylphenoxy)-4-(1-fluoroethyl)pyrimidine

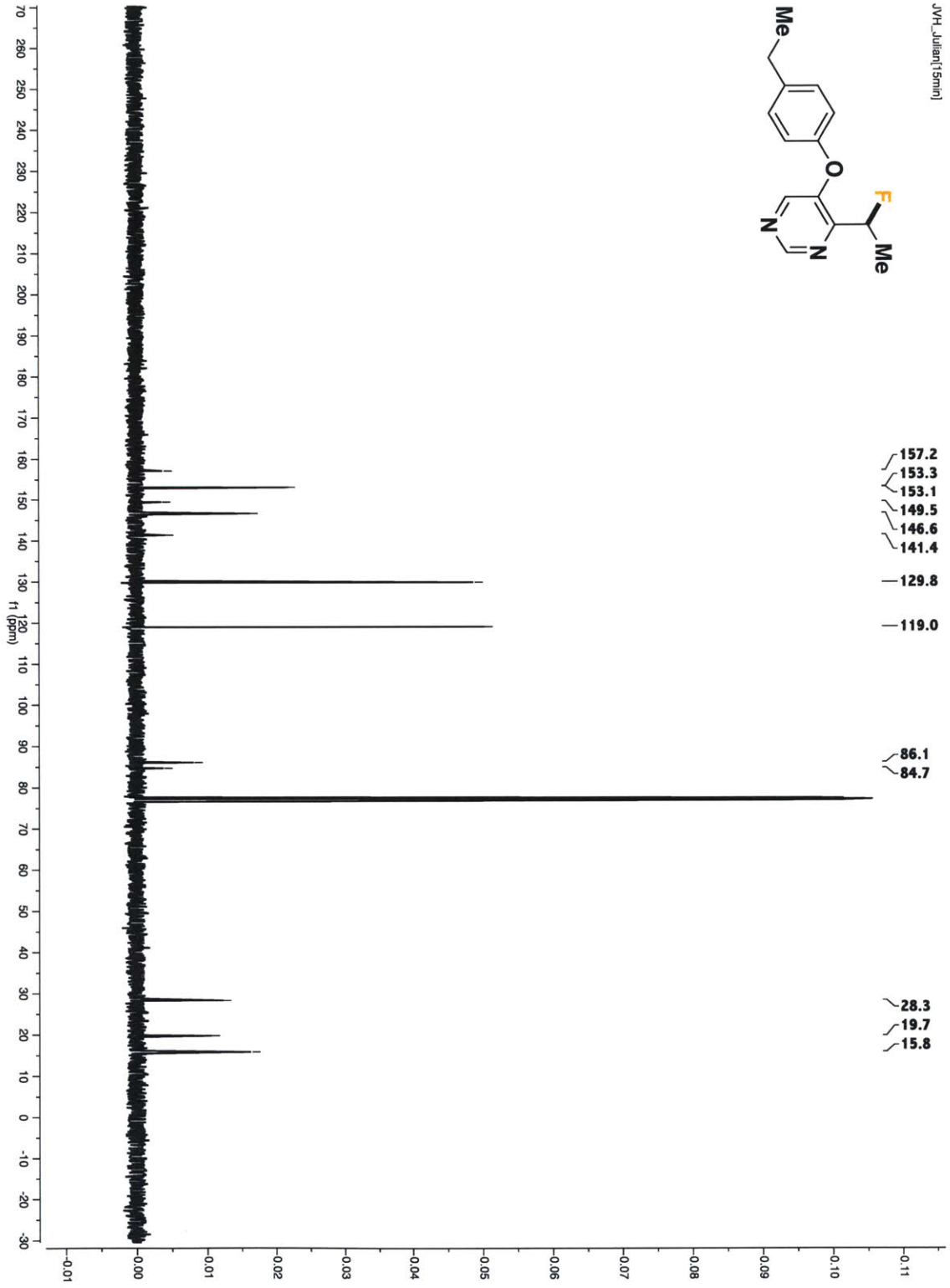

Figure S30. ^{13}C NMR spectrum of 5-(4-ethylphenoxy)-4-(1-fluoroethyl)pyrimidine

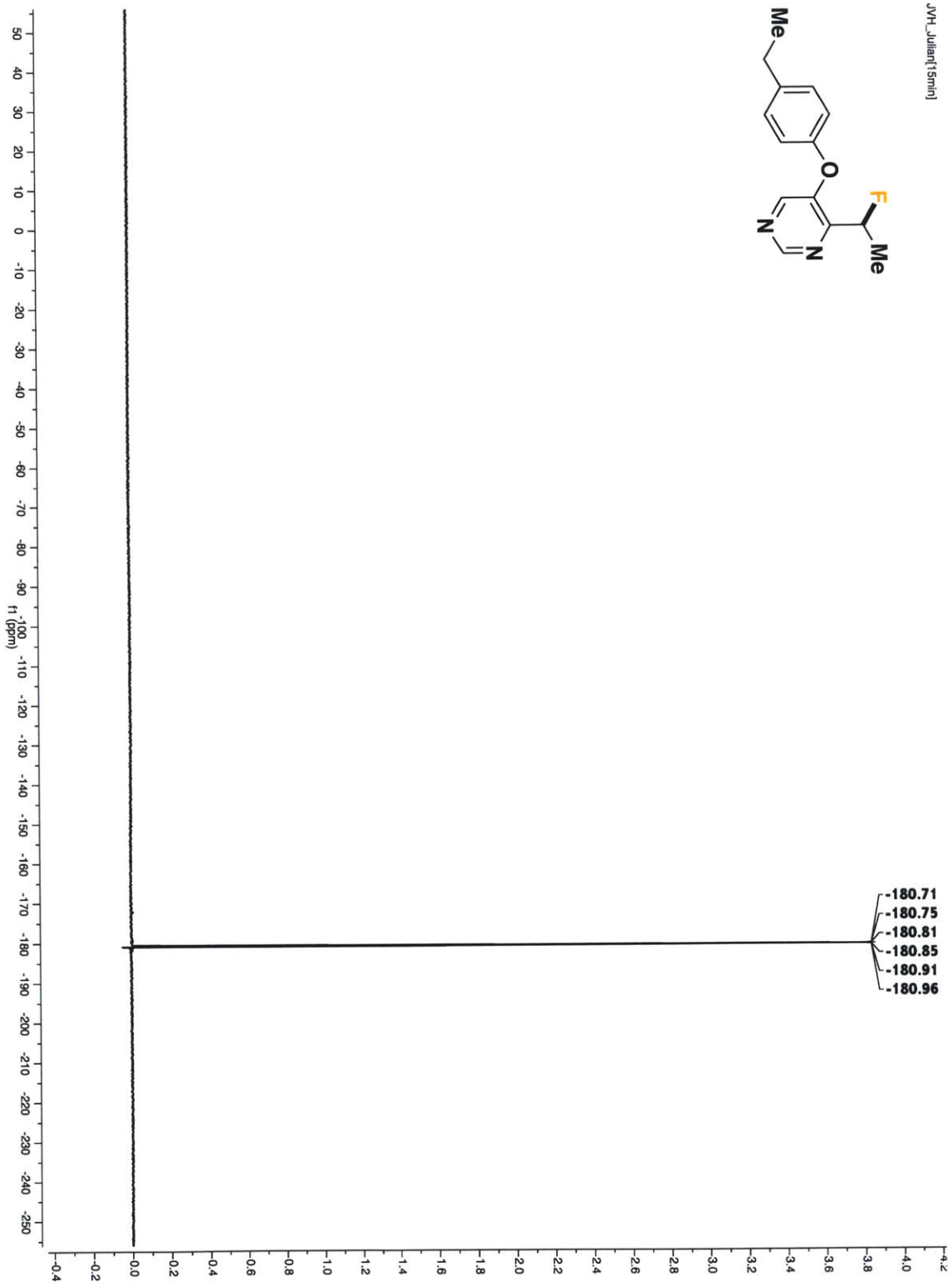

Figure S31. ^{19}F NMR spectrum of 5-(4-ethylphenoxy)-4-(1-fluoroethyl)pyrimidine

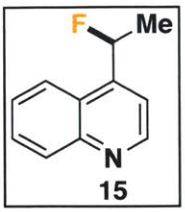

15

4-(1-fluoroethyl)quinoline: 56%, yellow oil. Purified via column chromatography on silica gel using 2-10% ethyl acetate/dichloromethane gradient elution.

^{1}H NMR (500 MHz, $CDCl_3$) δ 8.94 (d, *J* = 4.3 Hz, 1H), 8.16 (d, *J* = 8.4 Hz, 1H), 7.89 (d, *J* = 8.4 Hz, 1H), 7.73 (t, *J* = 7.6 Hz, 1H), 7.58 (t, *J* = 7.6 Hz, 1H), 7.51 (d, *J* = 4.3 Hz, 1H), 6.32 (dq, *J* = 46.9 Hz, *J* = 6.4 Hz, 1H), 1.80 (dd, *J* = 24.2 Hz, *J* = 6.5 Hz, 3H); ^{13}C NMR (126 MHz, $CDCl_3$): δ 150.5, 148.3, 146.8 (d, *J* = 19.4 Hz), 130.6, 129.4, 127.0, 124.7 (d, *J* = 4.7 Hz), 122.9, 116.6 (d, *J* = 11.0 Hz), 87.7 (d, *J* = 171.1 Hz), 22.7 (d, *J* = 24.6 Hz); ^{19}F NMR (471 MHz, $CDCl_3$): δ -176.7 (dq, *J* = 48.1 Hz, *J* = 24.2 Hz); HRMS (ESI/Q-TOF) [M + H]$^{+}$ m/z: Calcd for ($C_{11}H_{10}FN_2$) 176.0870; Found 176.0868.

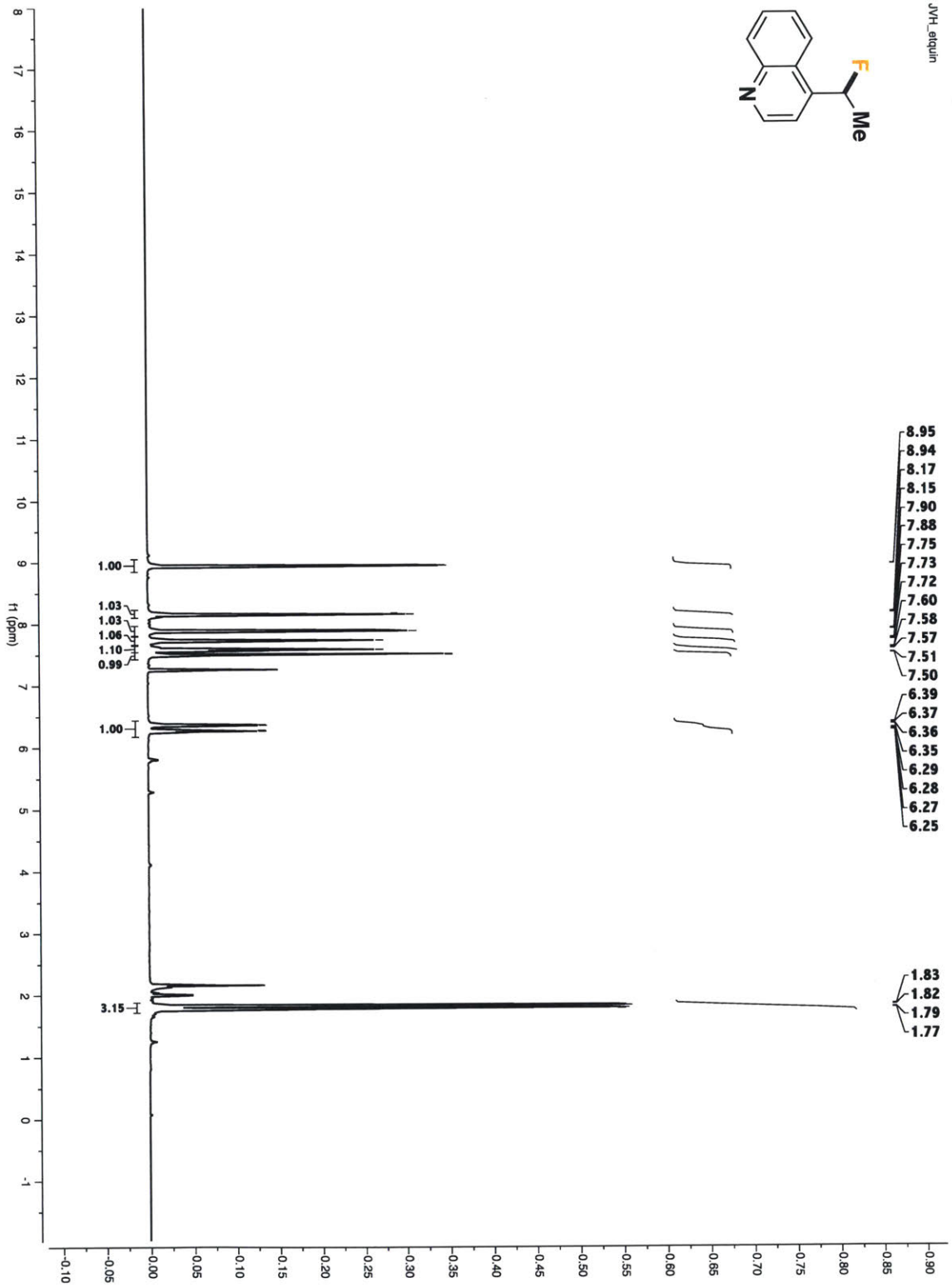

Figure S32. ^{1}H NMR spectrum of 4-(1-fluoroethyl)quinoline

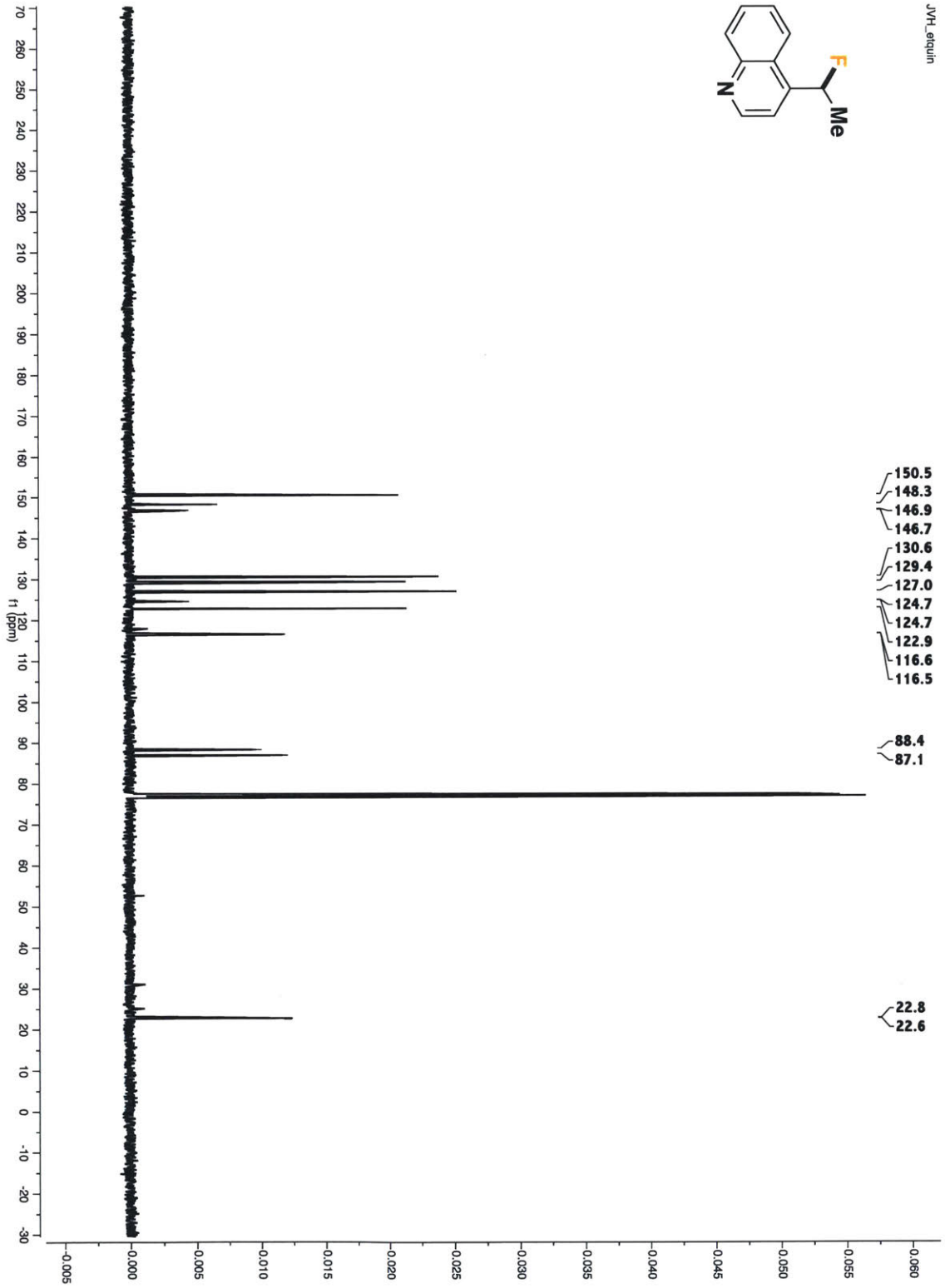

Figure S33. ^{13}C NMR spectrum of 4-(1-fluoroethyl)quinoline

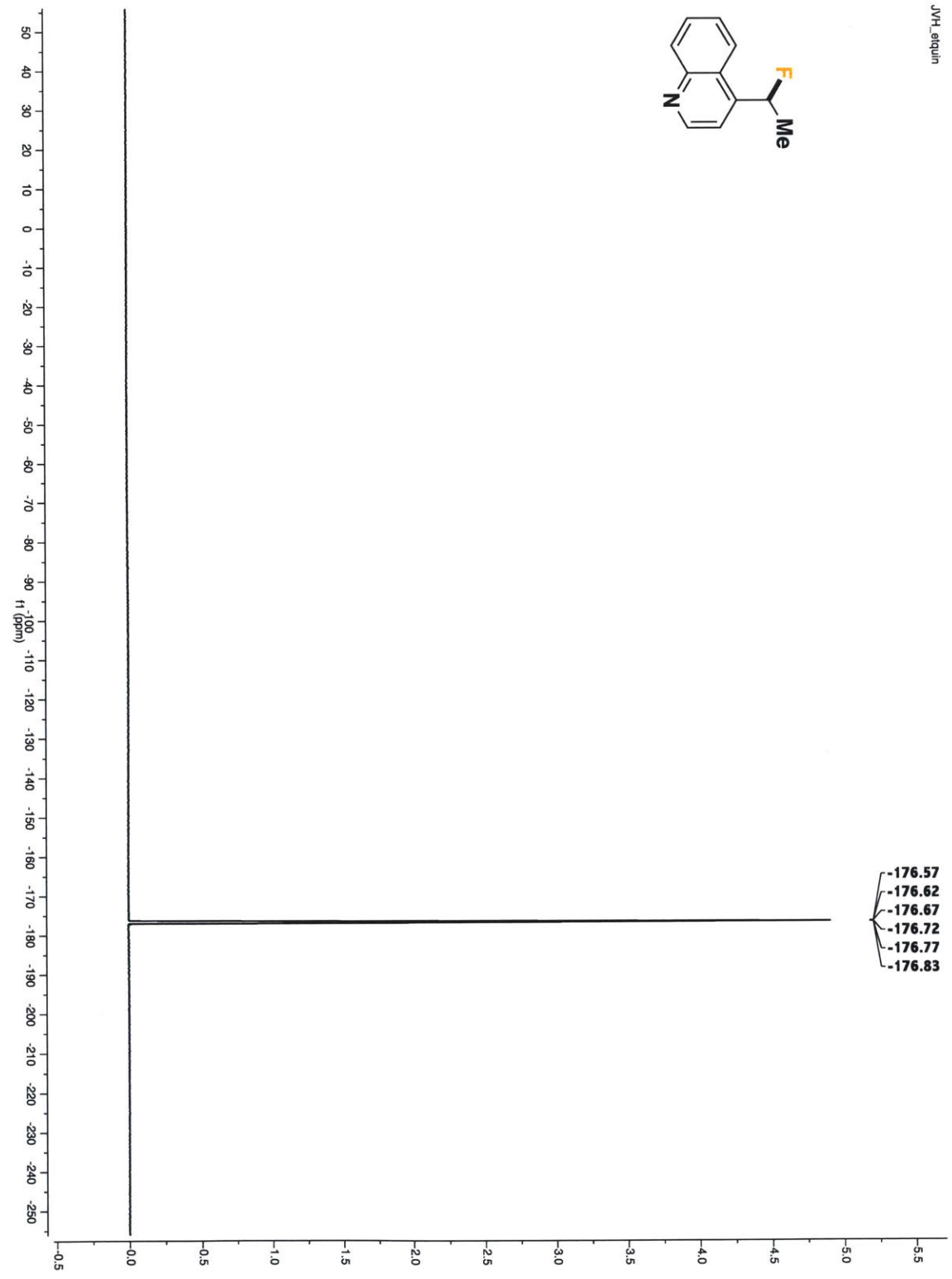

Figure S34. ^{19}F NMR spectrum of 4-(1-fluoroethyl)quinoline

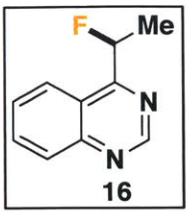

16

4-(1-fluoroethyl)quinazoline: 44%, yellow oil.. Purified via column chromatography on silica gel using 20% ethyl acetate/hexanes.

^{1}H NMR (500 MHz, $CDCl_3$) δ 9.31 (s, 1H), 8.35 (d, *J* = 8.5 Hz, 1H), 8.10 (d, *J* = 8.5 Hz, 1H), 7.94 (t, *J* = 7.1 Hz, 1H), 7.68 (t, *J* = 7.7 Hz, 1H), 6.24 (dq, *J* = 47.8 Hz, *J* = 6.6 Hz, 1H), 1.90 (dd, *J* = 24.2, *J* = 6.6 Hz, 3H); ^{13}C NMR (126 MHz, $CDCl_3$) δ 167.1 (d, *J* = 20.2 Hz), 154.3, 151.04, 134.1, 129.5, 128.1, 122.3, 90.9 (d, *J* = 173.0 Hz), 20.7 (d, *J* = 23.1 Hz); ^{19}F NMR (471 MHz, $CDCl_3$) δ -174.4 (dq, *J* = 48.1 Hz, *J* = 24.3 Hz). HRMS (ESI/Q-TOF) [M + H]$^{+}$ m/z: Calcd for ($C_8H_9FN_2$) 177.0823; Found 177.0818.

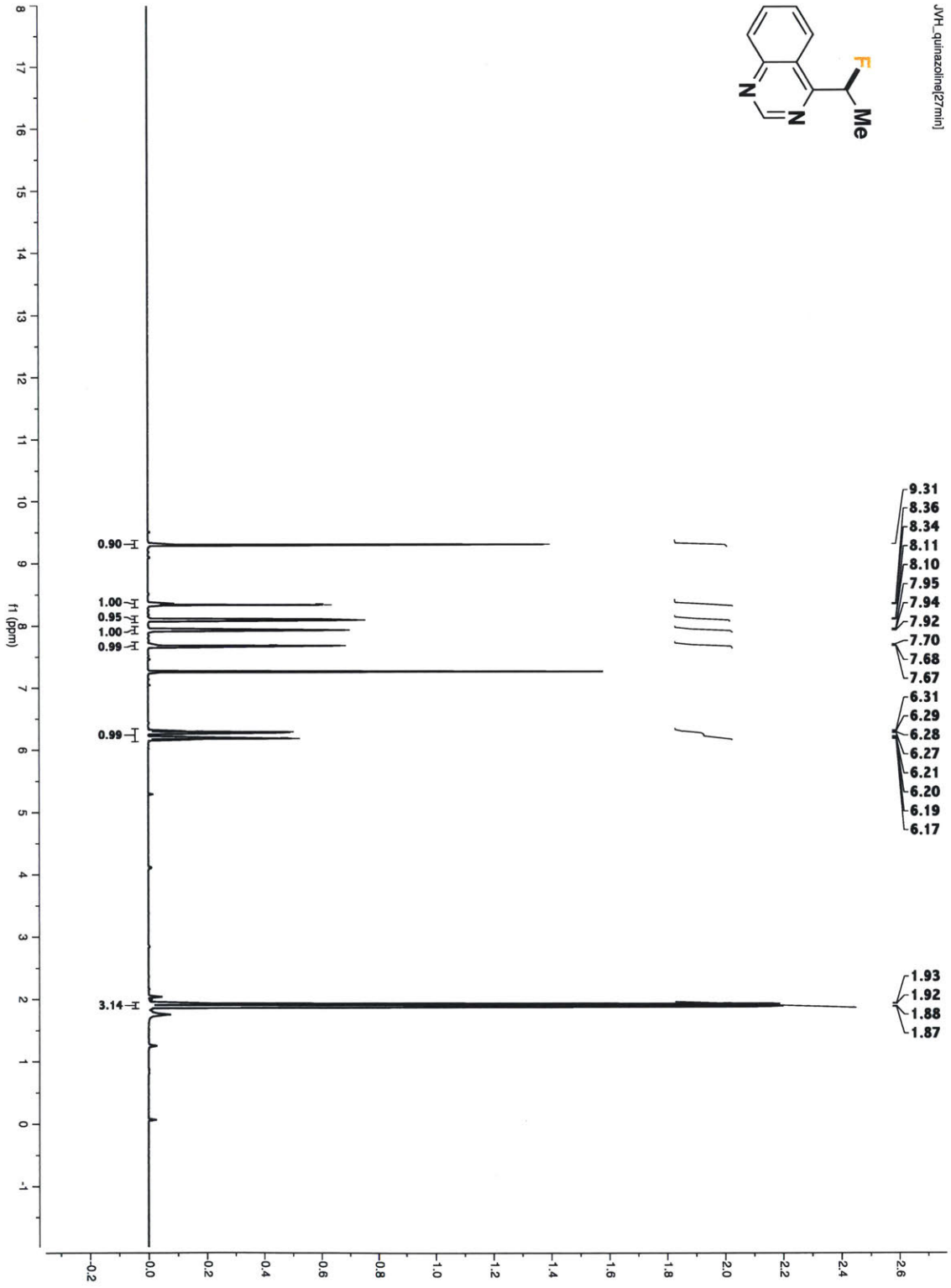

Figure S35. ^{1}H NMR spectrum of 4-(1-fluoroethyl)quinazoline

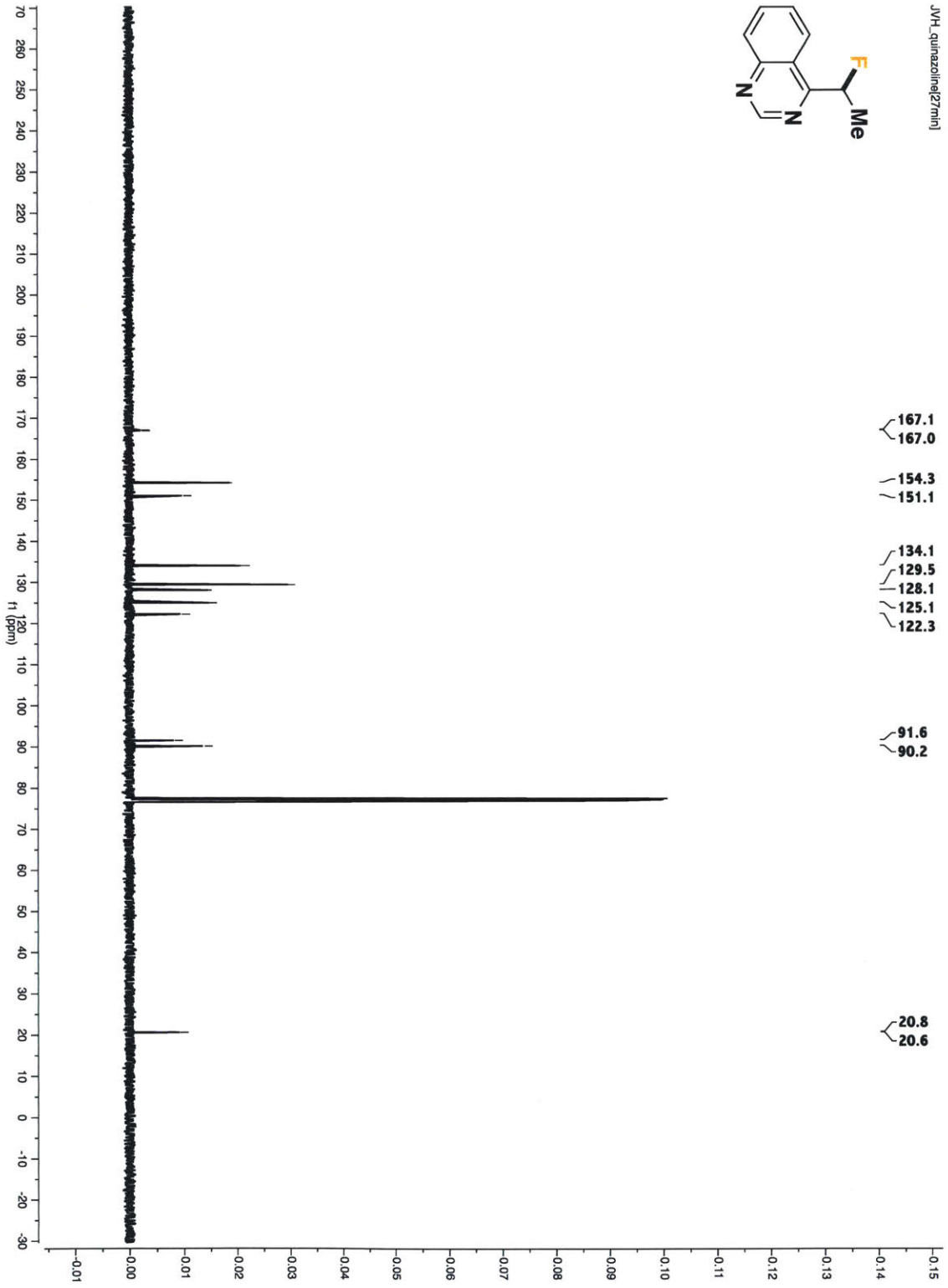

Figure S36. ^{13}C NMR spectrum of 4-(1-fluoroethyl)quinazoline

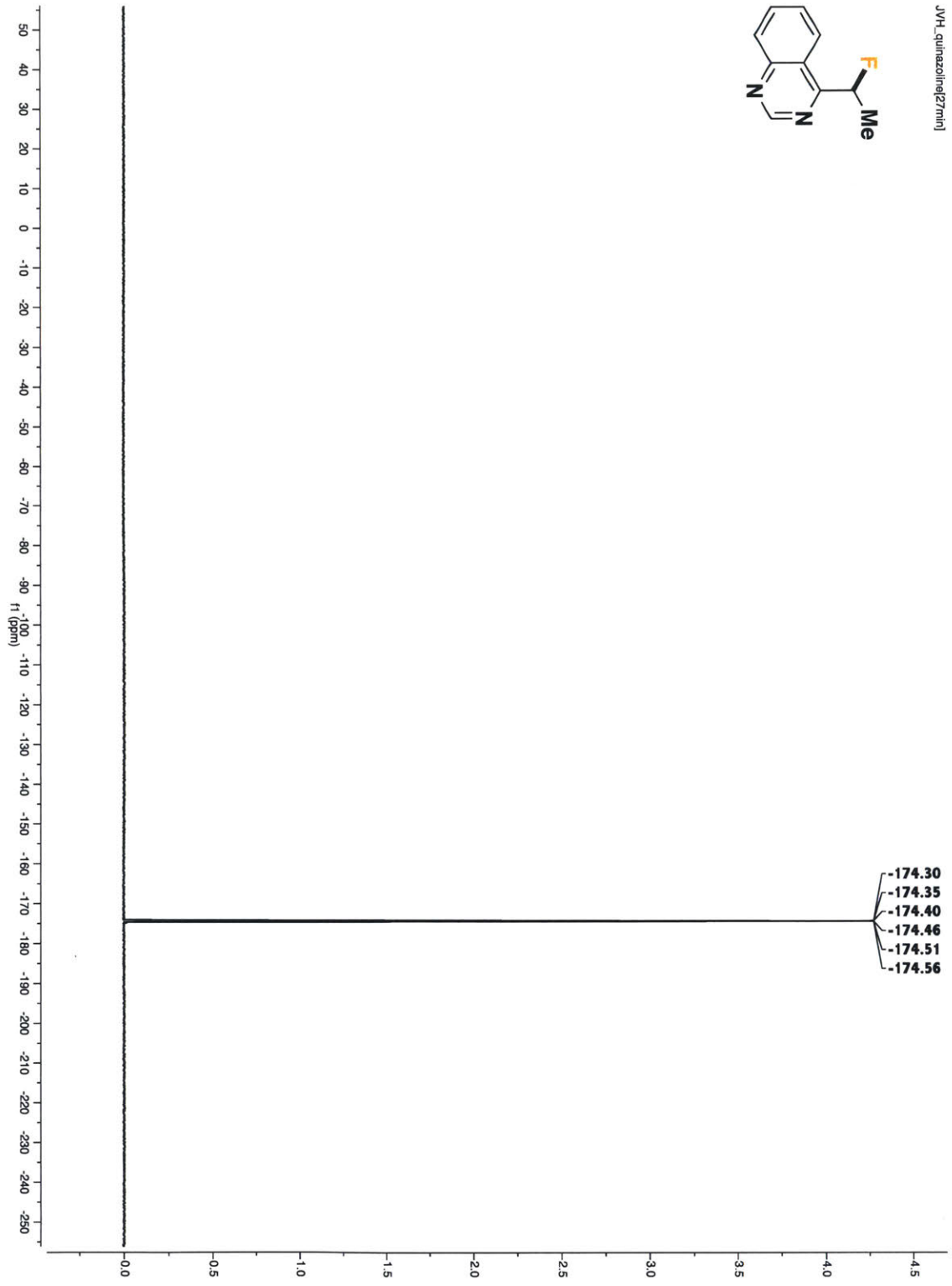

Figure S37. ^{19}F NMR spectrum of 4-(1-fluoroethyl)quinazoline

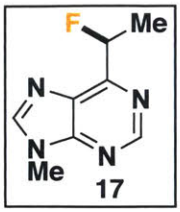

9-methyl-6-(1-fluoroethyl)-9*H*-purine: 49%, white solid. Purified via column chromatography on silica gel using 1 – 2% methanol/dichloromethane gradient elution. ^{1}H NMR (500 MHz, $CDCl_3$) δ 8.96 (s, 1H), 8.09 (s, 1H), 6.18 (dd, J = 47.6 Hz, J = 6.6 Hz, 1H), 1.84 (dd, J = 24.3 Hz, J = 6.6 Hz, 3H); ^{13}C NMR (126 MHz, $CDCl_3$) δ 158.3 (d, J = 20.1 Hz), 152.5, 145.6, 130.5, 88.3 (d, J = 173.3 Hz), 30.0, 20.6 (d, J = 24.6 Hz); ^{19}F NMR (471 MHz, $CDCl_3$) δ -180.0 (dq, J = 49.7, J = 24.0 Hz); HRMS (ESI/Q-TOF) $[M + H]^+$ m/z: Calcd for ($C_8H_9FN_4$) 181.0882; Found 181.0879.

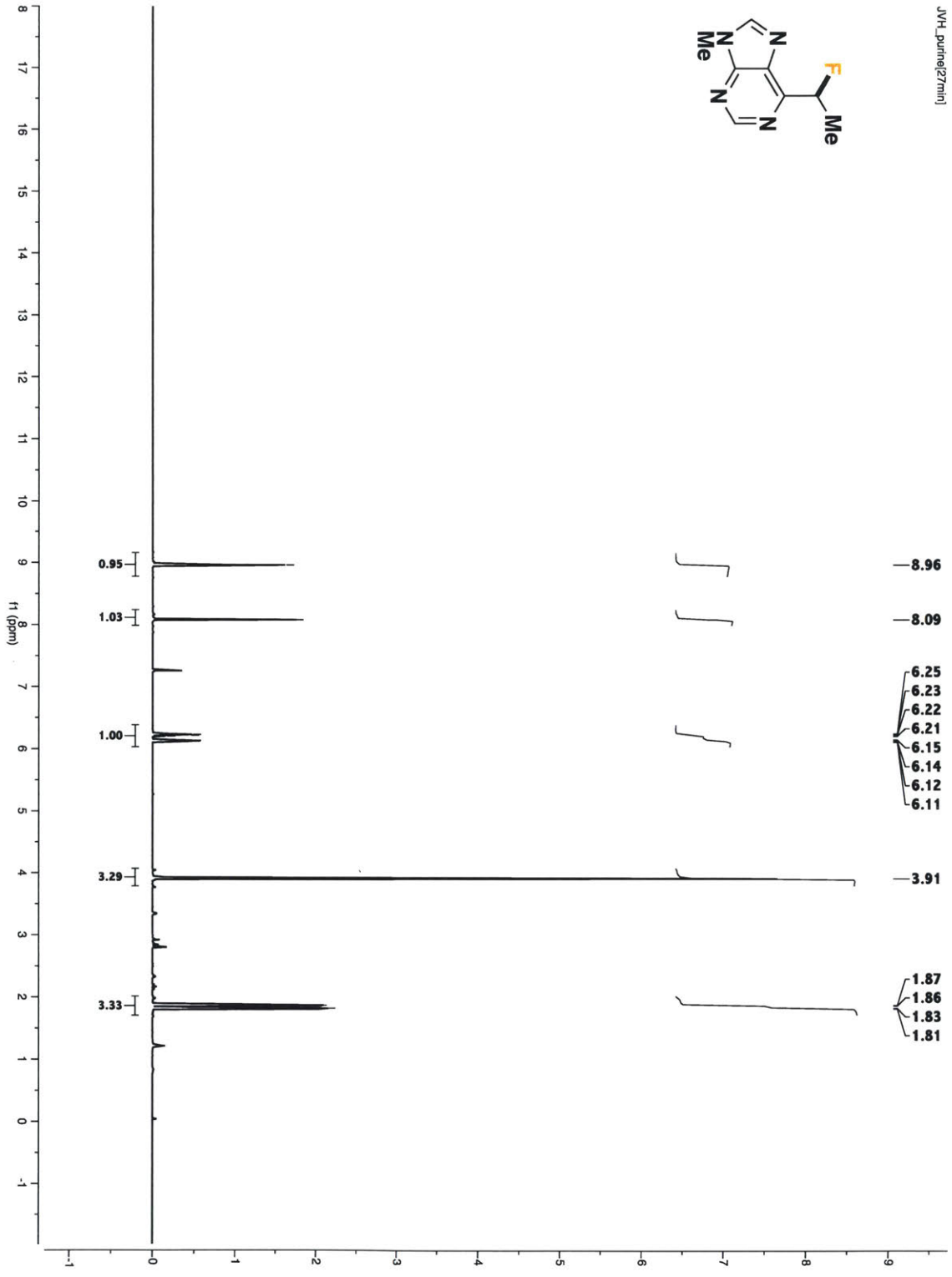

Figure S38. ^{1}H NMR spectrum of 9-methyl-6-(1-fluoroethyl)-9*H*-purine

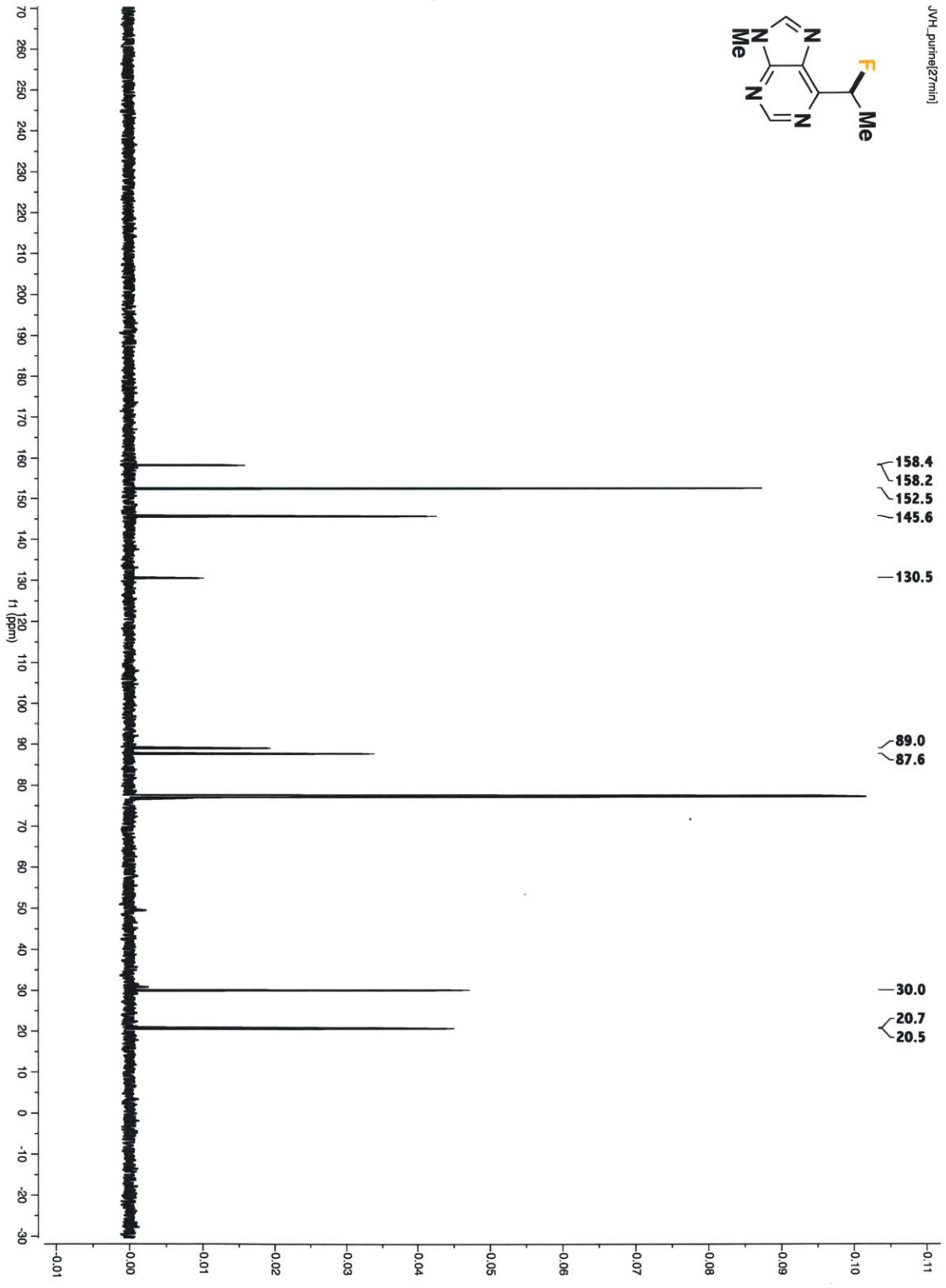

Figure S39. ^{13}C NMR spectrum of 9-methyl-6-(1-fluoroethyl)-9*H*-purine

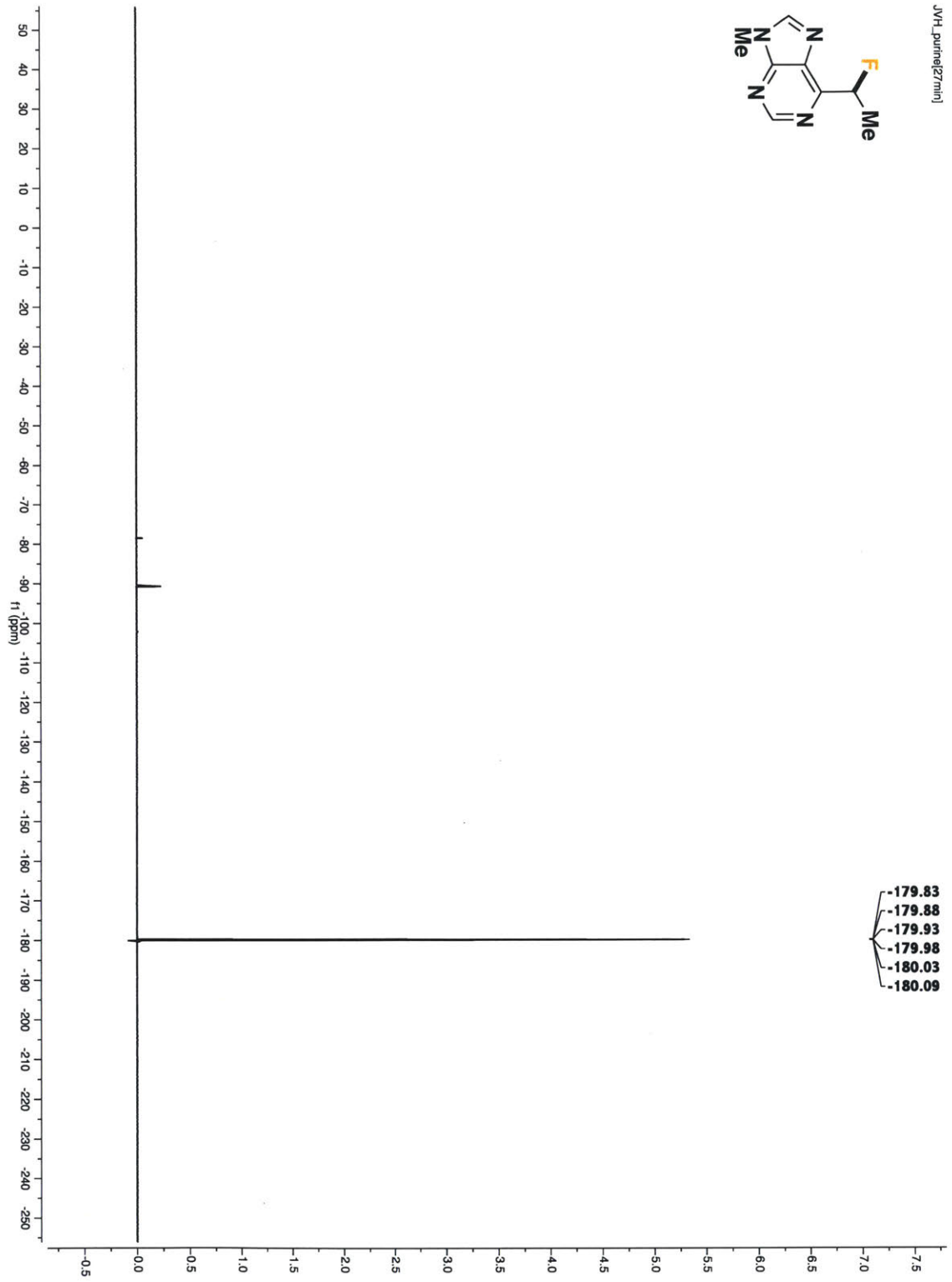

Figure S40. ^{19}F NMR spectrum of 9-methyl-6-(1-fluoroethyl)-9*H*-purine

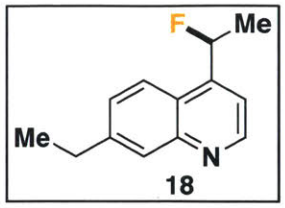

18

7-ethyl-4-(1-fluoroethyl)quinoline: 40%, yellow oil. Purified via column chromatography on silica gel using 5% ethyl acetate/dichloromethane.

^{1}H NMR (500 MHz, $CDCl_3$) δ 8.90 (d, *J* = 4.4 Hz, 1H), 7.95 (s, 1H), 7.81 (d, *J* = 8.6 Hz, 1H), 7.54 - 7.37 (m, 2H), 6.30 (dq, *J* = 46.9 Hz, *J* = 6.4 Hz, 2H), 2.87 (q, *J* = 7.5 Hz, 2H), 1.79 (dd, *J* = 24.2 Hz, *J* = 6.5 Hz, 3H), 1.35 (t, *J* = 7.6 Hz, 3H). ^{13}C NMR (126 MHz, $CDCl_3$) δ 150.5, 148.7, 146.6 (d, *J* = 19.5 Hz), 145.9, 128.3, 128.2, 122.9 (d, *J* = 4.9 Hz), 122.7, 115.8 (d, *J* = 10.7 Hz), 87.8 (d, *J* = 171.4 Hz), 29.0, 22.7 (d, *J* = 24.6 Hz), 15.3. ^{19}F NMR (471 MHz, $CDCl_3$) δ -176.6 (dq, *J* = 47.8 Hz, *J* = 24.5 Hz). HRMS (ESI/Q-TOF) $[M + H]^+$ m/z: Calcd for ($C_{13}H_{14}FN$) 204.1181; Found 204.1181.

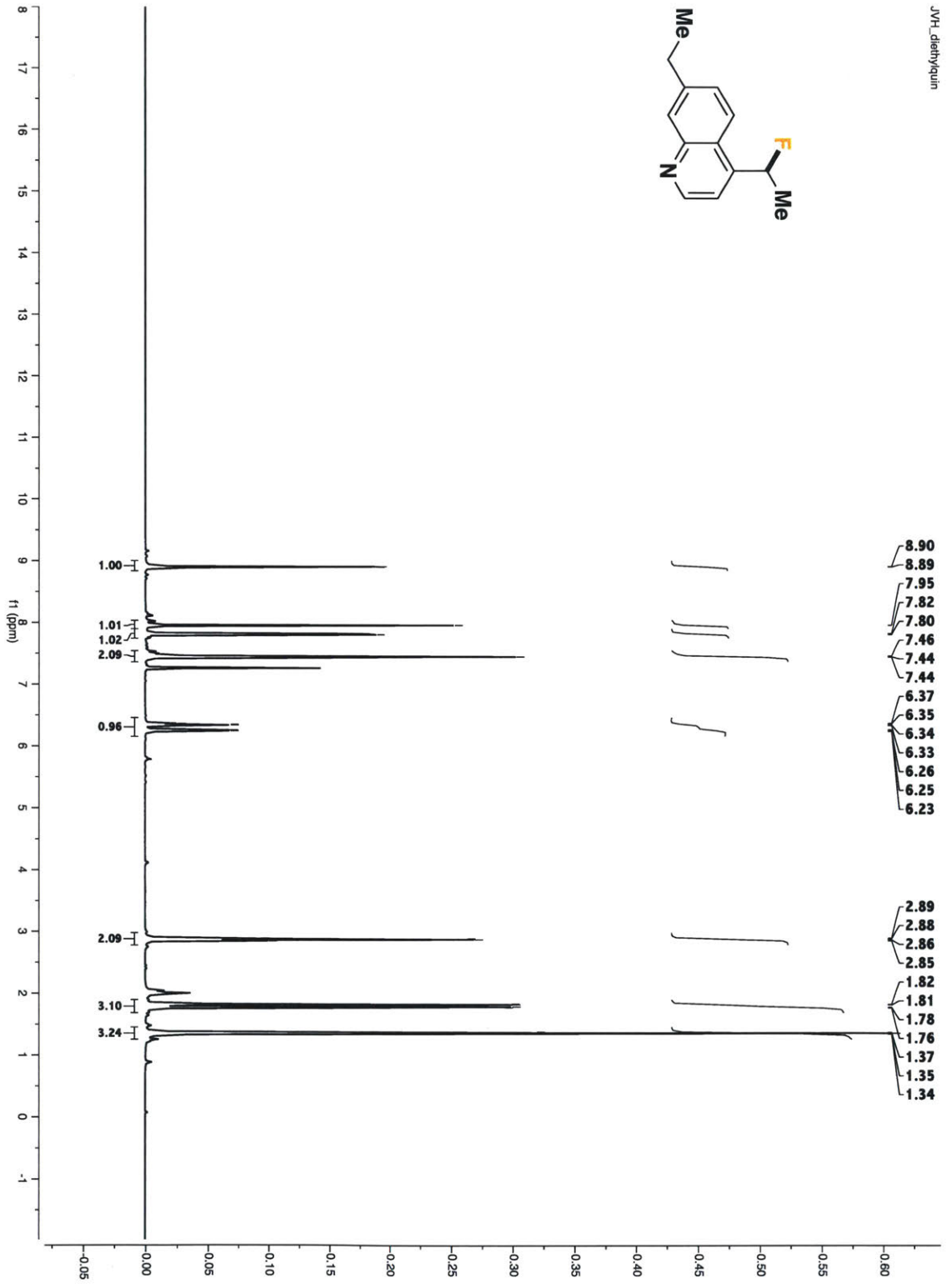

Figure S41. ^{1}H NMR of 7-ethyl-4-(1-fluoroethyl)quinoline

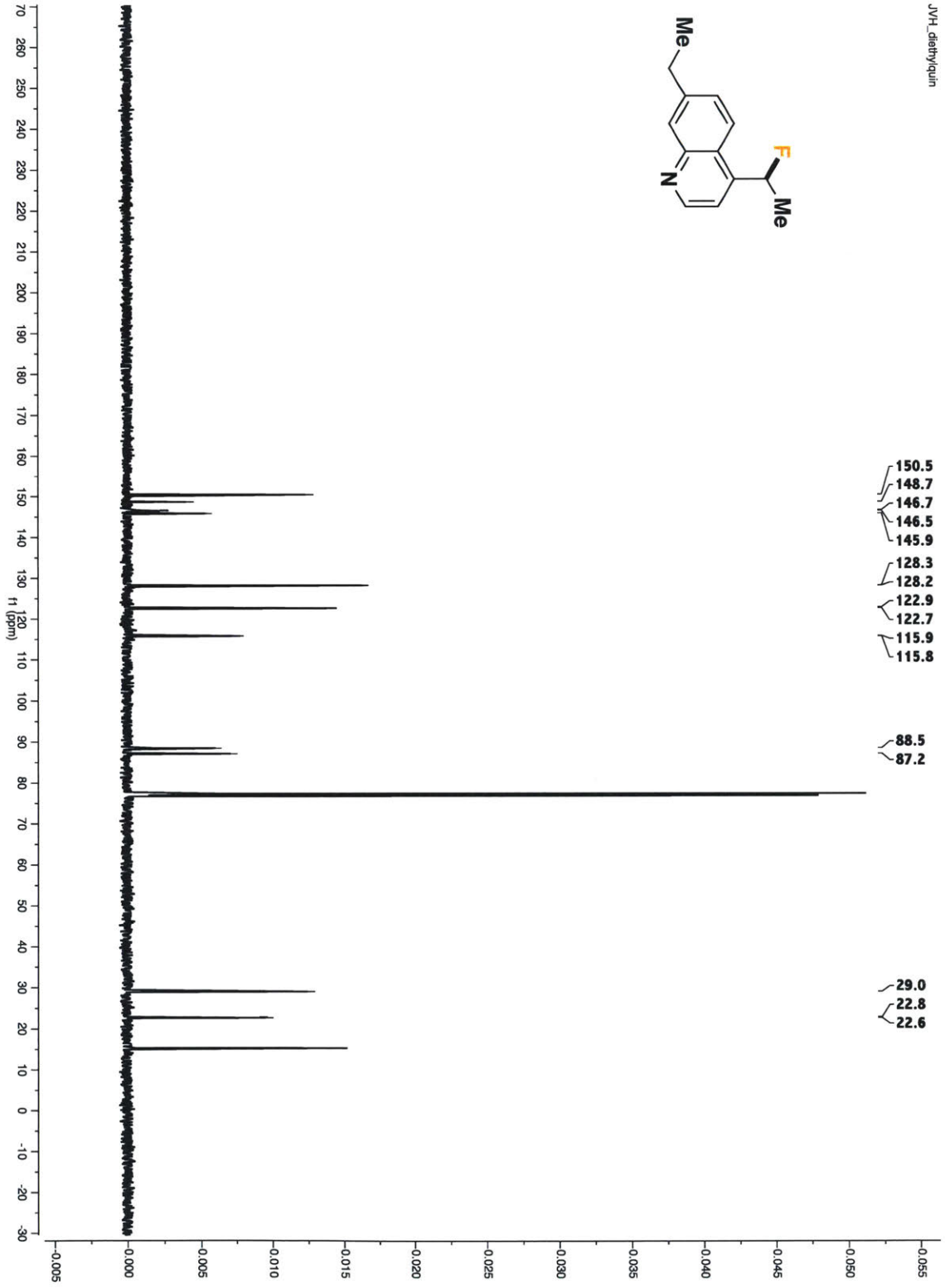

Figure S42. ^{13}C NMR of 7-ethyl-4-(1-fluoroethyl)quinoline

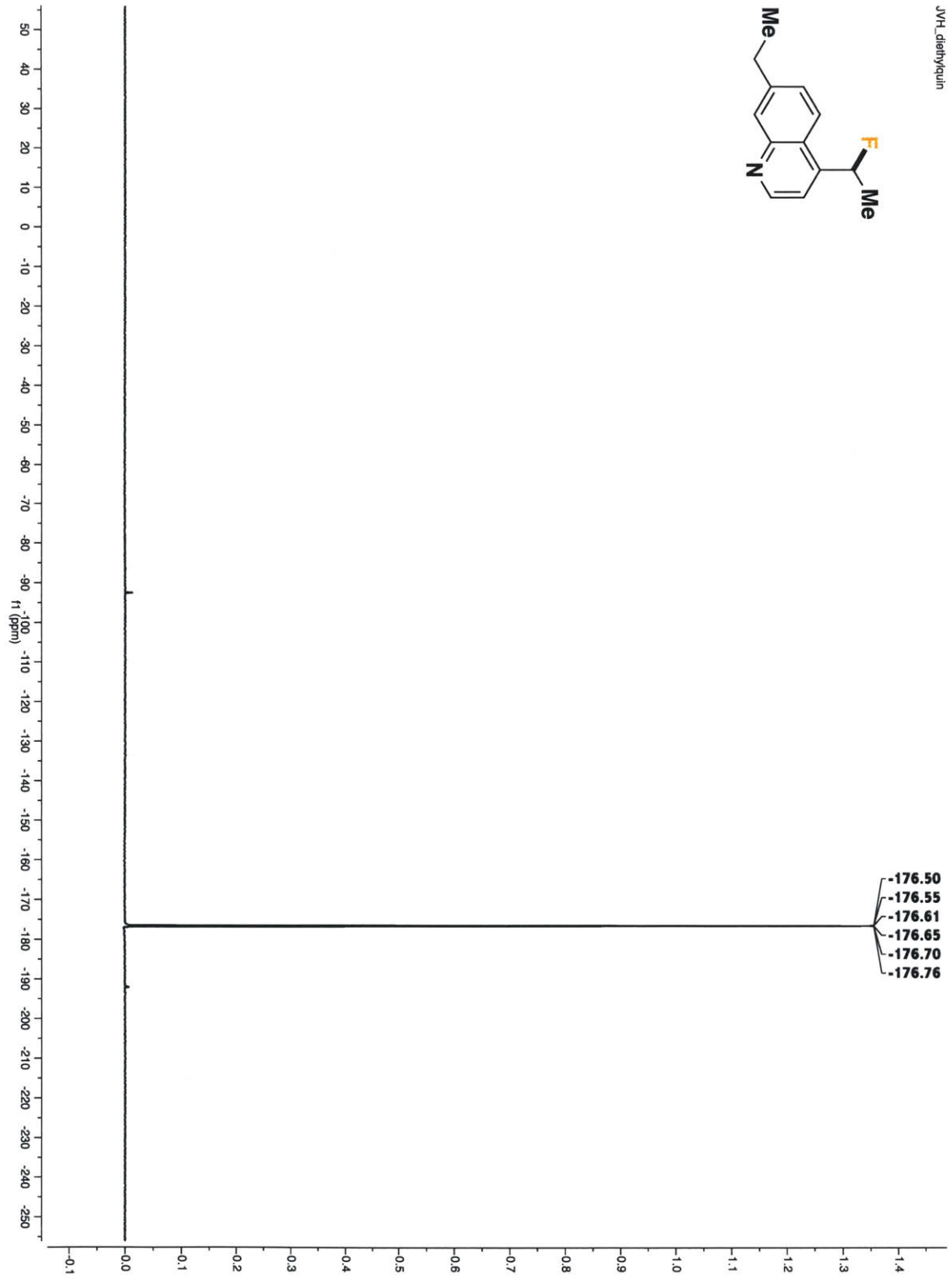

Figure S43. ^{19}F NMR of 7-ethyl-4-(1-fluoroethyl)quinoline

Dimer Characterization

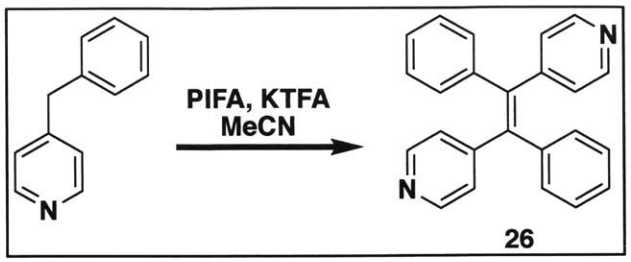

***E*-1,2-diphenyl-1,2-di(pyridin-4-yl)ethene:** 1.0 g (2.36 mmol) of [bis(trifluoroacetoxy)iodo]benzene and 477 mg (3.14 mmol) potassium trifluoroacetate were added to an oven-dried 8 mL scintillation vial, followed by dry acetonitrile (4 mL). 0.25 mL (1.67 mmol) 4-benzylpyridine were added via syringe, and the reaction was stirred for 18 hours at 80 °C. Subsequently, the reaction was cooled to room temperature, quenched with a saturated aqueous solution of sodium bicarbonate, and the product was extracted with 3 x 10 mL ethyl acetate. After drying over magnesium sulfate and concentrating on a rotary evaporator, the dimer was purified on silica gel via a 40 - 100% ethyl acetate/hexanes solution to yield 36 mg of the product as a white solid (7%, 0.11 mmol). The alkene was assigned as its *E*-isomer by hydrogenation to its known racemic (+/–)-1,2-diphenyl-1,2-di(pyridin-4-yl)ethane.

^{1}H NMR (400 MHz, CD_2Cl_2) δ 8.39 - 8.32 (m, 4H), 7.21 - 7.14 (m, 6H), 7.00 (dd, J = 7.9, J = 1.7 Hz, 4H), 6.94 - 6.87 (m, 4H); ^{13}C NMR (101 MHz, CD_2Cl_2) δ 151.3, 149.8, 141.8, 141.3, 131.5, 128.8, 128.2, 126.1; HRMS (ESI/Q-TOF) $[M + H]^+$ m/z: Calcd for ($C_{24}H_{18}N_2$) 335.1543; Found 335.1540.

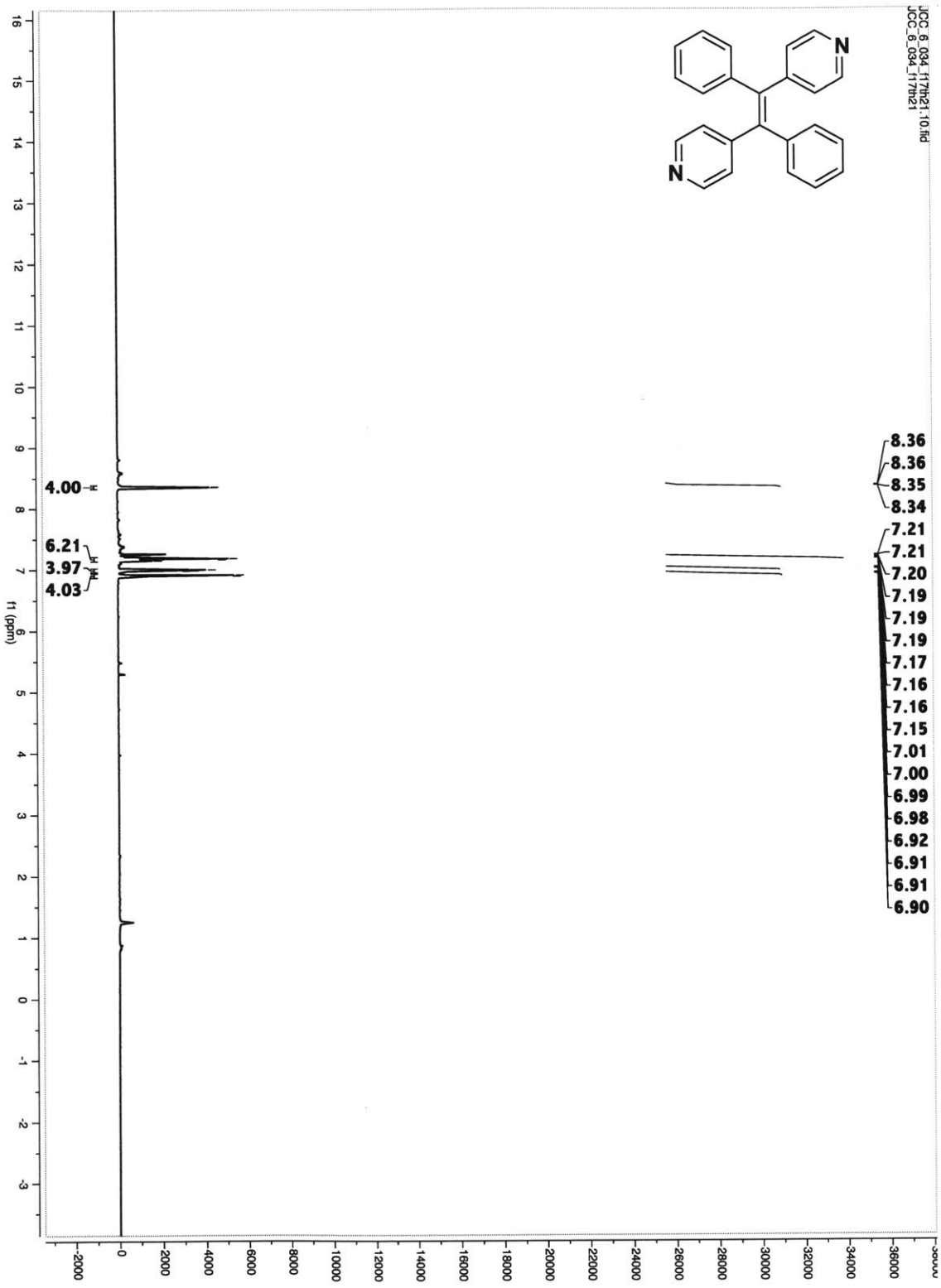

Figure S44. ^{1}H NMR spectrum of *E*-1,2-diphenyl-1,2-di(pyridin-4-yl)ethane

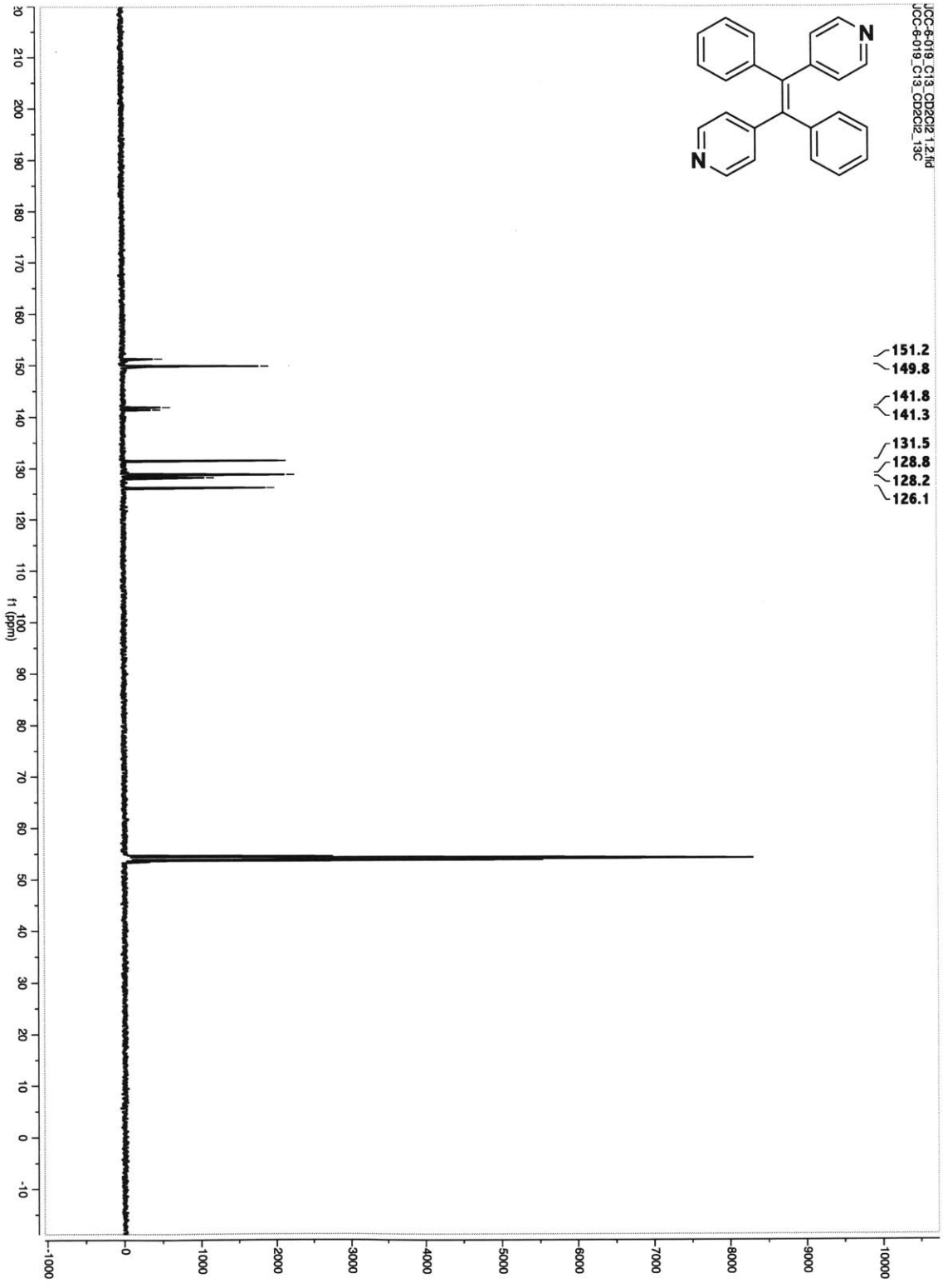

Figure S45. ^{13}C NMR spectrum of *E*-1,2-diphenyl-1,2-di(pyridin-4-yl)ethane

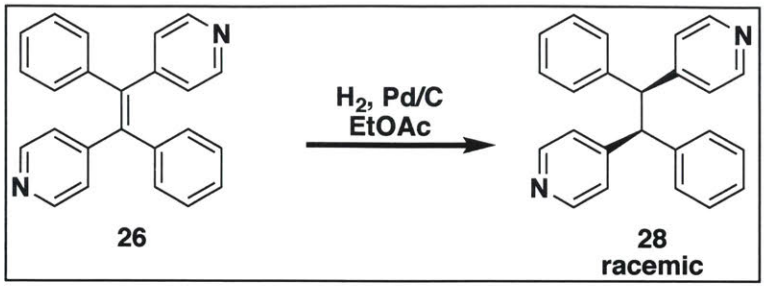

(+/–)-1,2-diphenyl-1,2-di(pyridin-4-yl)ethane: 20 mg of palladium on carbon (10% on activated wood carbon, 50% w/w with H_2O) added to a solution of 38 mg (0.11 mmol) dimer **12** in 10 mL ethyl acetate in a round bottom flask under nitrogen. A hydrogen balloon was added along with an outlet needle, and the flask was purged for five minutes to remove the nitrogen atmosphere. The reaction was stirred for 72 hours, with the hydrogen balloon replaced when needed. After completion of the reaction, the reaction was filtered through Celite® and the solvent evaporated via a rotary evaporator. The crude product was purified a silica gel plug, which was washed first with ethyl acetate to elute any trace remaining starting material, followed by 10% methanol/dichloromethane to yield 10 mg of a white solid (0.031 mmol, 28%). Upon comparison with previously reported spectra,[10] the product was determined to be the racemic stereoisomer.

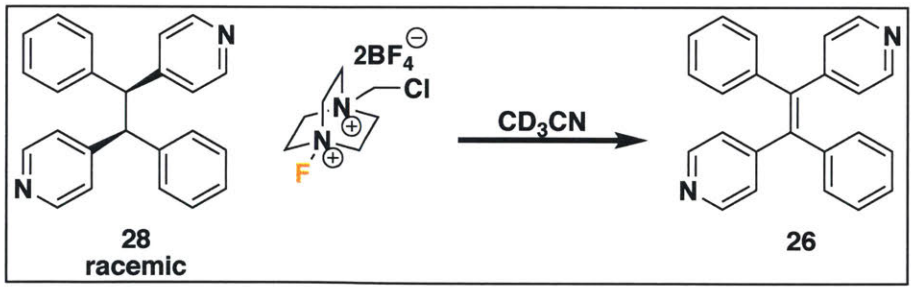

Oxidation of 23 to 24: (+/-)-1,2-diphenyl-1,2-di(pyridin-4-yl)ethane (10 mg, 30 umol) was dissolved in 0.3 mL deuterated acetonitrile. 12.6 mg (35 umol, 1.2 equivalents) of

Selectfluor® were added, and the reaction stirred 24 hours. The product was analyzed via GC/MS and confirmed as *E*-1,2-diphenyl-1,2-di(pyridin-4-yl)ethene.

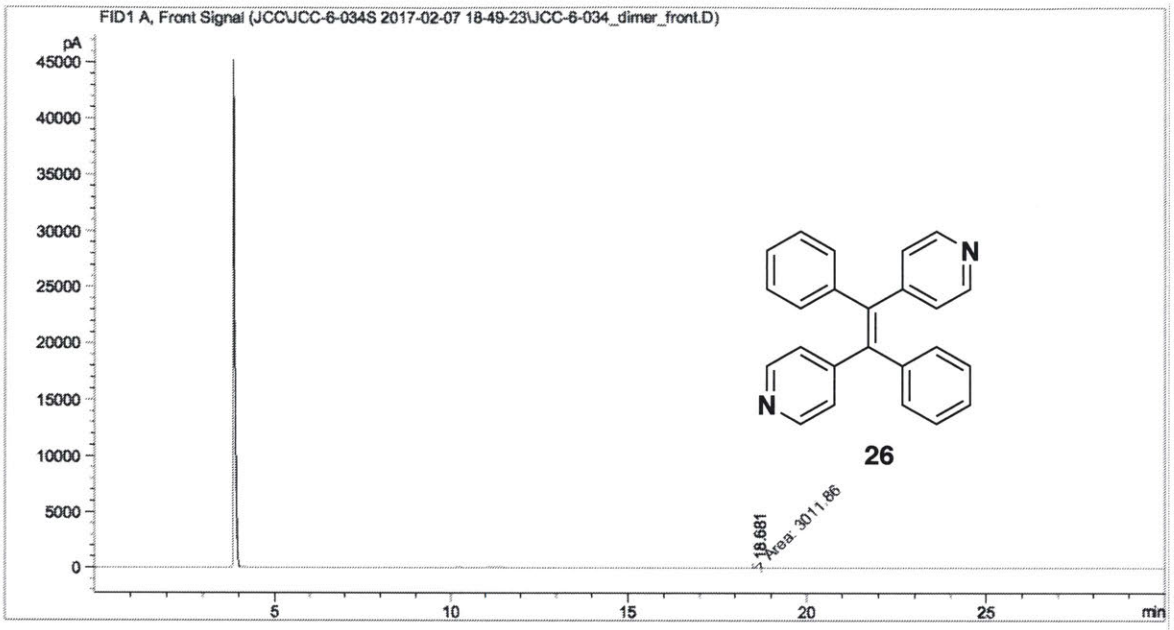

Figure S46. GC trace for pure olefin **25**

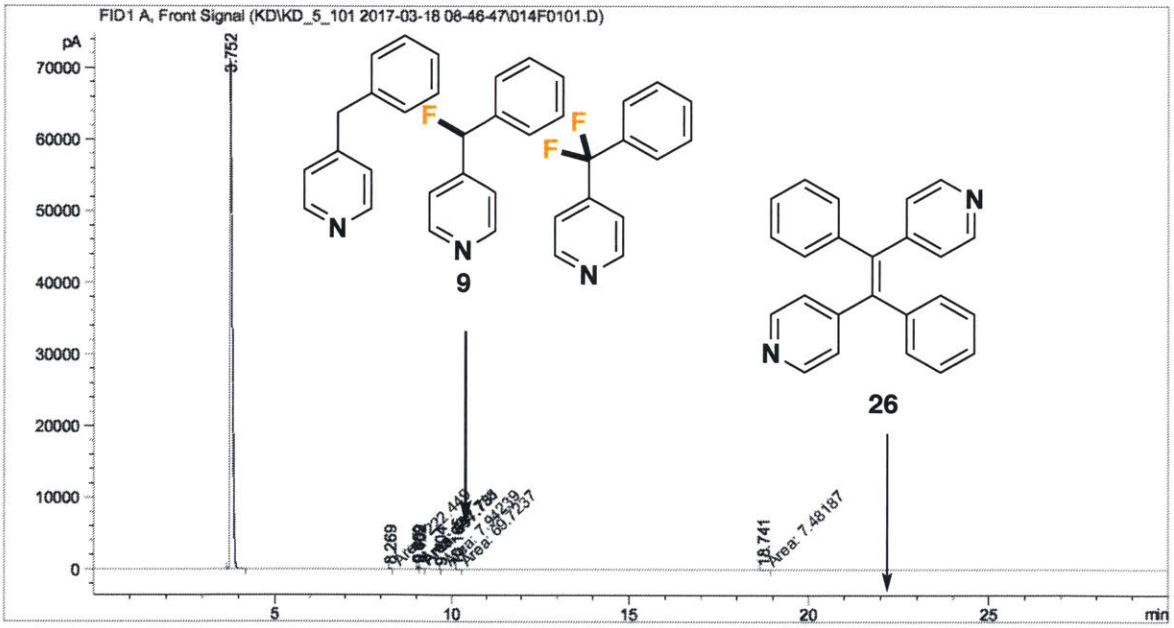

Figure S47. GC trace for fluorination reaction of 4-benzylpyridine showing *in situ* formation of dimer

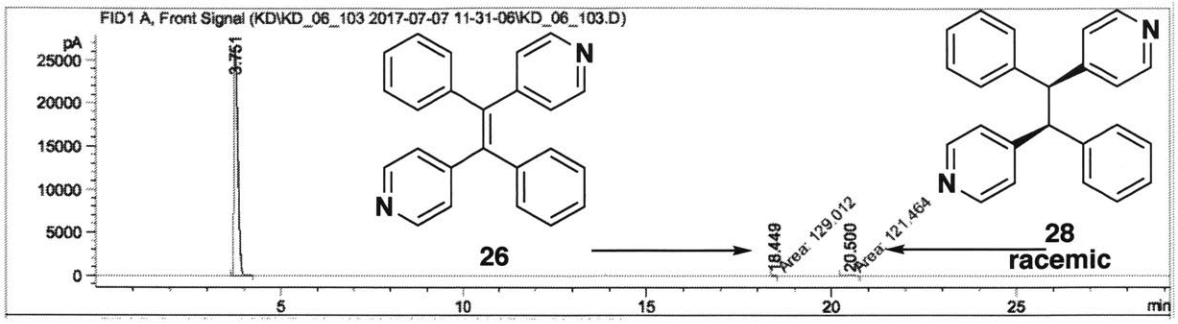

Figure S48. GC trace for oxidation of saturated racemic dimer (R_t 20.5) to olefin dimer

Selectivity

Under nitrogen, 4-ethylpyridine (0.5 mmol) and ethylbenzene (0.5 mmol) were added to an oven-dried 8 mL scintillation vial that had been purged with N_2 via a Teflon-faced septum. MeCN-d_3 (1 mL, stored over molecular sieves) was added, followed by 212 mg (0.6 mmol, 1.2 equivalents) Selectfluor®. The nitrogen needle was removed, and the cap sealed with melted parafilm. The suspension was stirred for 20 hours at 25 °C, gradually forming a pale yellow mixture. A saturated sodium bicarbonate solution was added to the reaction, and the product was extracted with 2 mL $CDCl_3$. 57 μL (0.5 mmol) of 4-fluoroanisole as an internal standard were added to the organic extract, and the yield analyzed via ^{19}F NMR. After removal of the solvent via rotary evaporation, the crude product was purified on silica or alumina to acquire clean NMR spectra. Besides the desired products, these reactions typically contained small amounts of remaining starting material and small amounts of difluorinated pyridine products. No fluorinated ethylbenzene was observed.

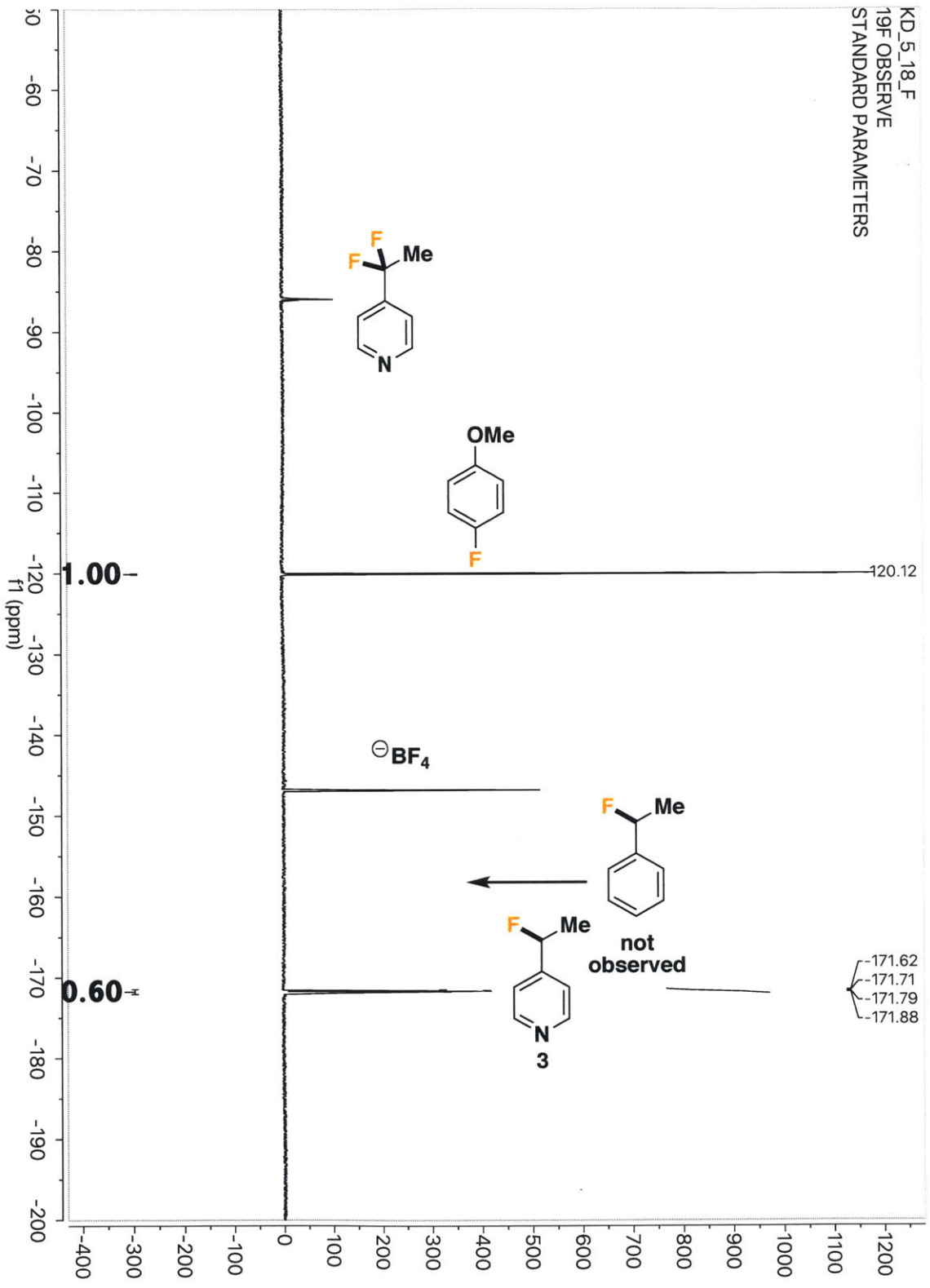

Figure S49. ^{19}F NMR of total selectivity for 4-ethylpyridine over ethylbenzene

Kinetic Isotope Effects

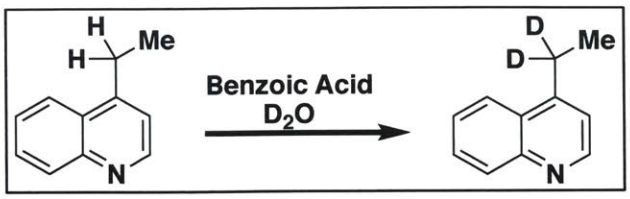

4-(ethyl-1,1-d_2)quinoline: Synthesized according to the procedure of Yin and coworkers.[12] Quinoline (800 mg, 5.09 mmol) was suspended along with benzoic acid (120 mg, 0.98 mmol) in 8 mL D_2O in a thick-walled glass pressure vessel. The suspension was capped and heated to 100 °C for six hours. After cooling to room temperature, the contents were transferred into a separatory funnel with the aid of ethyl acetate, washed with 10% K_2CO_3, dried over $MgSO_4$, filtered and concentrated *in vacuo* to yield the crude isotopically labelled substrate. After purification on silica gel (2:1 hexanes:ethyl acetate eluent), quantitative ^1H NMR analysis showed approximately 80% deuterium incorporation. A sample of this material (~270 mg) was re-subjected to the labeling procedure (with benzoic acid and D_2O amounts appropriately adjusted) to deliver 4-ethylquinoline that was now >98% isotopically labelled at the desired position, as judged by the disappearance of the CH_2 quartet resonance found at d 3.12 ppm (210 mg).

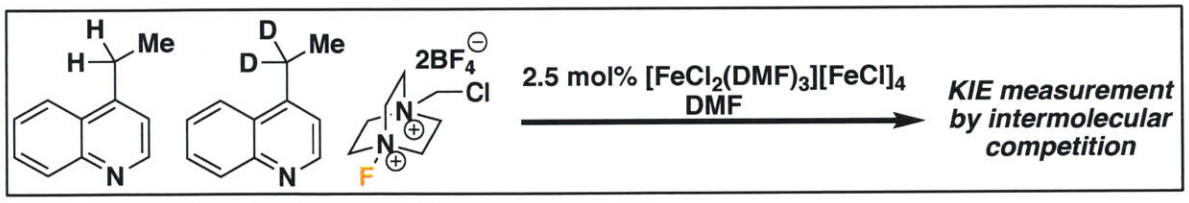

KIE measurement: 4-Ethylquinoline (78.6 mg, 0.5 mmol) and 4-(ethyl-1,1-d_2)quinoline (79.6 mg, 0.5 mmol) were transferred through a Teflon faces septum into an oven-dried 8

mL vial under nitrogen atmosphere using a tared and massed 100 μL syringe. DMF (1 mL) was added, followed by $[FeCl_4][FeCl_2(dmf)_3]$ (6.7 mg, 0.012 mmol, 0.025 mmol Fe) and finally Selectfluor® (177 mg, 0.5 mmol). The nitrogen inlet needle was removed, the reaction was sealed with melted parafilm and was heated to 40 °C for twenty hours. After that period, the reaction was cooled to room temperature and transferred to a separatory funnel with the aid of ethyl acetate. The organic layer was washed with a 1 M sodium L-ascorbic acid solution to remove the iron, which was then back extracted three times with ethyl acetate. The combined organic layers were dried with $MgSO_4$, filtered and concentrated *in vacuo*. The starting material and products were recovered together using silica gel chromatography (4:1 hexanes:ethyl acetate eluent). Quantitative ^{19}F NMR (relaxation delay = 10 s) showed a KIE (k_H/k_D) of 5.19.

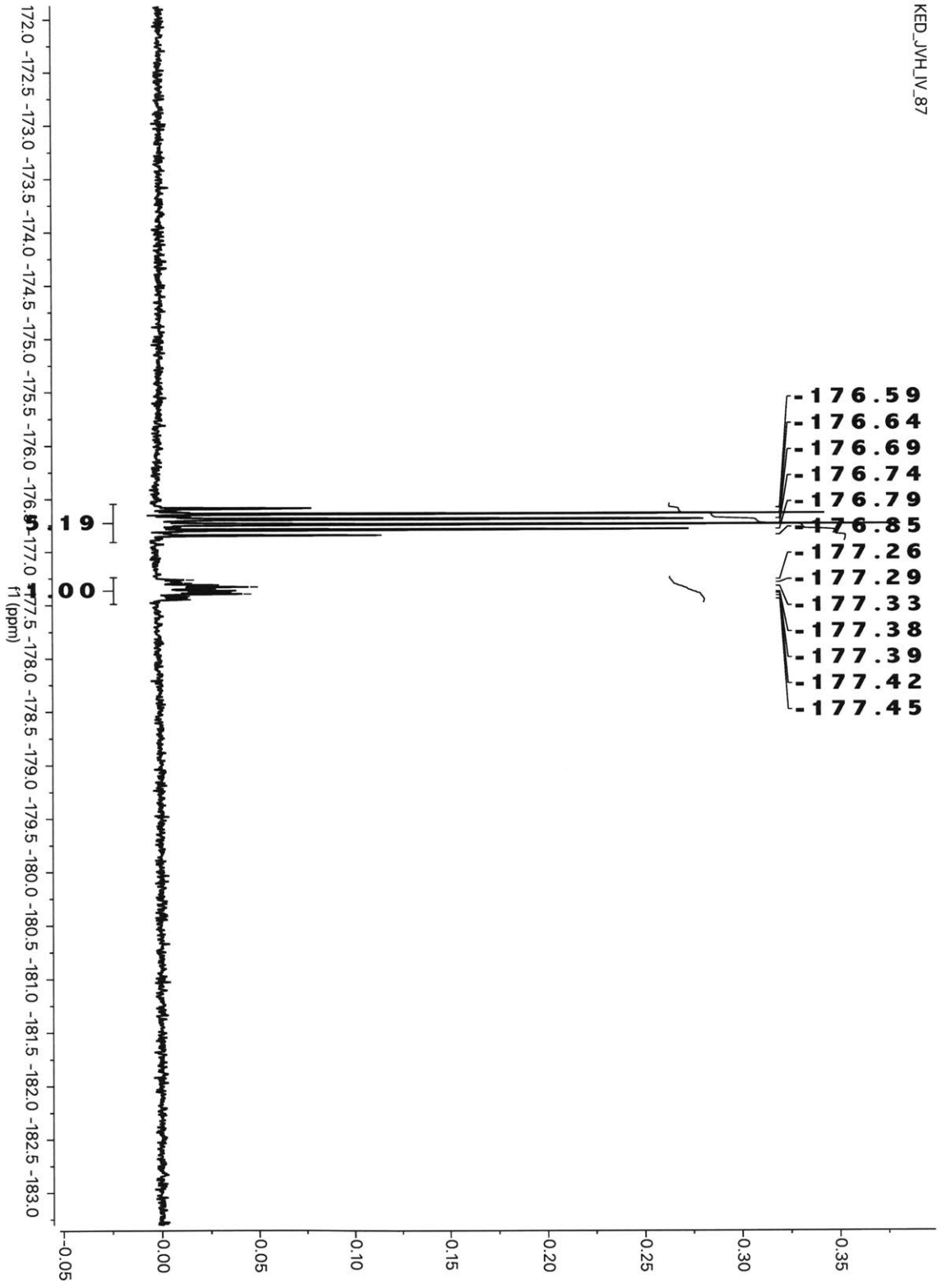

Figure S50. Measurement of KIE for intermolecular competition of ethylquinoline isotopomers

References

1. Steves, A.; Oestreich, M. *Org. Biomol. Chem.* **2009**, 7, 4464.
2. Wakiyama, Y.; Kumura, K.; Masaki, S.; Ueda, K.; Sato, Y.; Kikuchi, C.; Umemura, E.; Hirai; Y.; Kondo, H. PCT Intl. Apply. W.O. 2008146917. Dec. 4, 2008.
3. Antonsson, T. Bach, P.; Brickmann, K.; Bylund, R.; Giordanetto, F.; Johansson, J.; Zetterberg, F. PCT Intl. Appl. W.O. 2008085118. Jul. 17, 2008.
4. Felix, R. A.; Chin, H.-L. M.; Woodlard, F. X.; Lee, D. L.; Kanne, D. B. U.S. Patent 5707930, Jan 13, 1998.
5. Rodriguez, J. G.; Benito, Y. *J. Het. Chem.* **1988** *25* (3), 819.
6. Fürstner, A.; Leitner, A.; Méndez, M.; Krause, H. *J. Am. Chem. Soc.* **2002**, *124*, 13856.
7. Hahn, J. T.; Popp, F. D. *J. Het. Chem.* **1989**, *26* (5), 1357.
8. Chen, S.; Graceffa, R. F.; Boezio, A. A. *Org. Lett.* **2016**, *18* (1), 16.
9. Meanwell, M.; Nodwell, M. B.; Martin, R. E. Britton, R. *Agnew. Chem. Int. Ed.* **2016**, *55* (42), 13244.
10. Labrie, F.; Gauthier, S.; Cloutier, J.; Mailhot, J.; Potvin, S. Dion, S.; Sanceau, J. PCT Intl. Appl. W.O. 2008124922. Oct. 23, 2008.
11. Itoh, M.; Hirano, K.; Satoh, T.; Miura, M. *Org. Lett.* **2014**, *16* (17), 2050.
12. Liu, M.; Chen, X.; Chen, T.; Yin, S.-F. *Org. Biomol. Chem.* **2017**, *15*, 2507.

Chapter 2

Harnessing Chloramine as a Source of Electrophilic Nitrogen in Continuous-Flow

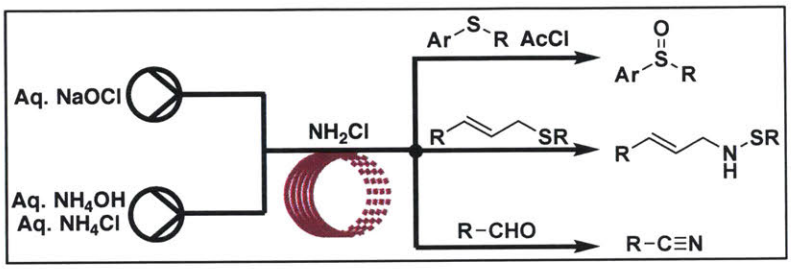

Abstract: Despite its atom economy, low cost, and straightforward synthesis, chloramine has not seen widespread use in organic synthesis due to its instability and toxicity. However, continuous-flow chemistry enables the safe and reliable generation of chloramine from aqueous ammonia and sodium hypochlorite solutions. Furthermore, an array of nucleophiles can rapidly react with chloramine as an electrophilic nitrogen source, enabling access to synthetically valuable nitriles, allylic sulfenamides, and sulfoxides in reaction times as brief as 3 seconds.

Thesis Supervisor: Timothy F. Jamison
Department Head and Robert R. Taylor Professor of Chemistry

Dr. Evan Styduhar carried out initial synthesis of chloramine and investigation of its reactivity. Dr. Laurel M. Heckman carried out the synthesis, isolation, and purification of unsaturated nitriles on scale. Kelley E. Danahy investigated and optimized the syntheses of primary hydrazines and sulfilimines from chloramine. Aria M. Fodness contributed to the optimization of pyrazole syntheses and exploration of chloramine reactivity.

Introduction

As of 2014, 84% of all small molecule pharmaceuticals contain at least one nitrogen atom.[1] The development of novel amination methods, therefore, has remained an active field of study.[2] Though nitrogen is typically treated as a nucleophile, the use of nitrogen-transfer reagents allows access to electrophilic nitrogen.[3] For instance, the nitrogen sources shown in **Figure 1** have been successfully employed in a variety of both electrophilic and ambiphilic aminations, such α-aminations[4] and hydrazine formations,[5] as well as nitrenoid reactions, such as olefin aziridinations and C–H insertions.[3]

However, despite their beneficial applications, **2** – **6** possess a number of undesirable features including poor atom economy, high cost, and explosive potential. In contrast, chloramine (**1**) is inexpensive and atom economical, yet its instability[6] and reputed toxicity[7] has thus far hindered its development as a versatile electrophilic nitrogen source.

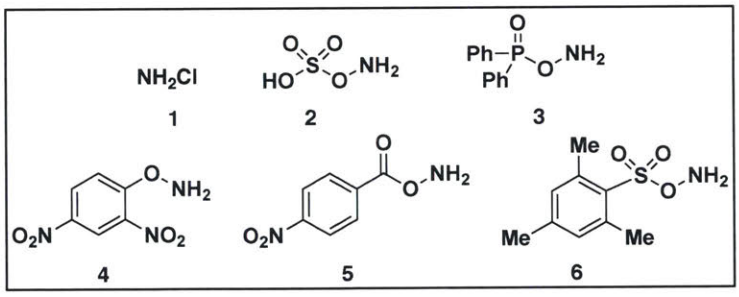

Figure 1. Common electrophilic amination reagents.

We hypothesized that continuous-flow chemistry could mitigate the disadvantages of **1**. Namely, the benefits of continuous-flow – superior temperature control, enhanced mixing leading to rapid reactions, and the ability to form and use potentially toxic reagents without the need for isolation[8] – precisely counter the disadvantages of **1**.

As shown in **Scheme 1**, **1** was prepared in a time of 1.6 minutes via three inexpensive and common reagents: aqueous ammonia and sodium hypochlorite, with ammonium chloride as a pH buffer. The reactor was cooled to 0 °C to attenuate any thermally-aided decomposition. A subsequent extraction into dichloromethane consistently yielded a solution between 0.16 and 0.18 M in **1**.

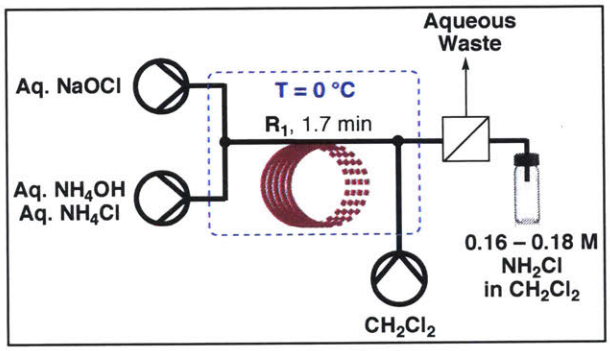

Scheme 1. Continuous-flow conditions for chloramine production.

Inspired by the work of Armstrong and coworkers, our initial test of **1** explored the formation of unprotected aziridines (**Scheme 2**).[9] As demonstrated, electrophilic amination agent **1** can react with tertiary amines to yield a highly reactive hydrazinium intermediate (**9**). Use of base deprotonates **9** to form zwitterion **10**, enabling transformation of chalcone **7** into aziridine **8**.[10] Under homogenous conditions, aziridine **8** was observed in 89% yield in just five minutes at room temperature.

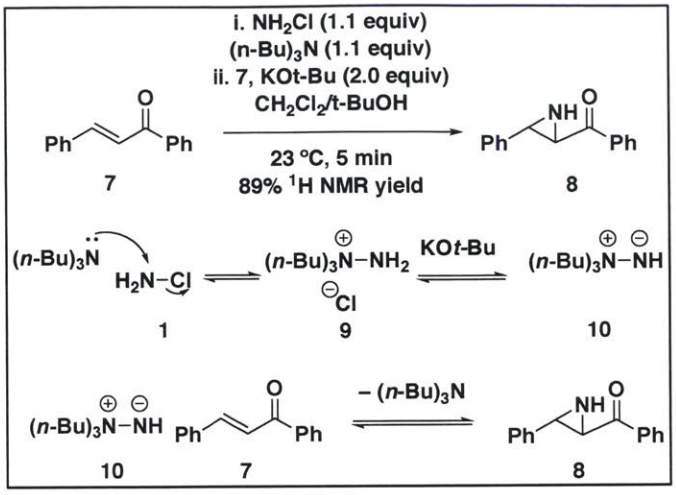

Scheme 2. Proposed mechanism for aziridine formation.[9,10]

However, while testing an aziridination on aldehyde **11a**, we discovered that the aldehyde cleanly converted to its nitrile. Examining the reaction scope showed that, using continuous-flow chemistry, unsaturated aldehydes gave their synthetically valuable nitriles in good to excellent yields in just three minutes (**Scheme 3**).

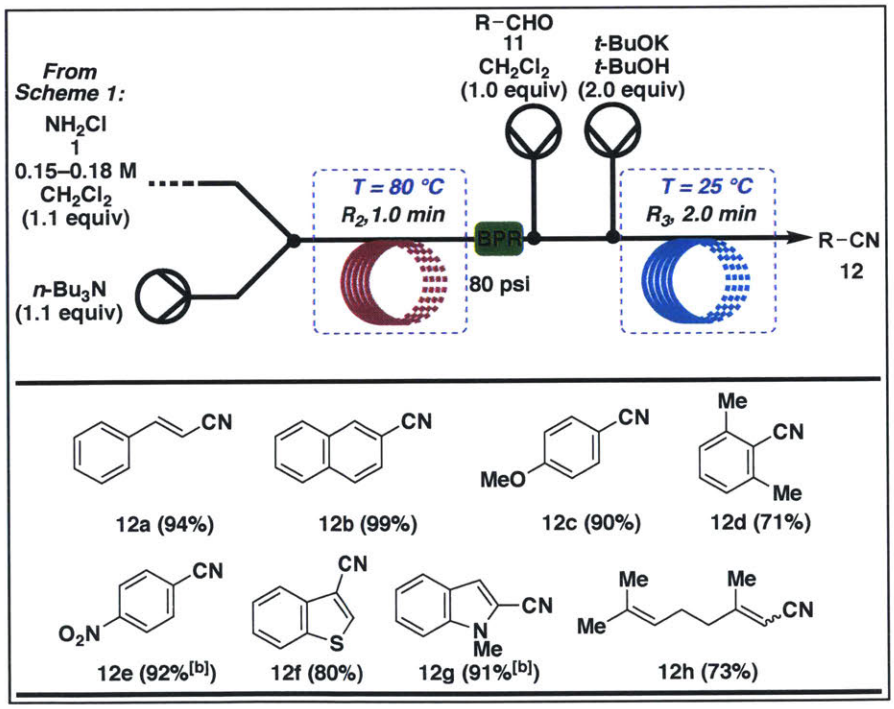

Scheme 3. Continuous-flow setup and scope of unsaturated nitrile formation.

Both electron-rich and electron-withdrawn aryl substituents were tolerated, as were benzothiophenes (**12f**) and protected indoles (**12g**). A potential mechanism is shown in **Scheme 4**, in which zwitterionic **10** condenses with aldehyde **11a** to form its imine, followed by loss of water. Under these basic conditions, removal of the α-proton provides the desired nitrile. This provides alternative conditions to typical methods for this transformation, which typically require a strong acid[11] or an additional chemical oxidant.[12]

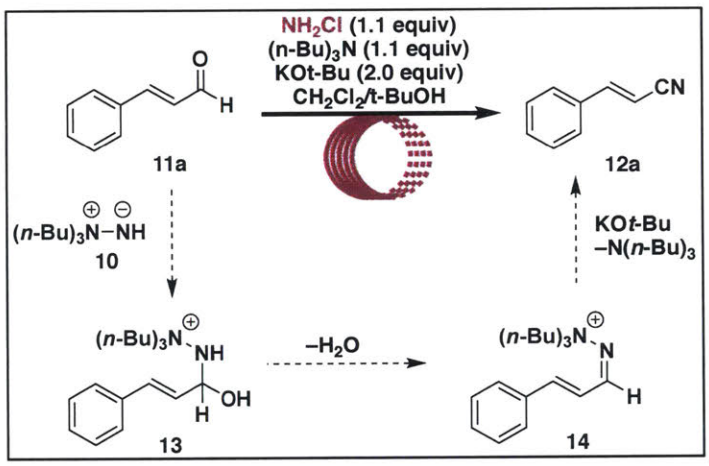

Scheme 4. A potential mechanism for the transformation of aldehydes to nitriles. mediated by **10**.

Noting the ready formation of hydraziniums from a combination of amines and **1**, we postulated that a variety of azaheterocycles could be formed from hydrazines, formed by a simple nucleophilic substitution on **1** by either secondary or primary amines. The use of chloramine to form substituted hydrazines has long been known, particularly in processes such as the Raschig process,[13] but, again, due to the unstable nature of **1**, which has a tendency to overreact to a variety of oxidized products,[6] this use has seen limited application thus far.

Optimization of Azaheterocycle Syntheses

With only 2 equivalents of alkyl-substituted amines, and the addition of a catalytic amount of potassium hydroxide to maintain a slightly basic pH,[14] the expected hydrazine was formed with quantitative conversion (**Table 1, entry 3**). Arylamines were not tolerated, presumably following the azo-mediated decomposition pathway available for arylhydrazines.[6, 15]

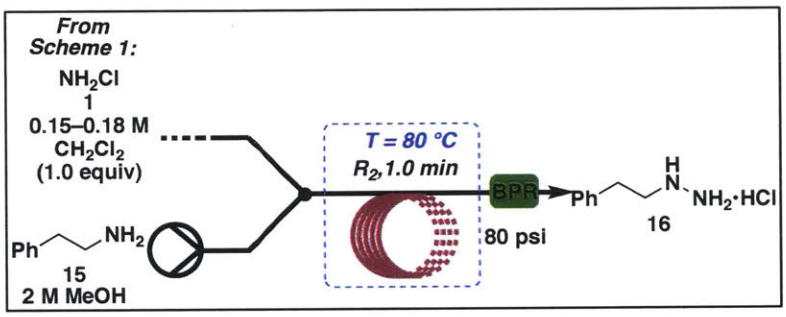

Entry	Additive (10%)	Equiv. RNH_2	Residence Time (min)	Conversion (%)
1	_	2	1	44
2	KOH	1	1	58
3	KOH	2	1	quant.
4	KOH	2	0.5	77
5	Bu_4NOH	2	1	quant.
6	KO*t*-Bu	2	1	84

Table 1. Conditions for formation of hydrazine **16** from **15** and **1**.

We had planned to telescope our hydrazine formation into a pyrazole synthesis by reacting with 1,3-diketones in a continuous system (**Scheme 5**). However, due to the diminished nucleophilicity of primary amines in comparison to tertiary amines,[16] titratable remnants of chloramine remained in our reaction. This proved challenging, as the hydrazine product is more nucleophilic than the amine starting material, resulting in ready decomposition of the hydrazine before forming our desired product.[7] Additionally, 1,3-

diketones are known to undergo their own decomposition with chloramine to form amides and α-chloroketones,[17] further hampering our efforts to isolate meaningful quantities of a pyrazole.

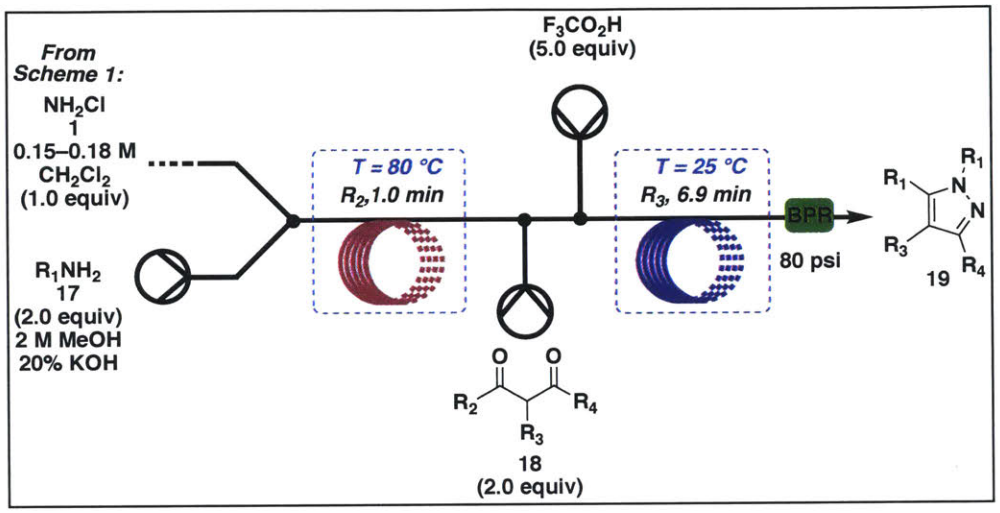

Scheme 5. Proposed continuous-flow setup for the synthesis of pyrazoles from alkyl amines and **1**.

Attempts to quench the residual chloramine with aqueous thiosulfate were unsuccessful, due to insufficient mixing between the dichloromethane and aqueous layer, even in continuous flow. Other reductants were tried: sodium sulfite, though more soluble in polar organic solvents than sodium thiosulfate, was insoluble under our conditions. Tertiary amines as quenching reagents, including tributylamine and pyridine, were unsuccessful. Ascorbic acid was not considered, as its acidic protons and multiple ketones resulting from oxidation would likely result in side reactions. Ultimately, a reductant soluble in organic solvents, with limited potential for side reactions, would be required for this method to succeed.

Exploration of Sulfilimine Reactivity

During our studies on the reactivity of **1**, we observed that polarizable, nucleophilic thioethers could readily undergo amination with chloramine as an electrophile, yielding salt **21** (**Scheme 6**). These salts can be deprotonated to form free sulfilimine **22**, which has limited use due to instability.[18] Though the methods to synthesize the analogous sulfoxides[19] and, more recently, the medicinally potent sulfoximines,[20] have received considerable attention, sulfilimines have been limited by the need for nitrogen protection.

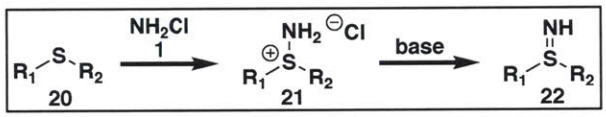

Scheme 6. Reaction of thioethers with **1**.

Current synthetic methods typically require the use of stoichiometric hypervalent iodine reagents, a transition metal catalyst, and/or variability in either the thioether reactant or the amine reactant, but rarely both.[21] However, taking advantages of the benefits of continuous-flow, we envisioned that addition of **1**, followed by an acylating electrophile, would result in a diverse array of desired sulfimilines without the need to isolate the unstable intermediates (**Scheme 7**).

Scheme 7. Proposed synthesis of *N*- and *S*-variable sulfilimines from **1**.

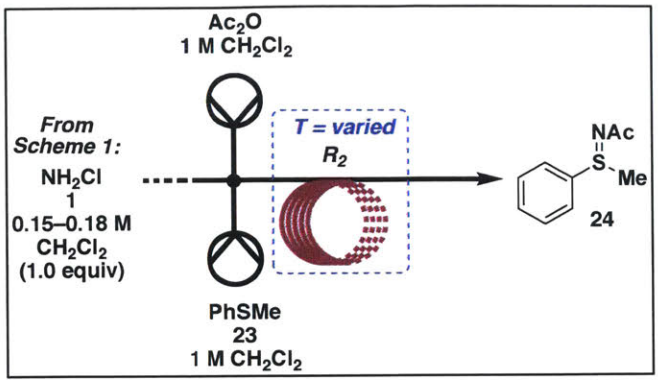

Entry	Equiv Ac_2O	Equiv 1	Temperature (° C)	Residence Time (min)	24 (%)
1	1	1	35	4	trace
2	1	1	25	4	7
3	1	2	25	4	19
4	1	2	0	4	18
5	1	2	0	2	33
6	1	2	0	0.5	39
7	10	2	0	0.5	60
8	1[a]	2	0	0.05	63

Table 2. All yields are estimated from LC-MS percent area, from product area, hydrolysis of incomplete acylated product, dimer, and starting material. [a]Acetyl chloride used instead of acetic anhydride.

For simplicity, thioanisole and acetyl chloride were chosen for optimization. Ultimately, as shown in **Table 2**, under continuous flow, reactivity to form the sulfilimines was near-instantaneous, requiring only a three second residence time at 0 °C, and thus, simultaneous addition of both acetyl chloride, thioanisole, and **1** was ideal. However, controlling the reactivity of the resulting sulfilimine proved challenging: though base was detrimental to sulfilimine stability, the production of one equivalent of HCl (**21**) began to shift the reactivity of chloramine from amination to chlorination.[22] As a result, a trace amount of byproduct was formed: dithianitronium cation **26**. As it is known that these

cations can form from the N–Cl bond,[23] most likely, reaction of sulfilimine **21** with a second equivalent of chloramine produces chlorinated **25**, and displacement by nucleophilic sulfur results in **26**. A potential mechanism for this transformation is shown in **Scheme** 8.

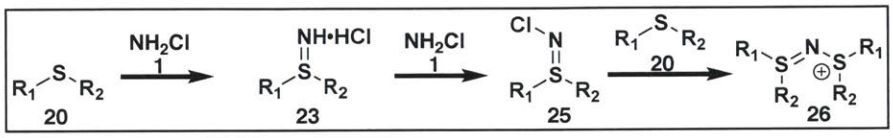

Scheme 8. Potential mechanism for formation of dimer **26** from **20** and **1**.

However, though *N*-acetyl sulfilimines were stable enough to allow us to observe their formation via LC-MS, their scale-up and isolation proved troublesome, providing sulfoxide **27** instead of sulfilimine **24** as the major product. Although a hydrolysis during workup was initially suspected, bypassing an aqueous quench still led to primarily sulfoxide **27** instead of sulfilimine **24**, indicating that perhaps another mechanism was at play. Moreover, the typical routes of decomposition for sulfilimines involves an extrusion of ammonia to revert to the thioether starting material, not hydrolysis to sulfoxide.[18] Furthermore, acetyl chloride was necessary to yield meaningful amounts of sulfoxide **27**; without an acylating reagent, only starting material, was observed – as expected for the decomposition of free sulfilimines.[18]

Overall, in continuous flow, a mere residence time of 3 seconds was optimal for sulfoxide formation, as shown in **Scheme 9**. Moreover, under these conditions, there was little risk of over-oxidation to sulfone, as sulfoxides were found to be unreactive in the presence of **1**. However, the conditions were rather niche, providing diarylsulfoxides and alkyl-aryl sulfoxides in moderate yield, while alkyl-alkyl thioethers tended to provide

numerous products, potentially from a Pummerer-type rearrangement,[24] alongside mixtures of sulfilimines and sulfoxides. Electron-withdrawn trifluoromethylaryl sulfides did not react, and electron-rich aryl rings, such as phenols, primarily gave chlorination instead of imidation.

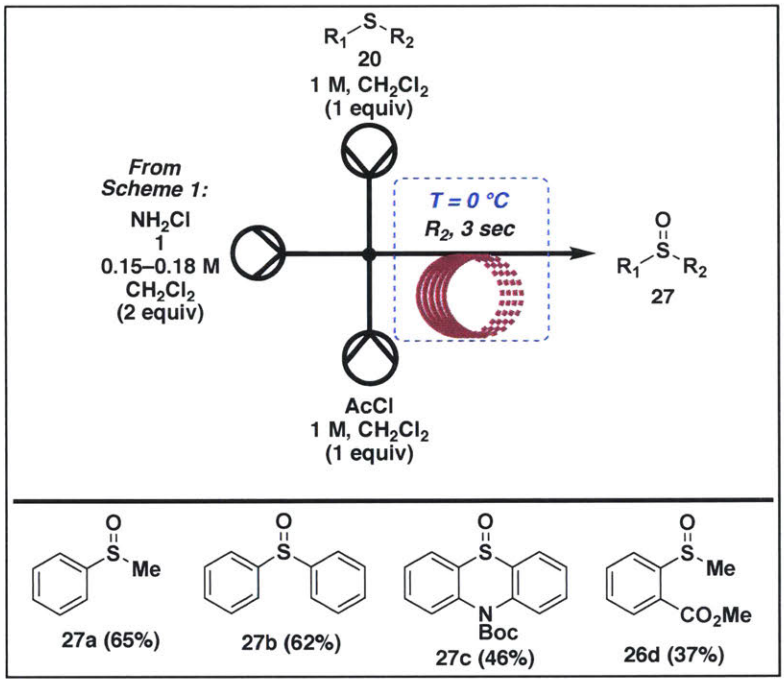

Scheme 9. Continuous-flow setup and substrate scope for sulfoxide formation from **20** and **1**.

Based on work by Vessière and coworkers, one potential mechanism requiring an acyl chloride involves an oxygen-nitrogen exchange to form sulfoxide **27** and acetonitrile, as shown in **Scheme 10**.[25] However, attempts to confirm this mechanism by replacing acetyl chloride with benzoyl chloride, with which we expected to observe the expected benzonitrile byproduct via GC-MS, were unsuccessful, casting doubt on this exact mechanism. Still, while the exact role of acetyl chloride remains unknown, an attempt to trap the unstable sulfilimine intermediate was successful.

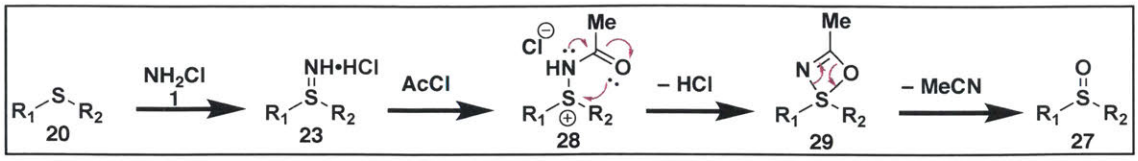

Scheme 10. Potential mechanism for the formation of sulfoxide **27**.

During an attempted oxidation of allylic thiothether **30**, approximately 15% of an unidentified side product was observed. NMR and mass spectrometry were able to confirm the product as rearranged sulfenamide **34**. Imidation of allylic thioether **31** can be followed by either an immediate [2,3]-sigmatropic rearrangement to allylic sulfenamide **32**,[18b] or acylation to **33** prior to rearrangement (**Scheme 11**). These rearrangements are known to occur spontaneously even at low temperatures,[26] and thus observation and isolation of **34** strongly suggests sulfilimine **31** as an intermediate.

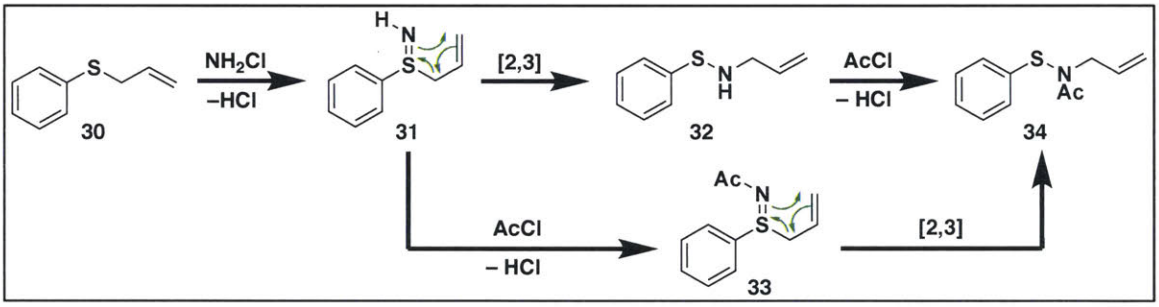

Scheme 11. Potential mechanisms for the sigmatropic rearrangement to form **34**.

Moreover, as the sulfenamide S–N bond is notoriously labile,[18b] this may represent a viable path to transform allylic thioethers into unprotected allylamines by excluding the acetyl chloride. As allylamines are common functional groups in pharmaceutical compounds, especially antifungal reagents,[27] methods for their syntheses remain in demand.[27] However, overall, exploration and optimization are required to transform this reaction into a useful and scalable route in continuous-flow.

Conclusion

In summary, we have successfully harnessed **1** as an inexpensive and rapidly formed source of nucleophilic and electrophilic nitrogen. The use of continuous-flow chemistry not only enables the generation and use of large amounts of **1** while minimizing risks to safety, but enables extremely fast syntheses of synthetically valuable nitriles in <2 minutes, as well as sulfoxides in <3 seconds. Additionally, though optimization is still required, the imidation of allylic thioethers offers the potential to synthesize a variety of allylic amines via a [2,3]-sigmatropic rearrangement.

References

1. Vitaku, E.; Smith, D. T.; Njardarson, J. T.; *J. Med. Chem.* **2014**, 57, 10257.
2. For recent examples, see the following and the references cited therein: a) Hong; S. Y.; Park; Y.; Hwang, Y.; Kim, Y. B.; Baik, M.; Chang, S. *Science*, **2018**, *359*, 1016.; b) Bentley; K. W. Dummit, K. A.; Van Humbeck, J .F. *Chem. Sci.* **2018**, *9*, 6440.; c) Ma; X.; Farndon, J. J.; Young; T. A.; Fey, N.; Bower, J. F.. *Angew. Chem. Int. Ed.* **2017**, *56*, 14531.
3. For recent examples on aminations with nitrogen transfer reagents, see the following and the references cited therein: a) Sabir, S.; Kumar, G.; Jat, J. L. *Org. Biomol. Chem.* **2018**, *16*, 3314; b) Svenstrup, N. ; Parachikova, A. I.; McArthur, J. *Imidazopyrazinones as PDE9 inhibitors for treatment of peripheral diseases and their preparation*, 2018, WO 2018009424; c) Ma, Z.; Zhou, Z.; Kürti., L. *Angew. Chem. Int. Ed.* **2017**, *56*, 9886.; d) Bronkhurst, C. E.; Koch, G.; Rothe-Pollet, S.; La Vecchia, S.. *Synlett.* **2017**, *28*, 1636. e) Paudyal, M. P.; Adebesin, A. M.; Burt, S. R.; Ess, D. H.; Ma, Z.; Kürti, L.; Falck, J. R.. *Science.* **2016**, *353*. 1144; f) Morales, S.; Aceña, J. L.; Garcia Ruano, J. L.; Belén Cid, M. *J. Org. Chem.* **2016**, *81*, 1001.; g) Jamison, T. F.; Marek, I. Chem. Eur. J. **2015**, *21*, 5278.
4. Zhou, Z.; Cheng, Q.-Q.; Kürti, L. *J. Am. Chem. Soc.* **2019**, *141*, 2242.
5. a) Panmand, D. S.; Jishkariani, D.; Hall, C. D.; Steel, P. J.; Asiri, A. M.; Katritzky, A. R. *J. Org. Chem.*, **2014**, *79*, 10593; b) Guernon, H.;. Legault, C. Y. *Organometallics*, **2013**, *32*, 1988.
6. a) Lawrence, S. A. Amines: Synthesis, Properties and Applications. Cambridge University Press: Cambridge, UK, 2004, pp 177; b) Cahn, J. W.; Powell. R. E. *J. Am. Chem. Soc.* **1954**. *76*, 2565.
7. Hall, S. M.; Lynn, R. *N. Engl. J. Med.* **1999**, *341*, 848.
8. Plutschack, M. B.; Piebers, B.; Gilmore, K.; Seeberger, P. H. *Chem. Rev.* **2017**, *117*, 11796.
9. a) Armstrong, A.; Pullin, R. D. C.; Scutt, J. N. *Synlett.* **2016**, *27*, 151.; b) Armstrong, A.; Pullin, R. D. C.; Jenner, C. R.. *Tetrahedron: Asymmetry.* **2014**, *25*, 74.; c) Armstrong, A.; Ferguson, A.. *Bellstein. J. Org. Chem.* **2012**, *8*, 1747; d) Armstrong, A.; Pullin, R. D. C.; Jenner, C. R.; Scutt, J. N. *J. Org. Chem.* **2010**, *65*, 3499.; e) Armstrong, A.; Baxter, C. A.; Lamont, S. G.; Pape, A. R.; Wincewicz, R.. *Org. Lett.* **2007**, *9*, 351.; f) Armstrong, A.; Carbery, D. R.; Lamont, S. G.; Pape, A. R.; Wincewicz, R. *Synlett.* **2006**, *15*, 2504.
10. Xu, J.; Jiao, P. *J. Chem. Soc. Perkin Trans. 1*, **2002**, *12*, 1491.
11. a) Quinn, D. J.; Haun, G. J.; Moura-Letts, G. *Tetrahedron. Lett.*, **2016**, *57*, 3844; b) An, X.-D.; Yu, S. *Org. Lett.* **2015**, *17*, 5064; c) Laulhé, S.; Gori, S. S.; Nantz, M. H. *J. Org. Chem*, **2012**, *77*, 9334.
12. a) Leggio, A.; Velsito, E. L.; Gallo, S.; Liguori. A. *Tet. Lett.* **2017**, *58*, 1512.; b) Hyodo, K.; Togashi, K.; Oishi, N.; Hasegawa, G.; Uchida, K.. *Org. Lett.* **2017**, *19*, 3005. c) Mitra, B.; Pariyar, G. C.; Singha, R.; Ghosh, P.. *Tet. Lett.* **2016**, 2298; d) Noh; J. H.; Kim, K.. *J. Org. Chem.* **2015**, *80*, 11624;
13. Jain, S. R.; Chellappa, D. *Proc. Indian. Acad. Sci.* **1985**, *95*, 381.; b) Wagle, U. D.; Belford, T. J.. *Manufacture of organic hydrazines*, 1979, US06022742; c) Clasen, H.. *Process for the manufacture of organic hydrazines*, 1974, US066694A; d) Sisler, H. H.;

Robert, M.. *Process of forming hydrazine,* 1950, US2710248A; e) Lawrence, S. A. *Amines: Synthesis, Properties, and Applications*; Cambridge University Press: Cambridge, UK, 2004, pp 177.
14. Darwich, C.; Elkhatib, M.; Pasquet, V.; Delalu, H. *Kinet. Catal,* **2013**, *54*, 649.
15. Clasen, H. *Process for the manufacture of organic hydrazines.* 1974, US4066698A
16. N-Nucleophiles. Mayr's Database of Reactivity Parameters. https://www.cup.lmu.de/oc/mayr/reaktionsdatenbank/fe/showclass/40 (accessed March 20, 2019).
17. Oda, J.; Horiike, M.; Inouye, Y. *Bull. Inst. Chem. Res., Kyoto. Univ.* **1972.** *50*, 183.
18. a) Yoshimura, T.; Omata, T. *J. Org. Chem.* **1976**, *41*, 1278; b) Tamura, Y.; Matsushima, H.; Minamikawa, J.; Ikeda, M.; Sumoto, K. *Tetrahedron.* **1975**, *31*, 3035; c) Kucsman, Á; Kapovits, I. *Phosphorus Sulfur Silicon Relat. Elem.* **1977**, *3*, 9.
19. For recent examples on sulfoxide synthesis, see the following and the references cited therein: a) Wang, L.; Chen, M.; Zhang, P.; Li, W.; Zhang, J. *J. Am. Chem. Soc.*, **2018**, *140*, 3467; b) Zhao, L.; Zhang, H.; Wang, Y. *J. Org. Chem.*, **2016**, *81*, 129; c) Yue, H.-L.; Klussmann, M. *Synlett,* **2016**, *27*, 2505; d) Lenstra, D. C.; Vedovato, V.; Flegeau, E. F.; Maydom, J.; Willis, M. C. *Org. Lett.*, **2016**, *18*, 2086; e) Imada, Y.; Tonomura, I.; Komiya, N.; Naota, T. *Synlett,* **2013**, *24*, 1679; f) Dai, W.; Li, J.; Chen, B.; Li, G.; Lv, Y.; Wang, L.; Gao, S. *Org. Lett.*, **2013**, *15*, 5658; g) Bahrami, K.;. Khodaei, M. M.; Arabi, M. S. *J. Org. Chem.*, **2010**, *75*, 6208.
20. For recent examples on sulfoximine synthesis, see the following and the references cited therein: a) Yu, H.; Li, Z.; Bolm, C. *Angew. Chem. Int. Ed.* **2018**, *57*, 324; b) Degennaro, L.; Tota, A.; De Angelis, S.; Andresini, M.; Cardellicchio, C.; Capozzi, M. A.; Romanazzi, G.; Luisi, R. *Eur. J. Org. Chem.* **2017**, 6486; c) Dannenberg, C. A.; Bizet, V.; Bolm, C. *Synthesis*, **2015**, *47*, 1951; d) Zenzola, M.; Doran, R.; Luisi, R.; Bull, J. A. *J. Org. Chem.*, **2015**, *80*, 6391; e) Lücking, U. *Angew. Chem. Int. Ed.* **2013**, *52*, 9399.
21. For recent examples on sulfilimine synthesis, see the following and the references cited therein: a) Dannenberg, C. A.; Fritze, L.; Krauskopf, F.; Bolm, C. *Org. Biomol. Chem.* **2017**, *15*, 1086; b) Bizet, V.; Hendriks, C. M. M.; Bolm, C. *Chem. Soc. Rev.*, **2015**, 44, 3378; c) Bizet, V.; Bolm, C. *Eur. J. Org. Chem.* **2015**, 2854; d) Candy, M.; Guyon, C.; Mersmann, S.; Chen, J.-R.; Bolm, C. *Angew. Chem. Int. Ed.* **2012**, 51, 4440.
22. Ura, Y.; Sakata, G. "Chloroamines." *Ullmann's Encyclopedia of Industrial Chemistry* (7th ed.). Wiley: Hoboken, NJ, 2007; pp. 5.
23. a) Furukawa, N.; Akasaka, T.; Oae, S.; Yoshimura, T. *Tetrahedron*, **1977**, *22*, 1061. ; b) Fernandez, I; Khiar, N. *Science of Synthesis*, **2007**, *31a*, 1001.
24. Laleu, B.; Machado, M. S.; Lacour, J. *Chem. Comm.* **2006**, 0, 2786.
25. a) Gelas-Mialhe, Y.; Vessière, R. *Synthesis*, **1980**, 1005; b) Georg, G. I.; Pfeifer, S. A. *Tetrahedron Letters*, **1985**, *26*, 2739.
26. Gilchrist, T. L.; Moody, C. *J. Chem. Rev.* **1977**, 77, 409.
27. a) Fan, C.; Lv, X.-Y.; Xiao, L.-J.; Xie, J.-H.; Zhou, Q.-L. *J. Am. Chem. Soc.* **2019**, *141*, 2889. b) Beck, J. F.; Samblanet, D. C.; Schmidt, J. A. R. *RSC. Adv.* **2013**, *3*, 20708; c) Birnbaum, J. E. *J. Am. Acad. Dermatol.* **1990**, *23*, 782.

Chapter 2
Supporting Information

General Considerations

All reactions were performed with commercial reagents and solvents that were used as received, unless otherwise specified. Reagents and starting materials were purchased from Sigma Aldrich, Alfa Aesar, Combi-Blocks, TCI America, and/or Ark Pharm; solvents were purchased from Fischer or Sigma-Aldrich. Concentration and removal of solvents was performed using a Buchi R-210 rotary evaporator with a dry ice/acetone condenser. Column chromatography was carried out using a prepackaged RediSep High-Performance silica column on a Biotage Isolera One flash chromatography system.

Nuclear magnetic resonance (NMR) spectra were recorded on a Bruker 400 or 500 (400 MHz or 500 MHz), using chloroform-d ($CDCl_3$). Chemical shifts are given in parts per million (ppm) from trimethylsilane (0.00) and measured relative to the solvent signal (^{1}H NMR: δ 7.26 for $CDCl_3$; ^{13}C NMR: δ 77.16 for $CDCl_3$). Coupling constants (*J* values) are reported in Hertz (Hz) to the nearest 0.1 Hz. ^{1}H NMR spectra are given in the following order: multiplicity (s, singlet; d, doublet; t, triplet; m, multiplet), coupling constants, number of protons. HRMS was performed using a Jeol Accu-TOF-DART® Mass Spectrometer.

Continuous-flow reactions were carried out in high-purity perfluoroalkoxy (HPFA) tubing, purchased from IDEX Health and Science Technologies. Harvard Apparatus syringe pumps were used to continuously deliver reagents, with either Harvard Apparatus stainless steel syringes or SGE Analytical Science glass syringes. Backpressure regulators were purchased from Zaiput Flow Technologies. For in-line extraction, Pall Zefluor PTFE microfiltration membranes (0.5 μm pore size) were placed inside liquid-liquid separators

from Zaiput Flow Technologies. For chloramine generation, reservoirs of bleach and an ammonium hydroxide/ammonium chloride solution were pumped through a Vaportec E-Series Integrated Flow Chemistry System.

General Procedure for the Continuous-flow Synthesis of Sulfoxides:

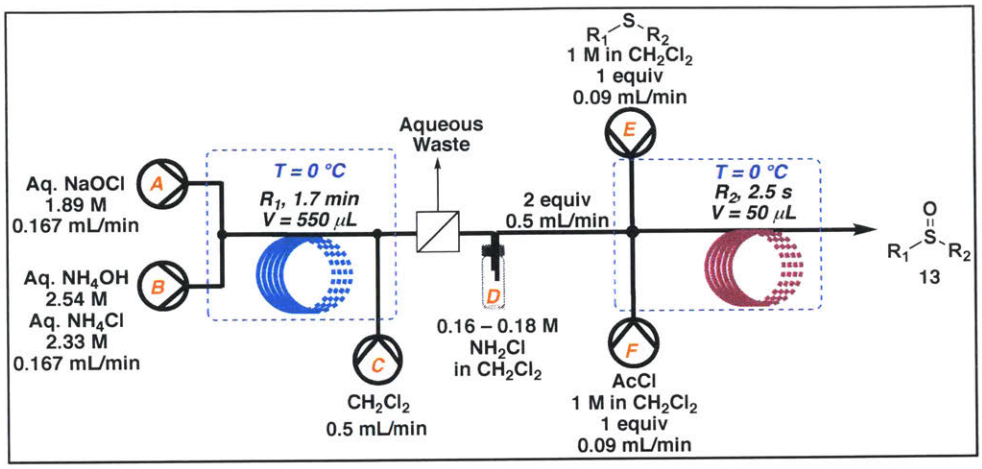

S1. Continuous-flow procedure for the syntheses of sulfoxides.

Stock solution preparation: Stock solution **A** was obtained from a bottle of 10–15% aqueous sodium hypochlorite, by which the exact concentration was determined by iodometric titration against a standardized aqueous sodium thiosulfate solution. For stock solution **D**, a 2 mL volumetric flask was charged with 2 mmol of the desired thioether. Dichloromethane was added to reach a volume of 2 mL. For stock solution **E**, 143 mL (2 mmol) of acetyl chloride were dissolved in dichloromethane up to 2 mL using a volumetric flask.

Procedure: Stock solutions **A** and **B** were separately loaded into glass jar reservoirs. Dichloromethane (**C**) was loaded into a 25 mL SGE glass syringe. Stock solutions **A** and **B** were pumped from a Vapourtec E-Series Integrated Flow Chemistry System at a rate of 167 μL/min each and combined for a residence time of 1.66 min in **R1** at 0 °C. Dichloromethane (**C**) was pumped from a Harvard Apparatus PhD Ultra syringe pump at a rate of 500 μL/min to combine with the outlet of **R1** at 0 °C before entering a membrane-based liquid-liquid separator. The resulting solution of chloramine in CH_2Cl_2 was

collected. The concentration of chloramine was then obtained by iodometric titration against a standardized 0.2 M aqueous sodium thiosulfate solution, typically giving concentrations of 0.15–0.18 M. Flow rates of solutions **D** (1 M, 1 equiv) and **E** (1 M, 1 equiv) were calculated by the concentration of chloramine (2 equiv). A collection time was calculated that would correspond to 1 mmol of starting thioether pumped into the system. Before collection, ten seconds were allowed to pass for equilibration. The heterogeneous product stream flowed into an Erlenmeyer flask filled with methanol as a mild quench (10 mL).

The solution was evaporated on a rotary evaporator, and the sulfoxide re-suspended in dichloromethane. The suspension was transferred to a separatory funnel and washed with saturated aqueous sodium bicarbonate. The organic layer was dried over sodium sulfate, filtered, and the dichloromethane evaporated. The crude sulfoxide was then purified via column chromatography with ethyl acetate and hexanes, using a RediSep High-Performance silica column on a Biotage Isolera One flash chromatography system.

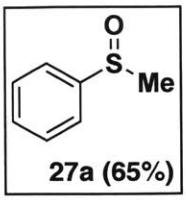

27a (65%)

(Methylsulfinyl)benzene: Purified on silica by eluting with hexanes and ethyl acetate. 65%, 90 mg, yellow oil.

^{1}H NMR (500MHz, $CDCl_3$) ò: 7.65 (dd, J = 8.1, J = 1.6 Hz, 2H), 7.56 – 7.47 (m, 3H), 2.72 (s, 3H); ^{13}C NMR (126 MHz, $CDCl_3$) ò: 131.2, 129.5, 123.6, 44.1. Data consistent with previously reported spectra.[1]

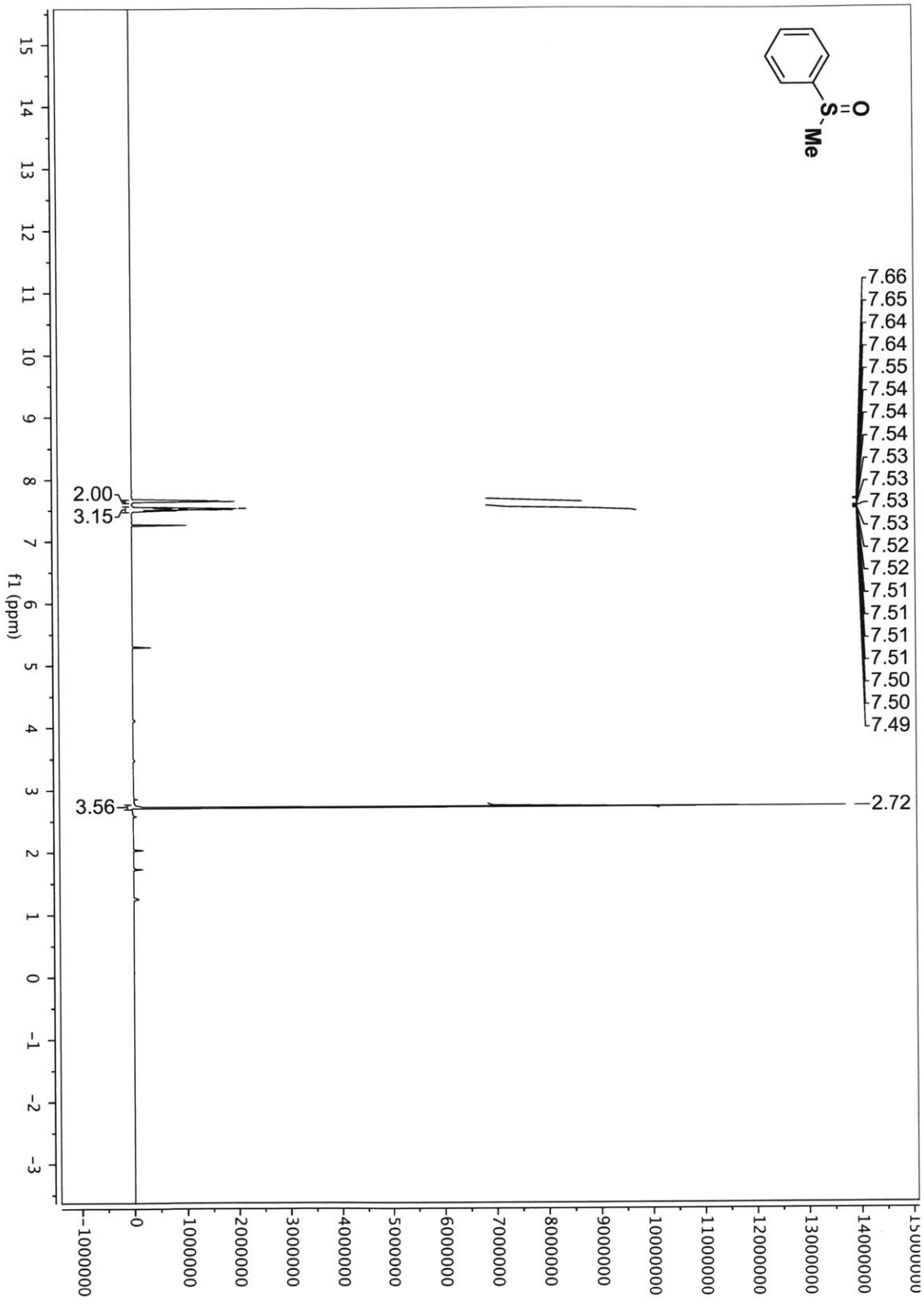

S2. ^{1}H NMR for **27a**.

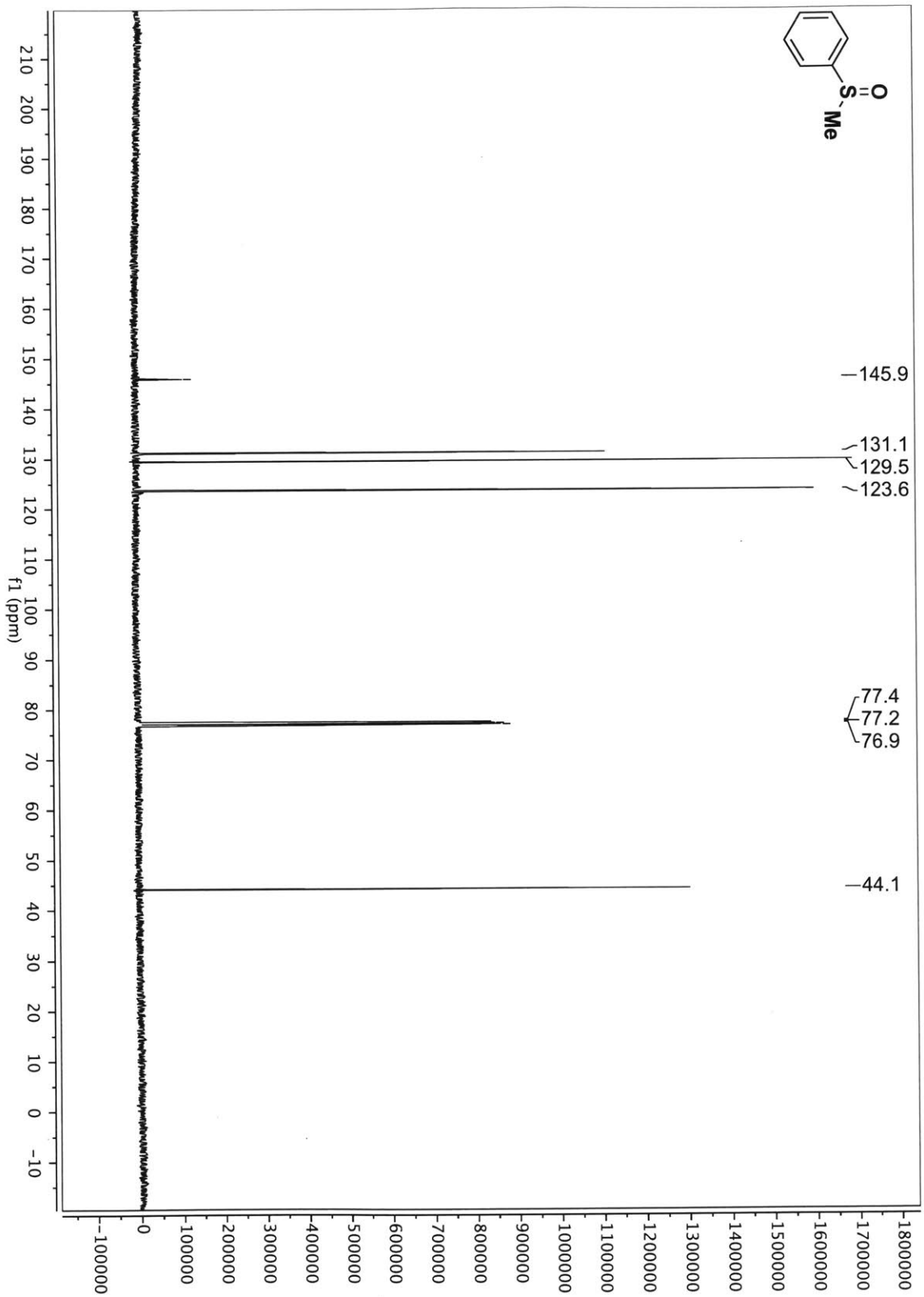

S3. ^{13}C NMR for **27a**.

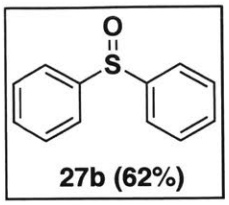

27b (62%)

Diphenyl sulfoxide: Purified on silica by eluting with hexanes and ethyl acetate. 62%, 126 mg, off-white solid.

^{1}H NMR (500MHz, $CDCl_3$) ð: 7.65 (dd, *J* = 7.9, *J* = 1.7 Hz, 1H), 7.51 - 7.39 (m, 2H);

^{13}C NMR (126 MHz, $CDCl_3$) ð: 131.2, 129.5, 124.9. Data consistent with previously reported spectra..[2]

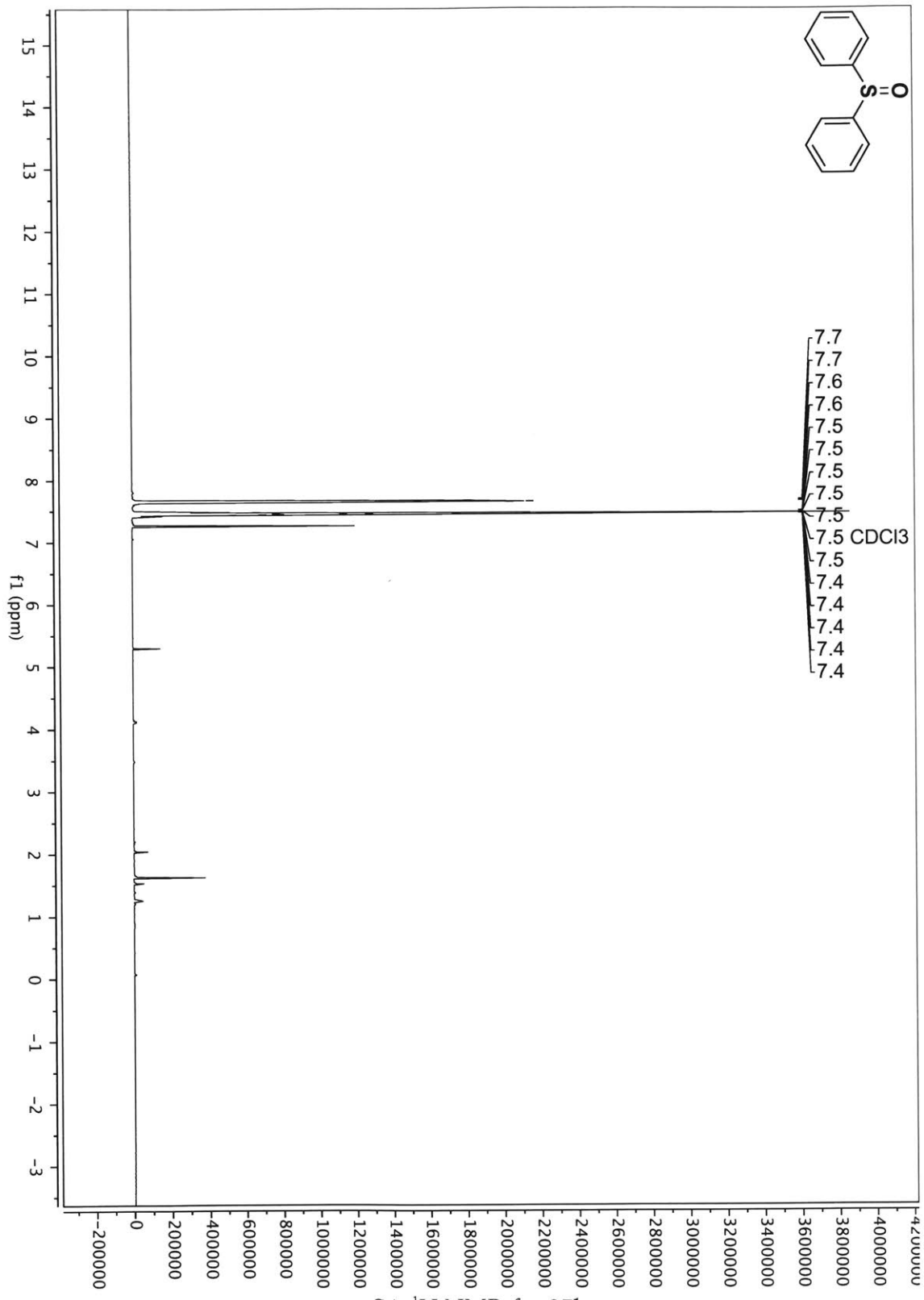

S4. ^{1}H NMR for **27b**.

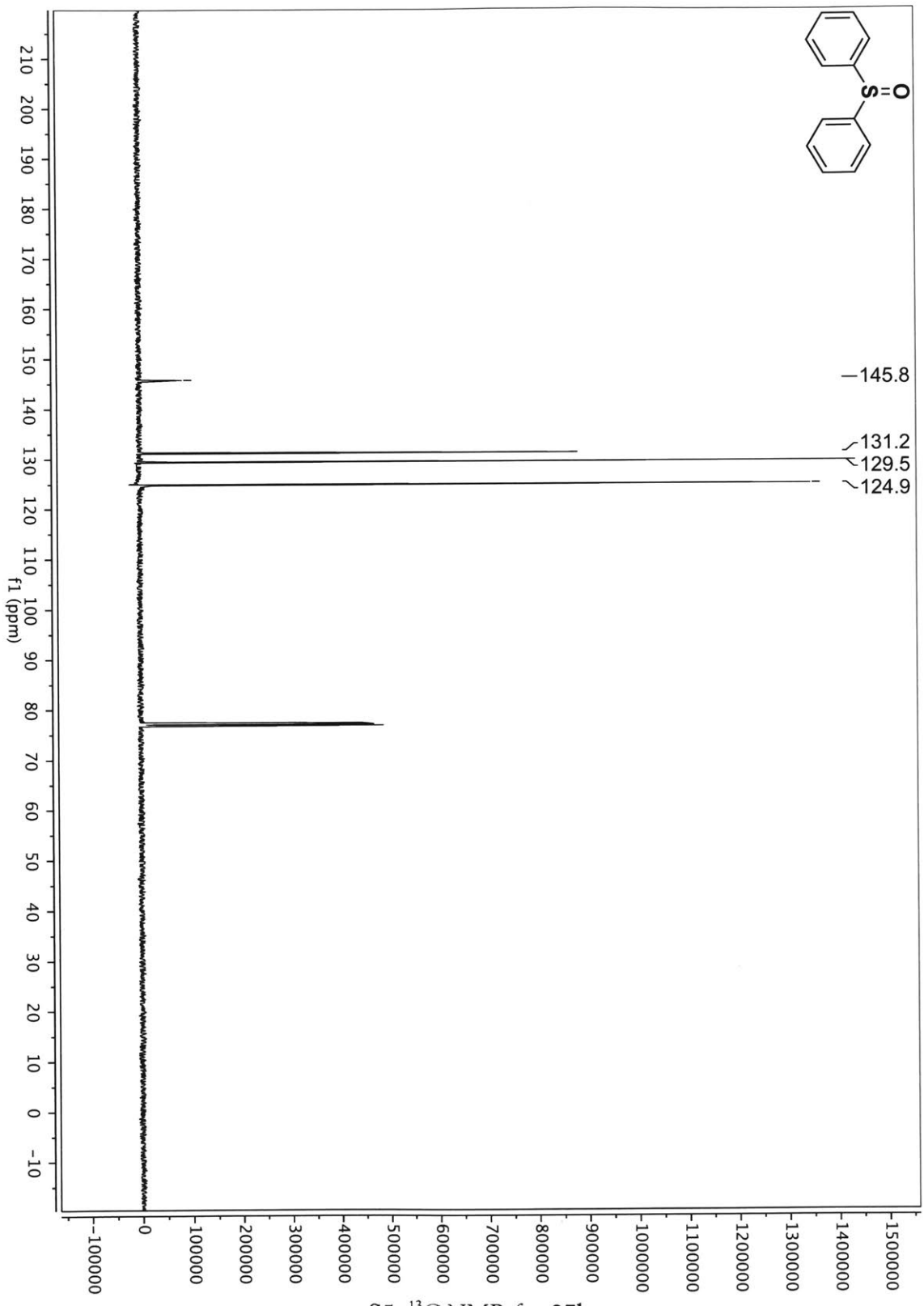

S5. ^{13}C NMR for **27b**.

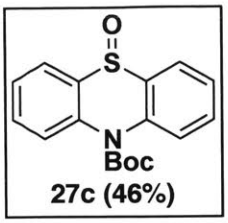

27c (46%)

tert-Butyl 10*H*-phenothiazine-10-carboxylate 5-oxide: Purified on silica by eluting with hexanes and ethyl acetate. 46%, 145 mg, off-white solid.

^{1}H NMR (400MHz, $CDCl_3$) ò: 7.84 (dd, *J* = 7.6, *J* =1.7 Hz, 2H), 7.74 (dd, *J* = 7.9, 1.3 Hz, 2H), 7.46 (ddd, *J* = 14.8, *J* = 7.7, *J* = 1.5 Hz, 4H), 1.54 (s, 9H); ^{13}C NMR (126 MHz, $CDCl_3$) ò: 130.2, 126.9, 126.4, 124.2, 28.3; HRMS (ESI/AccuTOF) $[M + H]^+$ m/z: Calcd for ($C_{17}H_{17}NO_3S$) 316.1002; Found 316.1019.

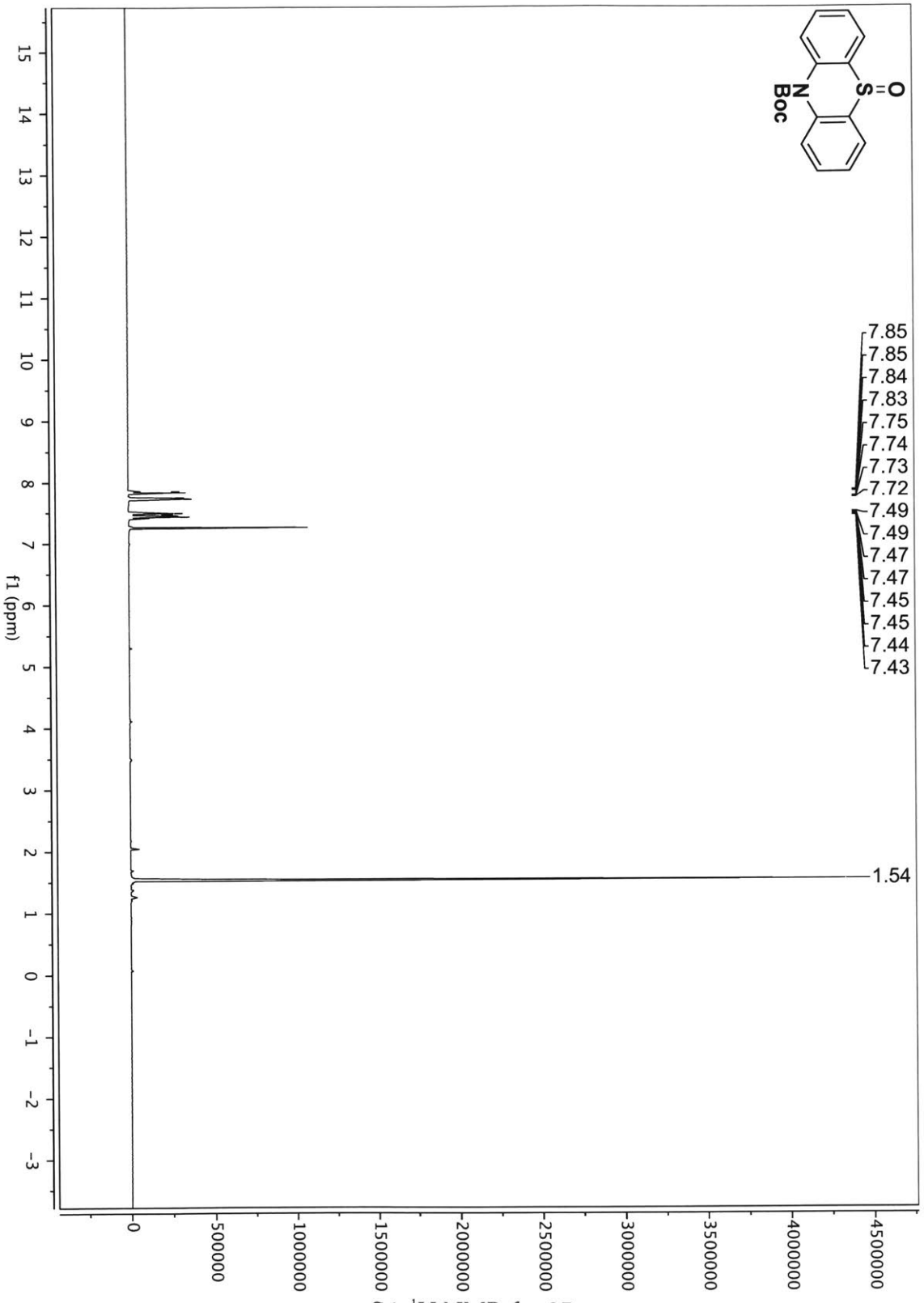

S6. ^{1}H NMR for **27c**.

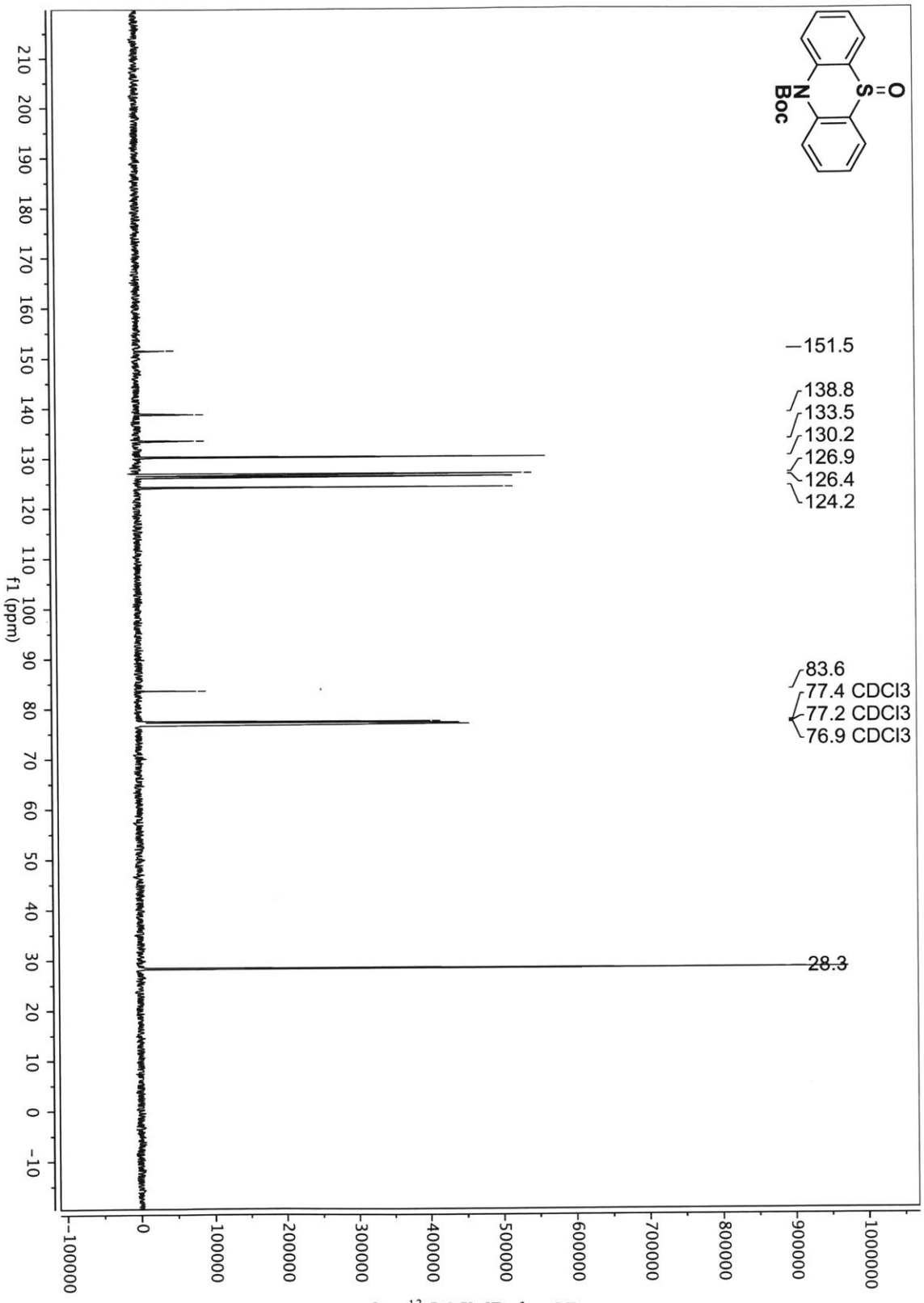

S7. ^{13}C NMR for **27c**.

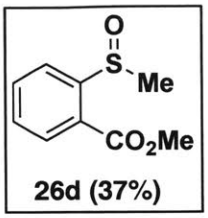

26d (37%)

Methyl-2- -(methylsulfinyl)benzoate: Purified on silica by eluting with hexanes and ethyl acetate. Mass balance was a mixture of products resulting from reaction between the preformed sulfilimines and the adjacent methyl ester. 36%, 73 mg, clear oil.

^{1}H NMR (400MHz, $CDCl_3$) ò: 8.32 (dd, *J* = 8.0 Hz, *J* =1.2 Hz, 1H), 8.09 (dd, *J* = 7.7 Hz, *J* = 1.3 Hz, 1H), 7.83 (d, *J* = 1.3 Hz, 1H), 7.58 (dd, *J* = 7.5 Hz, *J* = 1.3 Hz, 1H), 3.95 (s, 3H), 2.85 (s, 3H); ^{13}C NMR (125MHz, $CDCl_3$) ò: 165.9, 150.6, 134.3, 130.9, 130.3, 126.6, 124.3, 52.8, 44.2. Data consistent with previously reported spectra.[4]

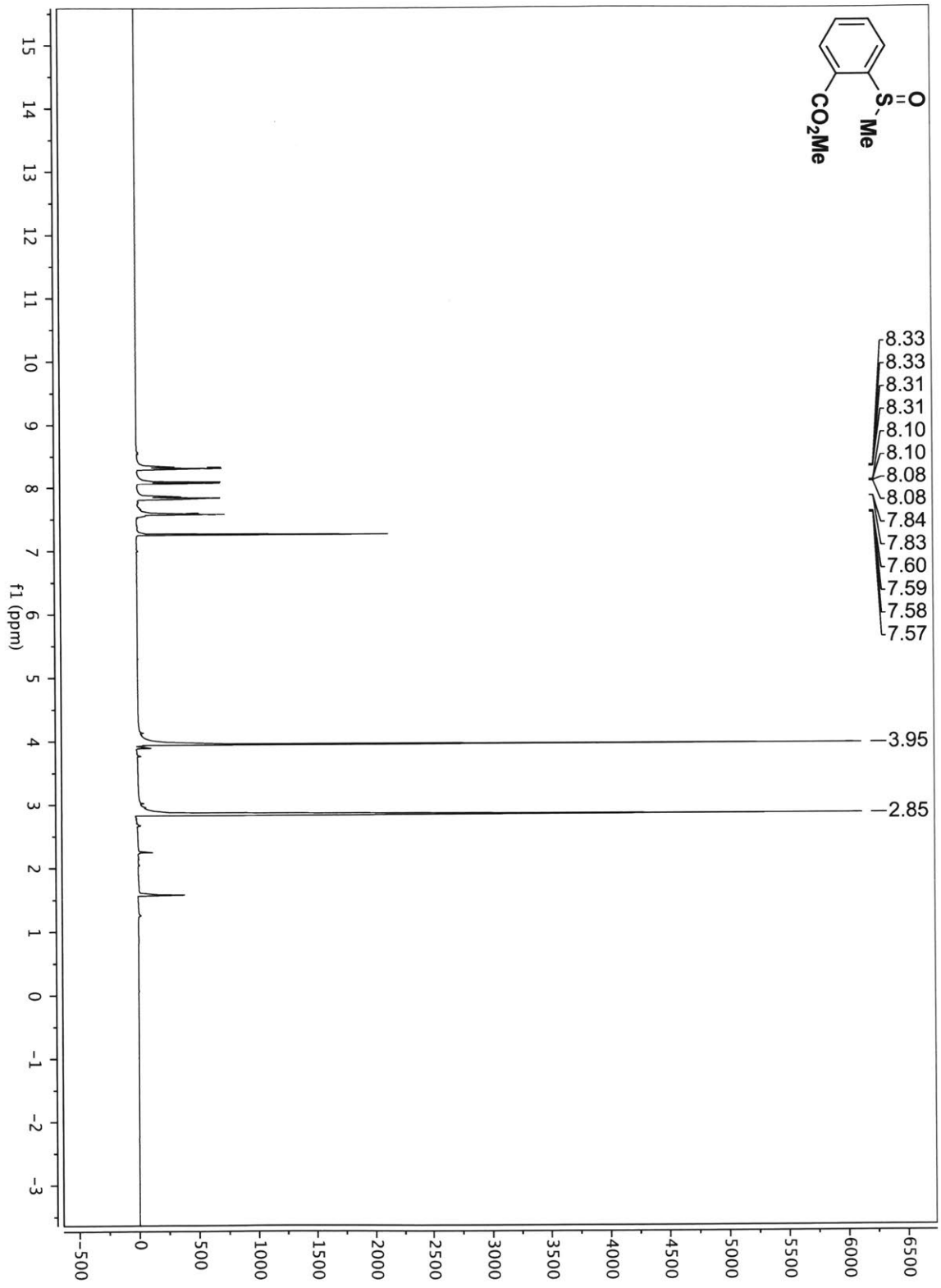

S8. ^{1}H NMR for **27d**.

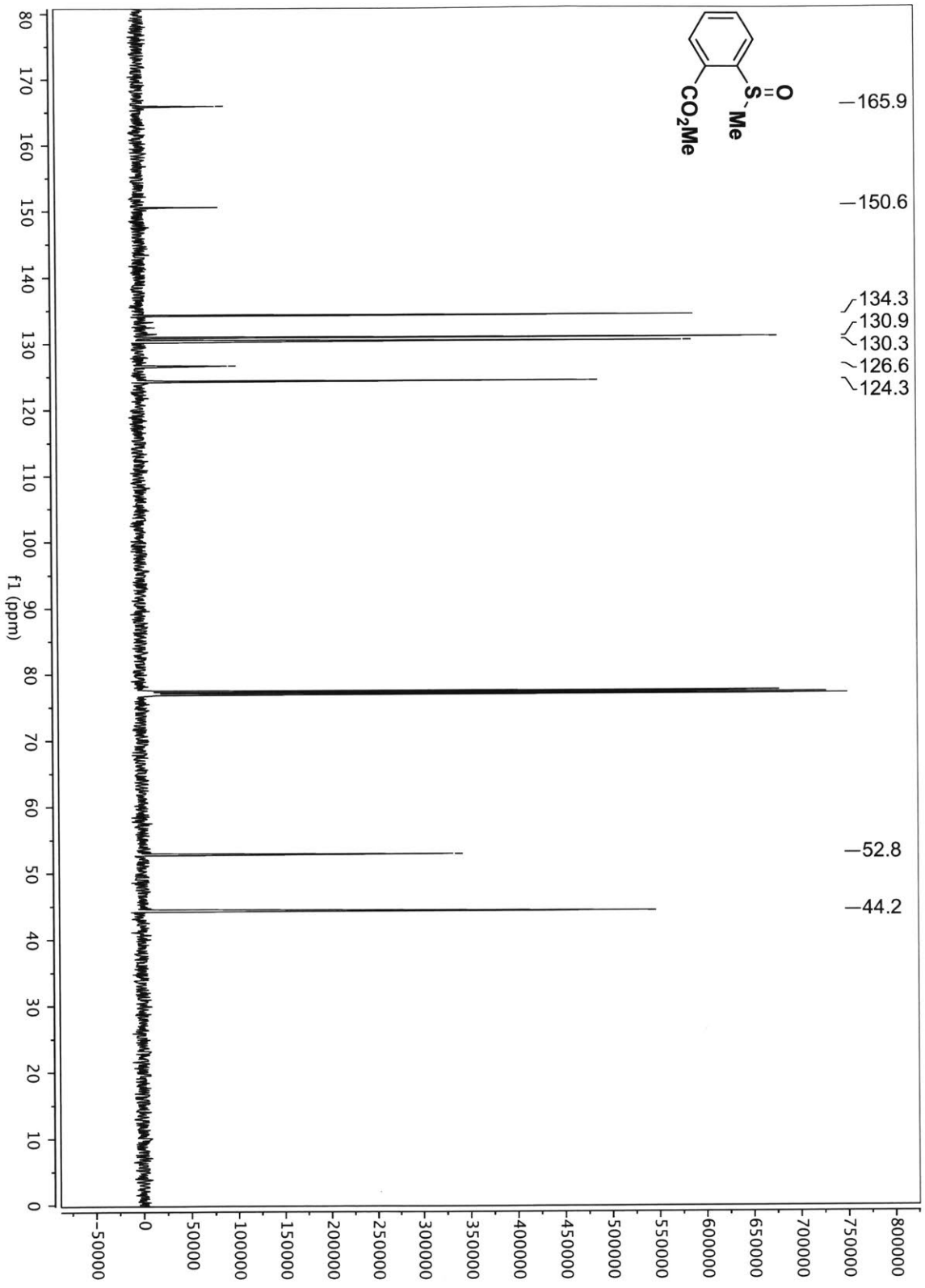

S9. ^{13}C NMR for **27d**.

Characterization of Allylic Sulfenamide

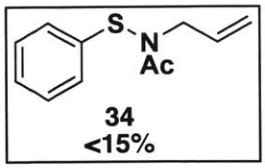

***N*-allyl-*N*-(phenylthio)acetamide:** The general procedure for sulfoxides was followed. Mass balance of the reaction was a mixture of starting material and sulfoxide. Purified on silica by eluting with hexanes and ethyl acetate. 32 mg, yellow oil. Complex mixture of compound, compound degradation, and methanol. Upon further attempts to purify and dry, the sample decomposed to various sulfonylated products, including *S*-phenyl benzene thiosulfonate as identified by GC-MS and confirmed by analysis of known spectra.[5] Comparisons are shown in the following spectra. ^{13}C NMR peaks were tentatively assigned by ruling out degradation peaks growing into the NMR.

^{1}H NMR (400MHz, $CDCl_3$) ð: 7.36 (t, *J* = 7.7 Hz, 3H), 7.25 – 7.18 (m, 1H), 7.11 (d, *J* = 7.8 Hz, 2H), 5.85 (ddt, *J* = 17.4 Hz, *J* = 9.8 Hz, *J* = 6.1 Hz, 1H), 5.24 – 5.11 (m, 2H), 4.25 (d, *J* = 6.1 Hz, 2H), 3.48 (s, 1H), 2.36 (s, 3H); ^{13}C NMR (100MHz, $CDCl_3$) ð: 176.4, 137.9, 132.9, 129.5, 126.7, 123.1, 118.2, 53.9, 22.2; HRMS (ESI/Accu-TOF) $[M + H]^+$ m/z: Calcd for ($C_{11}H_{13}NOS$) 208.0791; Found 208.0818.

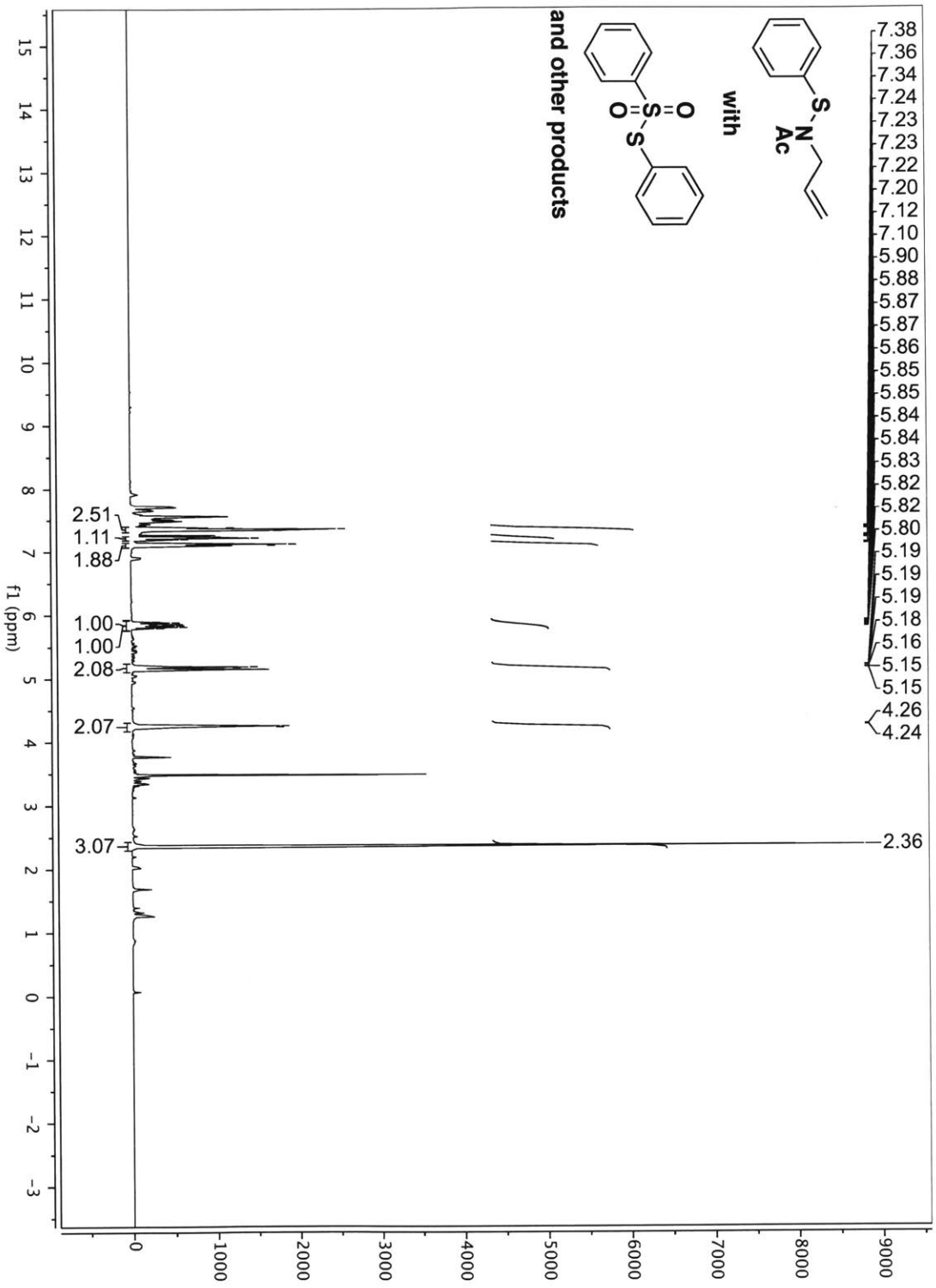

S10. ^{1}H NMR for **31**, contaminated with methanol and degradation products, including *S*-phenylbenezene thiosulfonate as the major impurity.

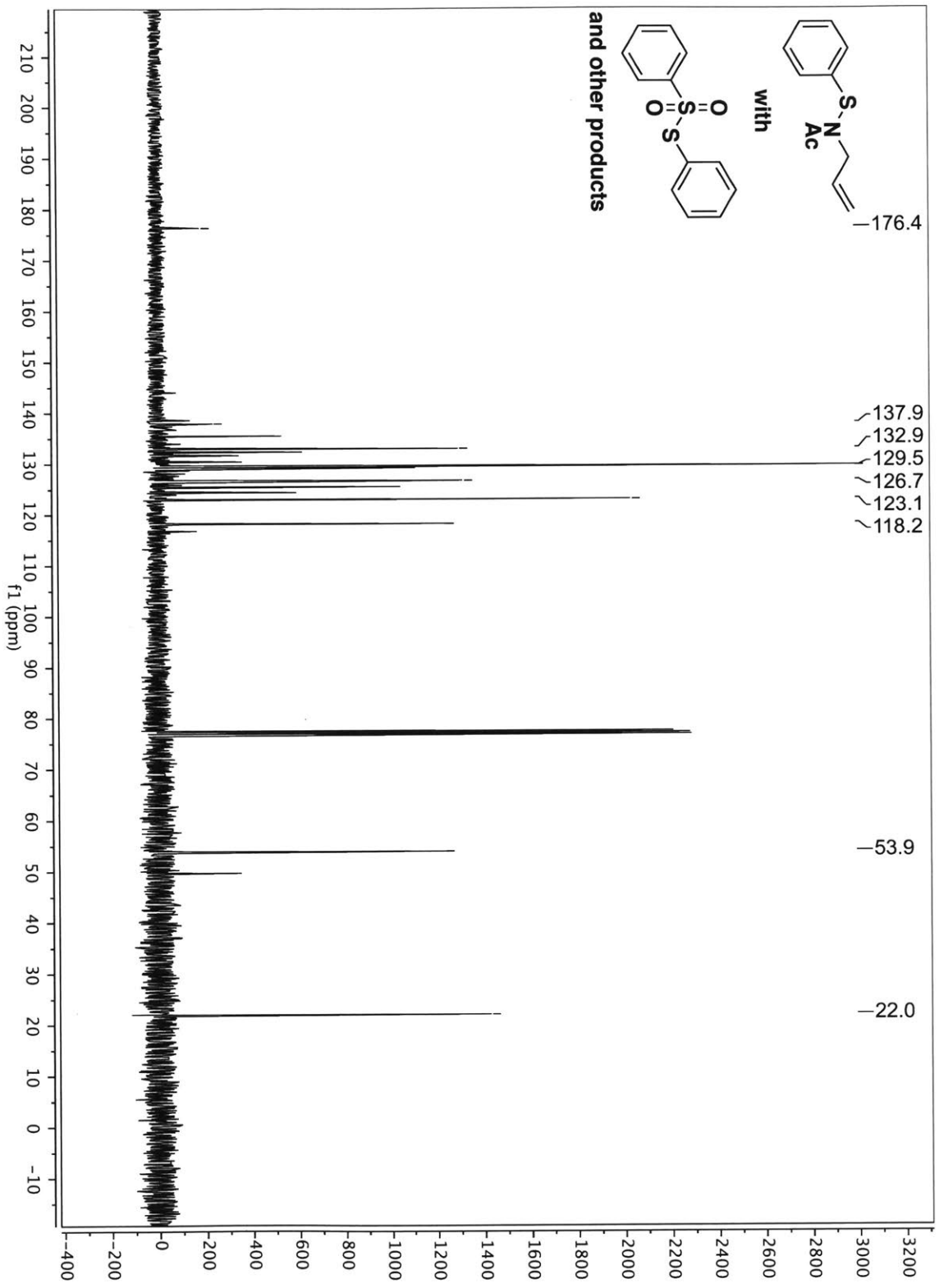

S11. ^{13}C NMR for **31**, contaminated with methanol and degradation products, including *S*-phenylbenezene thiosulfonate as the major impurity.

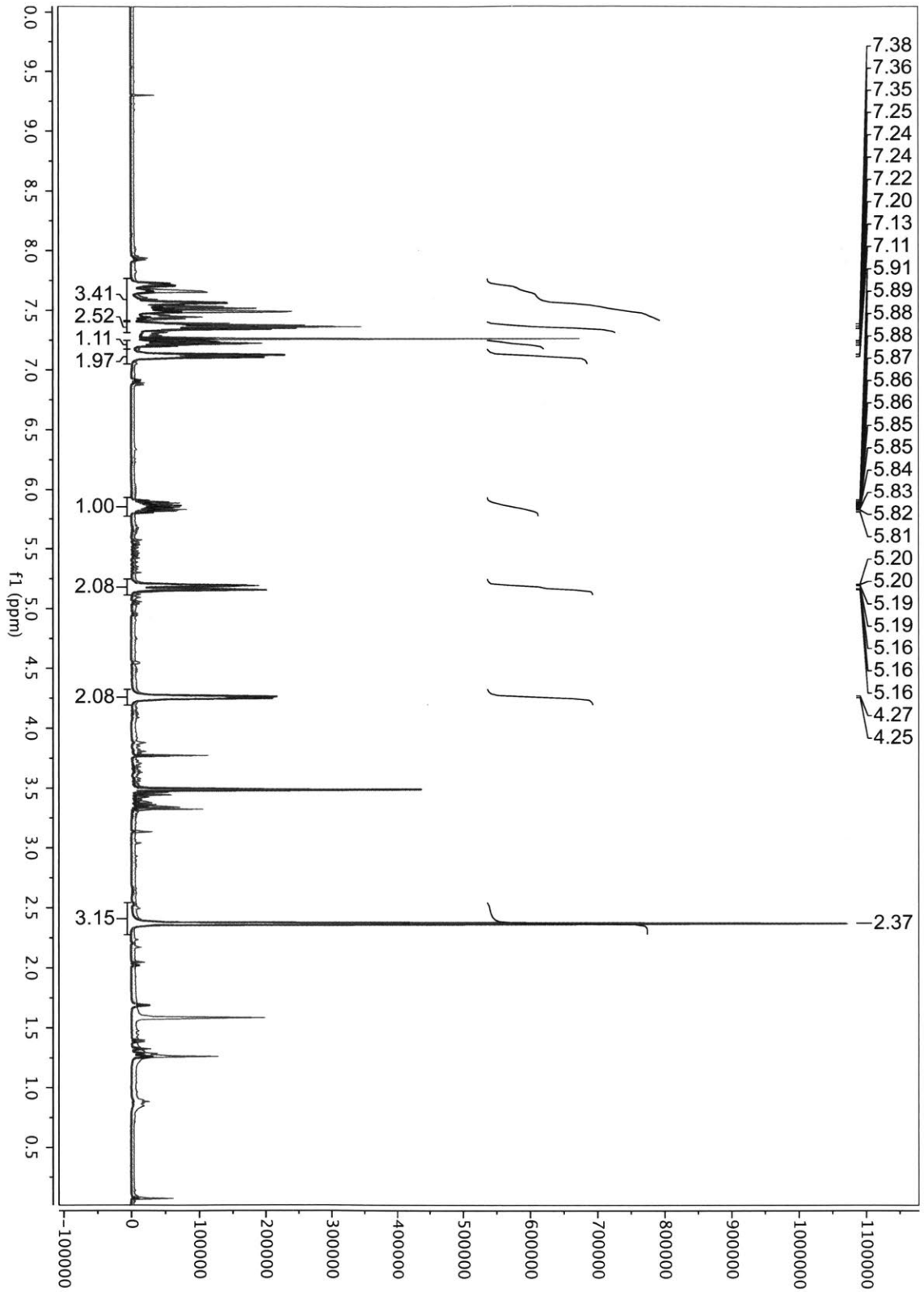

S13. ^{1}H NMR for **31**, before (red) and after (green) further drying and purification attempts, showing further degradation to *S*-phenylbenezene thiosulfonate and other impurities.

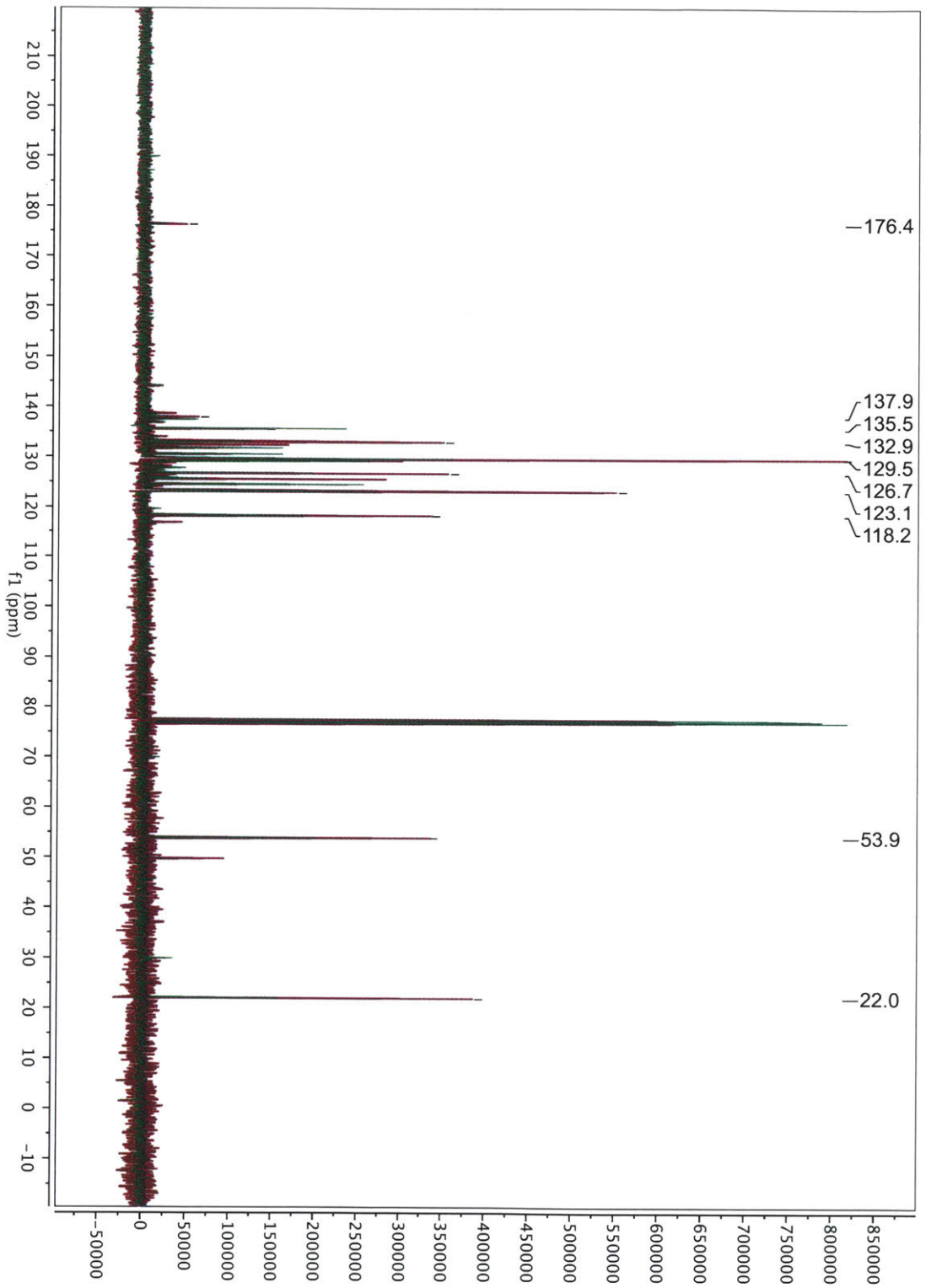

S14. ^{13}C NMR for **31**, before (red) and after (green) further drying and purification attempts, showing further degradation to *S*-phenylbenezene thiosulfonate and other impurities.

References

1. Yuan, Y.; Shi, X.; Liu, W. *Synlett.* **2011**, 559.
2. Jiang, J.; Luo, R.; Zhou, X.; Cheng, Y.; Ji, H. *Adv. Synth. Catal.* **2018**, 360, 4402.
3. Dai, W.; Shang, S. Lv, Y.; Li, G. Li, C.; Gao, S. *ACS. Catal.* **2017**, 7, 4890.
4. Dai, W.; Li, G.; Wang, L.; Chen, B.; Shang, S.; Lv, Y.; Gao, S. *RSC Adv.* **2014**, 4, 46545.
5. Sobhani, S.; Aryanejad, S.; Maleki, M. F. *Synlett.* **2011**. 319.

Chapter 3
Synthesis and Purification of (*S*)-Naproxen in Continuous-flow

Abstract

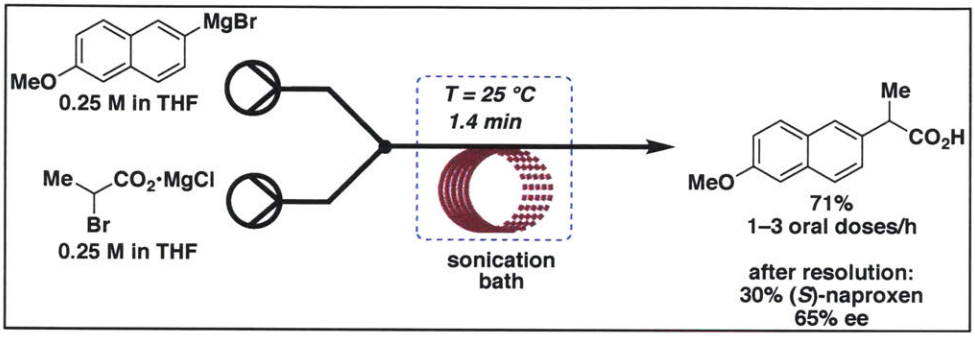

Thesis Supervisor: Timothy F. Jamison
Department Head and Robert R. Taylor Professor of Chemistry

Kelley E. Danahy optimized the synthesis and kinetic resolution of racemic naproxen in batch and continuous-flow. Both K. E. D. and Aria M. Fodness assisted in exploring the potential of enantioselective Kumada couplings and hydrocarboxylations in continuous-flow, and A. M. F. contributed to optimization of the batch enzymatic resolution and optimized the continuous-flow synthesis of racemic naproxen methyl ester. Justin A. M. Lummiss assisted with operation of a continuous oscillatory baffled reactor for handling solids in flow.

Introduction

Naproxen (**1**) has been a popular analgesic since its debut in 1975 and is perhaps best known by its current brand name, Aleve, as marketed by Bayer.[1] Structurally, naproxen is a member of the *propionic acid* class of non-steroidal anti-inflammatory drugs (NSAIDs). However, in contrast to its peers (**Figure 1**), naproxen has the distinction of being sold as the enantiopure (*S*)-naproxen, rather than a racemate. As the (*R*)-enantiomer is a suspected liver toxin,[2] all current processes to produce naproxen rely on a chiral resolution, as shown in **Scheme 1**.[1]

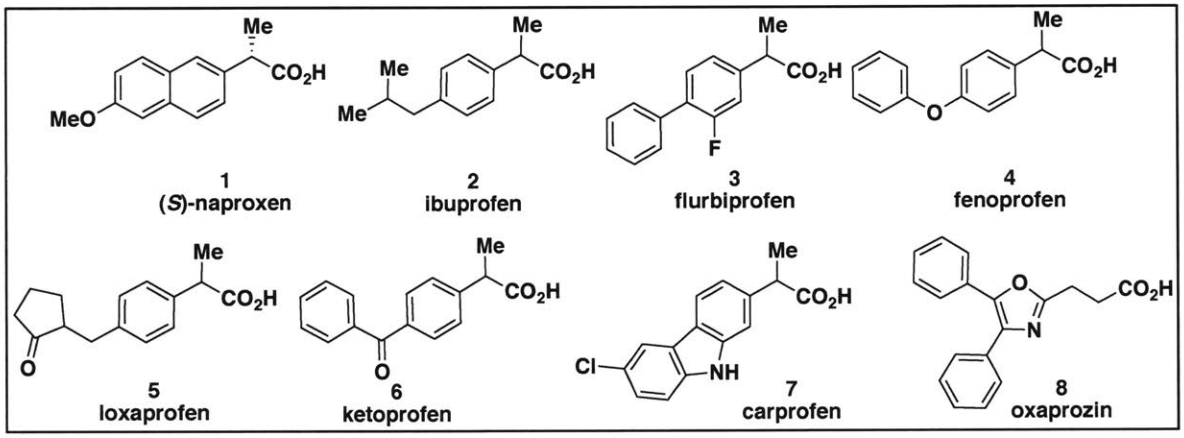

Figure 1. The structures of a variety of propionic acid NSAIDs currently on the market. All except naproxen are sold as their racemates.

Many laboratory routes to enantiopure naproxen have been developed, including enantioselective hydrogenation,[3] asymmetric Kumada couplings,[4] and hydrocyanations.[5] However, though these results avoid the necessary 50% loss in yield during chiral resolutions, they are limited by expensive asymmetric ligands, flammable gases at high pressures, need for robust temperature control, and/or toxicity. Altogether, the use of a cheap resolving agent such as *N*-octylglucamine (**Scheme 1**), followed by racemization and

recycling of the undesired *R*-enantiomer, remains the most cost-effective and economical route.[1]

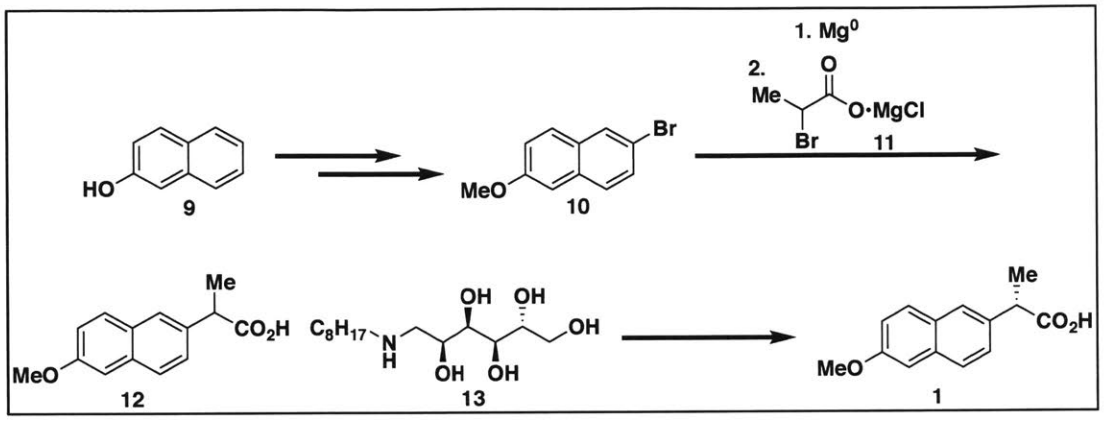

Scheme 1. Typical batch process for the synthesis of **1**.[1]

However, the batch route still has a number of limitations. Namely, the key, exothermic addition of Grignard **10** into an α-haloacid such as **11** (**Scheme 1**) requires stable temperatures, as well as sufficient mixing to prevent side reactions, such as carbonyl addition or deprotonation of the enolizable product. To us, therefore, this represented an opportunity to adapt the synthesis of naproxen to continuous-flow, where superior mixing and temperature control are often easier to achieve.[6]

Optimization of Gringard in Continuous-flow

As shown in **Scheme 1**, the key steps for the synthesis of naproxen involve a Grignard addition to an α-halopropionic acid, followed by chiral resolution using the cheap resolving reagent *N*-octylglucamine. Overall, solid formation proved the main challenge in adapting both steps to a continuous-flow system. Magnesium salts from the Grignard, in addition to our desired recrystallization in a continuous system, frequently clogged the reactor. Additionally, the use of reactors designed to accommodate solids in continuous systems, such as a continuous-stirred tank reactor (CSTR) or a continuous oscillatory baffled reactor (COBR), were ineffective to prevent clogging.

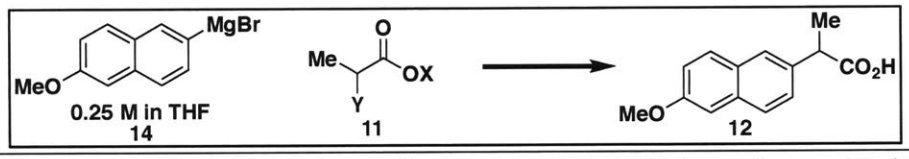

Entry	X	Y	Equiv Gringard	Yield (%)
1	Me	Br	1	44[a]
2	Me	Br	2	74[a,b]
3	Me	Cl	1	7[a]
4	Et	OTf	1	24[a]
5	H	Br	2	36[c]
6	½ Mg	Br	1	35[a,c]
7	MgCl	Br	1	71[d]

Table 1. Yields obtained via a calibration curve on gas chromatography using 1,3,5-trimethoxybenzene as an internal standard. [a]Reaction done in batch, stirred 30 minutes at room temperature. [b]Reaction done in continuous-flow. [c]Yield determined by ^{1}H NMR, using 1,3,5-trimethoxybenzene as an internal standard. [d]Yield determined by isolation of crude material, with a small amount of 2-methoxynapthalene as a contaminant.

Regarding the Grignard addition, we attempted a variety of conditions to enhance the solubility of our reaction system. As shown in **Table 1 (entry 2)**, use of the methyl ester of **11** and two equivalents of Grignard **14** was sufficiently soluble to allow adaptation to continuous-flow. In contrast, the limited solubility of the preformed magnesium salt of **11** rendered this reagent only suitable for batch conditions (**entry 5**). The lower yield from this

result, while precedented in a patented process by Matthews and Arnold (35%), can be at least partially attributed to the difficulty drying the hygroscopic magnesium salt.[7]

Use of different coordinating solvents such as 2-methyltetrahydrofuran worsened solubility and led to no improvement in yield. However, again, based on the procedure of Matthews and Arnold,[7] deprotonation of **14** with one equivalent of methylmagnesium chloride to form the mixed magnesium salt **11** led to 71% yield of the desired racemic product **12** (entry 6). The resulting reaction (t_R = 1.4 minutes) continuously synthesized racemic naproxen with a throughput of 863 mg (3.75 mmol) per hour. Notably, after approximately forty minutes of runtime, magnesium salt accumulation eventually began to clog the system, as before. Use of a sonication bath, however, eliminated this issue, and allowed naproxen to be run for over three hours without clogging (**Scheme 2**).

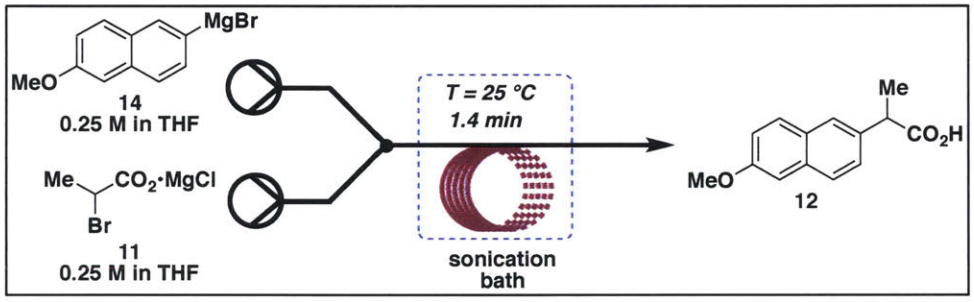

Scheme 2. Continuous-flow production of racemic naproxen.

Optimization of Chiral Resolution in Batch and Continuous-flow

Chemical Kinetic Resolution

The issue of kinetic resolution in continuous-flow proved more difficult to overcome. While kinetic resolutions are known in continuous systems,[8] the current reagent for naproxen is *N*-octylglucamine[1] (**12**), a modified sugar residue that we discovered was insoluble in most organic solvents below 50 °C. Use of more soluble chiral amines, such as α-methylbenzylamine,[9] only yielded racemic naproxen when telescoped with the preceding Grignard step (**Scheme 3**).

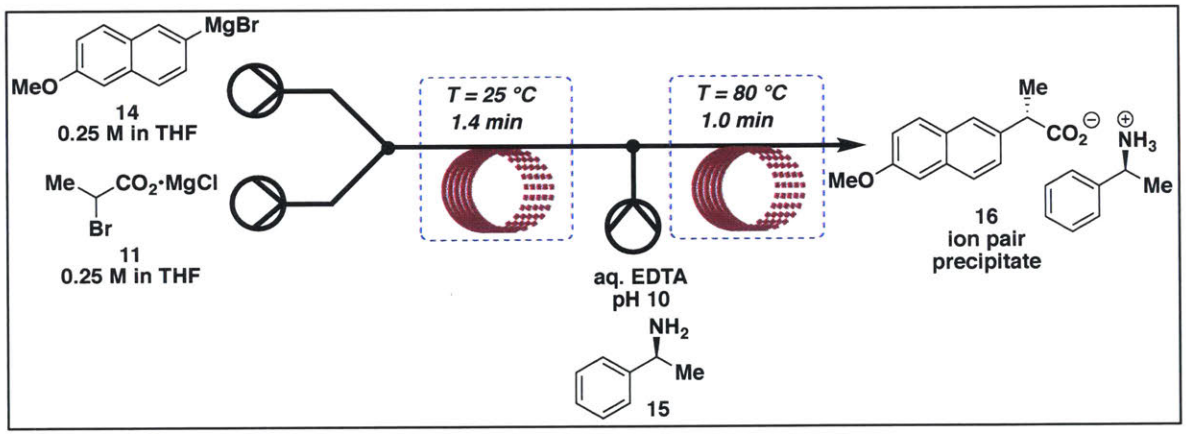

Scheme 3. Attempted telescoped synthesis and chiral resolution of (*S*)-naproxen in continuous-flow.

We postulated that our inefficient resolution could be explained by favored coordination of the leftover magnesium by the chiral amine, rather than formation of the desired carboxylic acid salt. Although a wash with ethylenediamine tetraacetic acid (EDTA), carefully basified to pH 10 to deprotonate all chelating carboxylic acids while avoiding formation of insoluble magnesium hydroxide, improved our ee to >90% during

small scale batch reactions, this was insufficient for adaptation to a continuous system. Ultimately, to ensure all magnesium was removed, the crude racemic naproxen had to be eluted through a small amount of silica gel, offline from a continuous-flow system.

However, as resolution in flow no longer seemed feasible within our desired conditions, we then attempted several reported procedures to resolve naproxen in batch. Despite previous reports, methanol[10a] and acetonitrile[10b] proved inefficient for our material, giving only 51% and 28% ee, respectively. However, use of a Pope-Peachy method,[10c] in which 0.5 equivalents of triethylamine solubilized the undesired *R*-enantiomer, led to our desired (*S*)-naproxen in 65% ee and 30% yield (of 50% expected) after workup (**Scheme 4**).

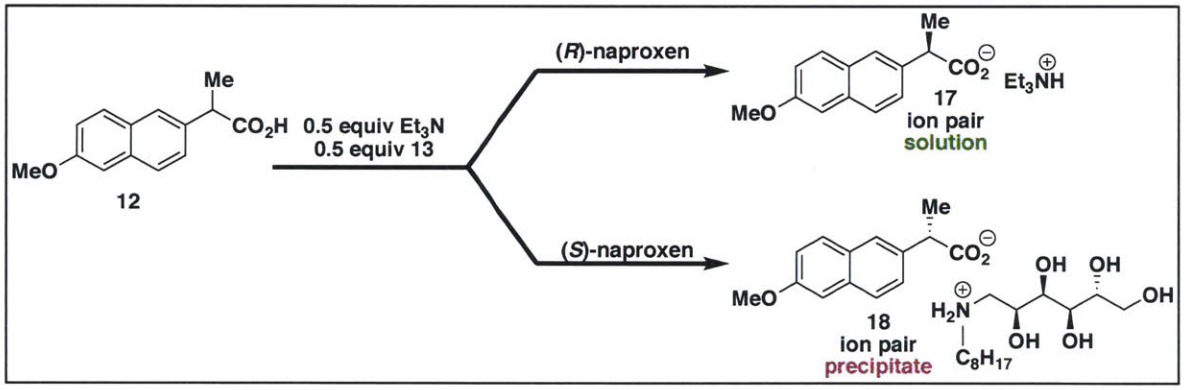

Scheme 4. Chiral resolution of (*S*)-naproxen via a Pope-Peachy method.

Enzymatic Kinetic Resolution

Enzymatic kinetic resolution offered an alternative approach to bypass the solubility issues we had using chiral amines as crystallization reagents. With this method, we envisioned a packed bed of immobilized enzyme that would selectively hydrolyze the methyl ester of racemic naproxen, allowing easy separation of the (*S*)-acid from the (*R*)-ester, as shown in **Scheme 5**.

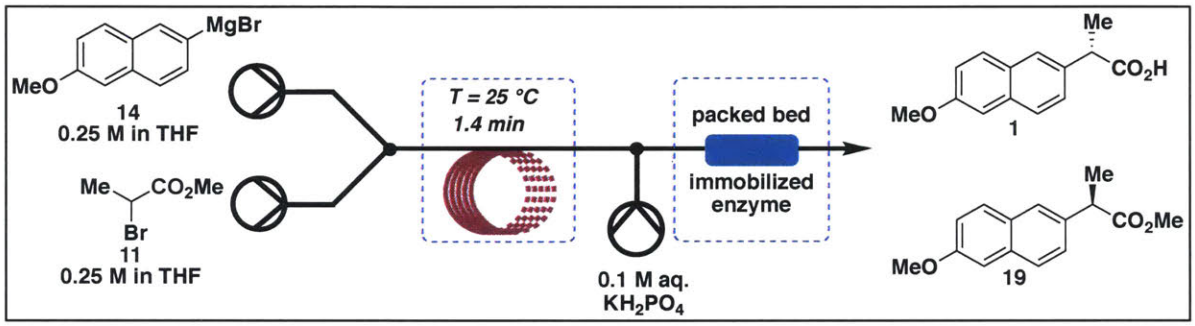

Scheme 5. Proposed enzymatic resolution to (*S*)-naproxen in continuous flow.

Our initial screen of enzymes identified lipase from *Candida rugosa* as the most promising enzyme (**Table 2, entry 1**), in good agreement with previous literature.[11] Though this reaction typically takes ≥12 hours for completion in batch, we ultimately found that a 3:2 mixture of DMSO[12] and 0.1 M aqueous KH_2PO_4 buffered to pH 8, at 42 °C (**Table 2, entry 10**), allowed 70% cleavage in a time of just one hour, and up to 90% in two hours.

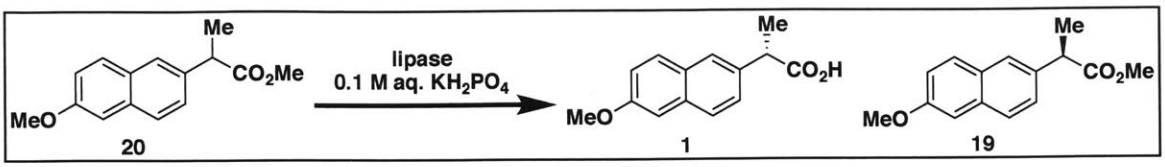

Entry	Enzyme	Additive	pH	Temperature (°C)	ee (%) 1 h	ee (%) 2h
1	*Candida rugosa*	-	7	37	21	46
2	*Candida antartica*	-	7	37	42	33
3	Amano	-	7	37	0	15
4	*Candida rugosa*	-	6[a]	37	35	16
5	*Candida rugosa*	-	8[b]	37	31	66
6	*Candida rugosa*	-	9[b]	37	23	50
7	*Candida rugosa*	-	8[b]	39	37	53
8	*Candida rugosa*	-	8[b]	42	45	75
9	*Candida rugosa*	-	8[b]	45	51	64
10	*Candida rugosa*	DMSO[c]	8[b]	42	67	90

Table 2. ee observed via a Chiralpak® OD-H column on HPLC. Loading was 150 mg enzyme and 10 mg methyl ester **20**. [a] Buffer was treated with 1 M hydrochloric acid to pH 6, as indicated by pH paper. [b] Buffer was treated with 2.5 M sodium hydroxide to desired pH, as indicated by pH paper. [c]A 3:2 ratio of DMSO to aqueous buffer was used.

However, three problems emerged when telescoping this route with the Gringard reaction. First, the Gringard step required high flow rates to avoid clogging, which would thereby necessitate an impractically long packed bed to achieve a residence time of two hours. Second, quenching of the Gringard was required prior to reaching the packed bed of enzyme, yet, even if our potassium phosphate buffer was used as a quench, significant solid formation was observed upon quenching. This would likely clog our system before reaching the packed bed.

The third concerns the effects of organic solvents on enzymes. Namely, THF was found to completely inhibit enzymatic activity. Thus, for this reaction to succeed, THF

would have to be mixed with an aqueous buffer and DMSO before heating to the point that all THF would evaporate. 2-MeTHF was not an alternative, because, while 2-MeTHF is immiscible in water, it too inhibited the reaction once DMSO was added as a cosolvent, as did diethyl ether and *tert*-butyl methyl ether. Most likely, DMSO allowed enough solvent mixing to inhibit the lipase from *Candida rugosa*. Potentially inert solvents, such as hexanes or toluene, also showed no activity. However, for these solvents, we believe that the issue was less enzyme inhibition than naproxen's lipophilicity, which kept naproxen in the organic phase, rather than the aqueous phase necessary to observe enzymatic activity. Addition of tetrabutylammonium bromide as a phase-transfer catalyst did not substantially enhance the reaction progression, and thus the enzymatic resolution route was abandoned.

Conclusion

The efficient, racemic synthesis of (S)-naproxen in continuous-flow requires only 1.4 minutes, allowing for up to 863 mg/h of the desired analgesic, or about 1–3 oral doses per hour.[13] A chiral resolution in batch with commercially available *N*-octylglucamine then yield (*S*)-naproxen in 30% yield and 65% ee. This efficient continuous route may be further adapted to other racemic propionic acid NSAIDs, such as ibuprofen, fenoprofen, and flurbiprofen via a simple change of Grignard reagent.

References

1. Harrington, P. J.; Lodewijk; E. *Org. Process Res. Dev.*, **1997**, *1*, 72.
2. Caron, G.; Tseng, G. W.-M.; Kazlauskas, R. J. *et al. Tetrahedron: Asymmetry* **1994**, *5*, 83.
3. Ohta, T.; Takaya, H.; Kitamura, M.; Nagai, K.; Noyori, R. *J. Org. Chem.* **1987**, *52*, 3174.
4. a) Mao, J.; Liu, F.; Wang, M.; Wu, L.; Zhang, B.; Liu, S.; Zhong, J.; Bian, Q.; Walsh, P. J. *J. Am. Chem. Soc.* **2014**, *136*, 17662; b) Jin, M.; Adak, L.; Nakamura, M. *J. Am. Chem. Soc.* **2015**, *137*, 7128.
5. a) Casalnuovo, A. L., RajanBabu, T. V., Ayers, T. A.; Warren, T. H. *J. Am. Chem. Soc.* **1994**, *116*, 9869; b) RajanBabu, T. V.; Casalnuovo, A. L. *J. Am. Chem. Soc.* **1996**, *118*, 6325.
6. Plutschack, M. B.; Pieber, B.; Gilmore, K.; Seeberger, P. H. *Chem. Rev.* **2017**, *117*, 11796.
7. Matthews, G. J.; Arnold, R. A. *Preparation of 2-arylpropionic acids by direct coupling utilizing a mixed magnesium halide complex*,1977, US414397A.
8. For recent reports, see the following and the references cited therein: a) Escribà-Gelonch, M.; Hessel, V.; Maier, M. C.; Noël, T.; d'Angelo, M. F. N.; Gruber-Woelfler, H. *Org. Process Res. Dev.* **2018**, *22*, 178; b) Vartak, S.; Myerson, A. S. *Org. Process Res. Dev.* **2017**, *21*, 253; c) Quon, J. L.; Zhang, H.; Alvarez, A.; Evans, J.; Myerson, A. S.; Trout, B. L. *Cryst. Growth Des.* **2012**, *12*, 3036; d) Narducci, O.; Jones, A. G.; Kougoulos, E. *Chem. Eng. Sci.* **2011**, *66*, 1069; e) Lawton, S.; Steele, G.; Shering, P. *Org. Process Res. Dev.* **2009**, *13*, 1357.
9. Chodankar, N. K.; Oak, G. M. *Resolution of alpha-arylpropionic acids*, 1999, EP1029846A1.
10. a) Syntex Corp. *6-methoxy-methyl-2-napthalene-acetic acid resolution.* 1978, GB20225968A; b) Yuan, X.; Li, J.; Tian, Y.; Lee, G.-H.; Peng, X.-M.; Zhu, R.; You, X. *Tetrahedron: Asymmetry*. 2001, *12*, 3015; c) Von Morze, H. *Process for the preparation of (d) 2-(d-methoxy-2-naphthyl) propionic acid and pharmaceutically acceptable salts thereof and new intermediates therefor.* 1983, EP0095901A1.
11. a) Sayin, S.; Akoz, E.; Yilmaz, M. *Org. Biomol. Chem.* **2014**, *12*, 6634; b) Yilmaz, E.; Sezgin, M.; Yilmaz, M. *J. Mol. Catal. B. Enzym.* **2011**, *69*, 35; c) Yilmaz, E.; Can, K.; Sezgin, M.; Yilmaz, M. *Bioresour, Technol.* **2011**, *102*, 499.
12. Watanabe, K.; Ueji, S. *J. Chem. Soc., Perkin Trans. 1*, **2001**, 0, 1386.
13. Naproxen (Oral Route) Proper Use. https://www.mayoclinic.org/drugs-supplements/naproxen-oral-route/proper-use/drg-20069820 (accessed 18 March 2019).

Chapter 3
Supporting Information

General Considerations

All reactions were performed with commercial reagents and solvents that were used as received, unless otherwise specified. Reagents and starting materials were purchased from Sigma Aldrich, Alfa Aesar, Combi-Blocks, TCI America, and/or Ark Pharm; solvents were purchased from Fischer or Sigma-Aldrich. Concentration and removal of solvents was performed using a Buchi R-210 rotary evaporator with a dry ice/acetone condenser. Column chromatography was carried out using a prepackaged RediSep High-Performance silica column on a Biotage Isolera One flash chromatography system.

Nuclear magnetic resonance (NMR) spectra were recorded on a Bruker 400 (400 MHz), using chloroform-d ($CDCl_3$). Chemical shifts are given in parts per million (ppm) from trimethylsilane (0.00) and measured relative to the solvent signal (^{1}H NMR: δ 7.26 for $CDCl_3$; ^{13}C NMR: δ 77.16 for $CDCl_3$). Coupling constants (*J* values) are reported in Hertz (Hz) to the nearest 0.1 Hz. ^{1}H NMR spectra are given in the following order: multiplicity (s, singlet; d, doublet; t, triplet; m, multiplet), coupling constants, number of protons.

Continuous-flow reactions were carried out in high-purity perfluoroalkoxy (HPFA) tubing, purchased from IDEX Health and Science Technologies. Harvard Apparatus syringe pumps were used to continuously deliver reagents, with either Harvard Apparatus stainless steel syringes or SGE Analytical Science glass syringes. Backpressure regulators were purchased from Zaiput Flow Technologies. For in-line extraction, Pall Zefluor PTFE microfiltration membranes (0.5 μm pore size) were placed inside liquid-liquid separators from Zaiput Flow Technologies.

HPLC was performed using an Agilent Technologies 1290 Infinity II High Performance Liquid Chromatography sampler, using a Chiralpak® AD-H column. UV wavelengths at 220 nm were used to observe naproxen.

Procedure for the Syntheses of Starting Materials

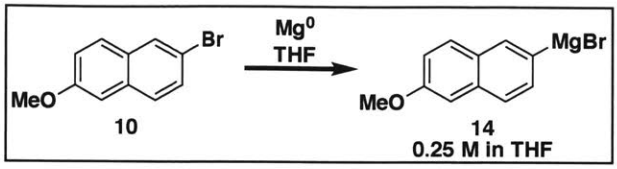

(6-methoxynaphthalen-2-yl) magnesium bromide, 0.25 M in THF: 6-methoxy-2-bromonaphthalene (10.43 g, 40 mmol) was added to an oven-dried Schlenk flask. The flask was purged with nitrogen three times, and 1.06 g (44 mmol, 1.1 equivalents) Mg powder, obtained from a glovebox, were added. Dry THF was added until the total volume of solution equaled 150 mL, and the reaction was stirred overnight. The resulting Gringard was titrated with phenanthroline and dry methanol to yield a concentration of 0.25 M.

2-bromopropionate magnesium chloride, 0.25 M in THF: 2-bromopropionic acid (3.6 mL, 40 mmol) was added to an oven-dried Schlenk flask under nitrogen, followed by 137 mL THF. The solution was cooled to 0 °C and 13.3 mL methyl magnesium chloride (3 M in THF) were added slowly. Bubbling was observed. After addition, the reaction was warmed to room temperature overnight and stored under inert atmosphere for use in the continuous-flow synthesis of naproxen.

Procedure for the Synthesis and Chiral Resolution of (S)-Naproxen

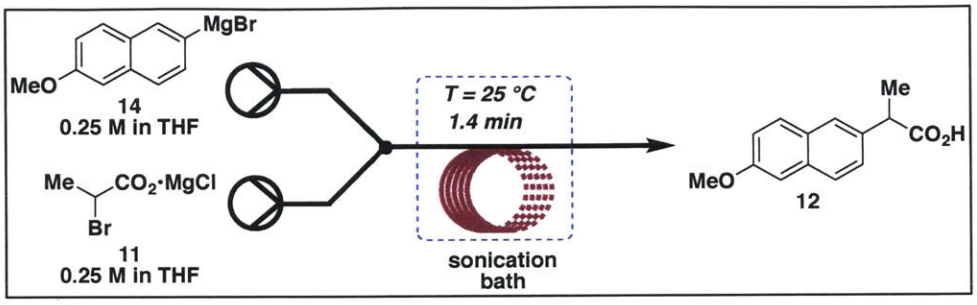

2-(6-methoxynaphthalenyl)propanoic acid: Two 50 mL Harvard stainless steel syringes were flushed with dry THF three times prior to use. Under nitrogen, one syringe was filled to 50 mL with (6-methoxynaphthalen-2-yl) magnesium bromide, 0.25 M in THF. The second syringe was filled with 50 mL 2-bromopropionate magnesium chloride, 0.25 M in THF. Using a Harvard Apparatus pump, each syringe was run at 0.25 mL/min, and the reactor was submerged in a sonication bath for the duration of the reaction. A fine white precipitate was observed. After 4 minutes 12 seconds (3 times the residence time), the reaction was collected in an Erlenmeyer flask filled with 1 N hydrochloric acid as a quenching solution. After 2.5 hours of smooth running, a malfunction of the sonication bath caused immediate clogging. Turning the sonication bath back on, after another 4 minutes 12 seconds of equilibration, the reaction was run until the syringes were empty, for a total time of 3 h 20 minutes. The biphasic mixture in the Erlenmeyer flask was transferred to a separatory funnel, and ethyl acetate added to extract the product three times. The organic layer was removed, dried over sodium sulfate, filtered, and concentrated. To remove any traces of magnesium, the resulting off-white residue was flushed through a RediSep High Performance silica column using hexanes and ethyl

acetate, yielding racemic naproxen (1.94 g, 71%, crude with 2-methoxynaphthalene as a byproduct).

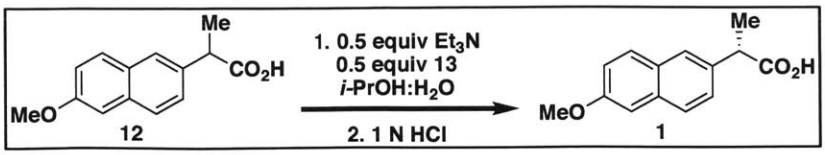

(S)-2-(6-methoxynaphthalenyl)propanoic acid (Naproxen): Following the procedure of Von Morze,[1] the crude material of racemic naproxen and 2-methoxynaphthalene (1.94 mg, 8.44 mmol based on naproxen) was dissolved in 12.7 mL isopropanol and 0.6 mL deionized water. 0.5 equivalents of triethylamine (0.59 mL, 4.22 mmol) and 0.5 equivalents of *N*-octyl-*D*-glucamine (1.124 g, 4.22 mmol) were added as a chiral resolving agent. The suspension was heated to 84 °C, at which point all materials dissolved, then slowly cooled to room temperature. A seed of (*S*)-naproxen-*N*-octyl-*D*-glucamine salt was added, and the solution was allowed to crystalize at room temperature overnight. The resulting crystals were filtered and washed with cold isopropanol, followed by 1 M HCl and extraction with ethyl acetate (three times). After drying over sodium sulfate, filtering, and concentrating on a rotary evaporator, an HPLC trace (Chiralpak® AD-H, 10% isopropanol: 90% hexanes) was taken showing 65% ee in (*S*)-naproxen. The material was then recrystallized in toluene to yield 580 mg (*S*)-naproxen (30% of 50% expected). Chiral HPLC by the aforementioned method revealed an ee of 65%.

^{1}H NMR (400MHz, $CDCl_3$) ð: 7.75–7.66 (m, 3H), 7.42 (d, *J* = 8.5 Hz, 1H), 7.18–7.02 (m, 2H), 3.91 (s, 3H), 3.87 (q, J = 7.2 Hz, 1H), 1.59 (d, *J* = 7.2 Hz, 3H); ^{13}C NMR (100 MHz, $CDCl_3$) ð: 179.2, 157.9, 135.0, 134.0, 129.4, 129.0, 127.4, 126.3, 126.3, 119.2, 105.7, 55.5, 45.3, 18.3. Data consistent with previously reported spectra.[2]

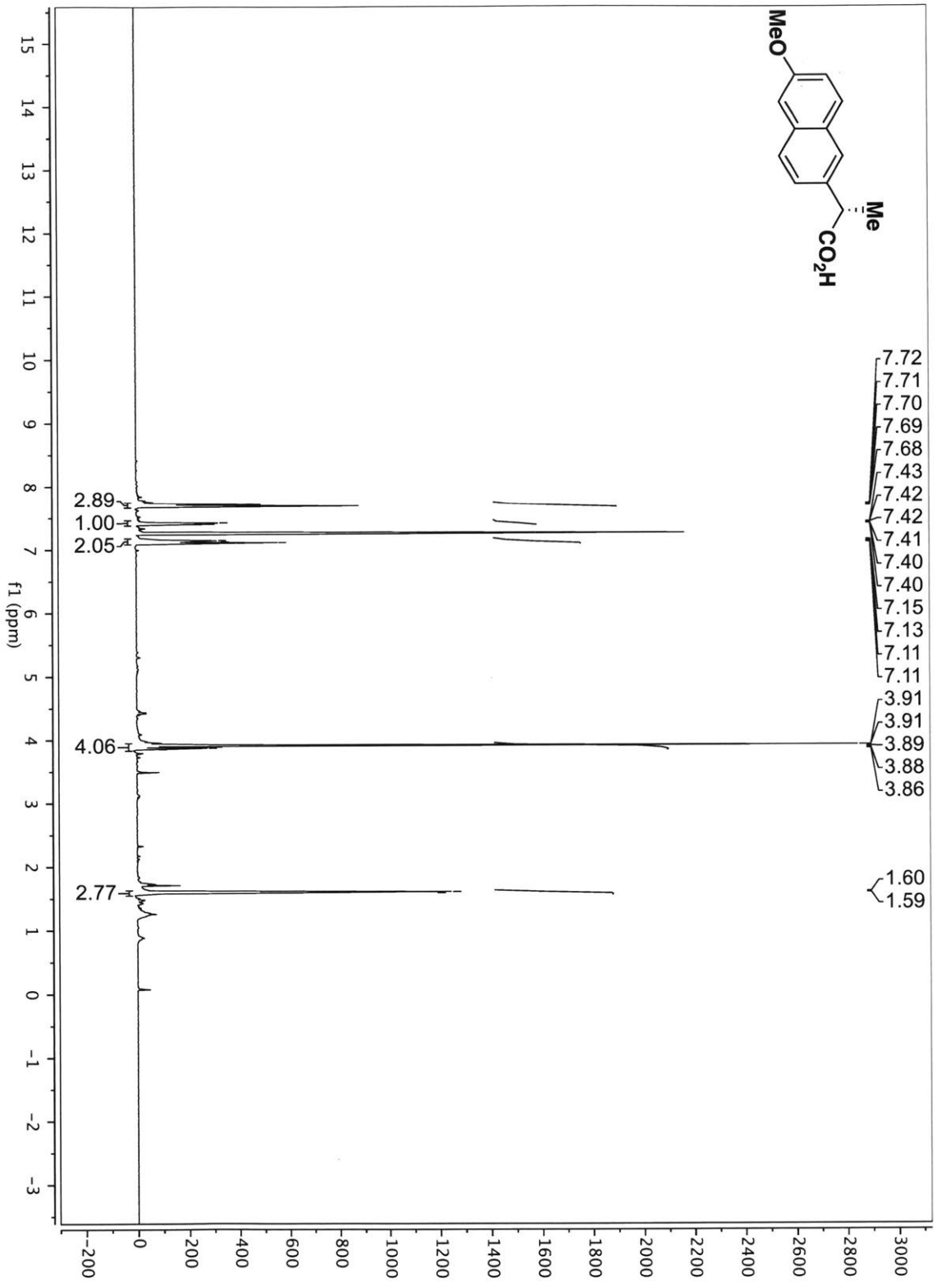

Figure S1. ^{1}H NMR for (*S*)-Naproxen.

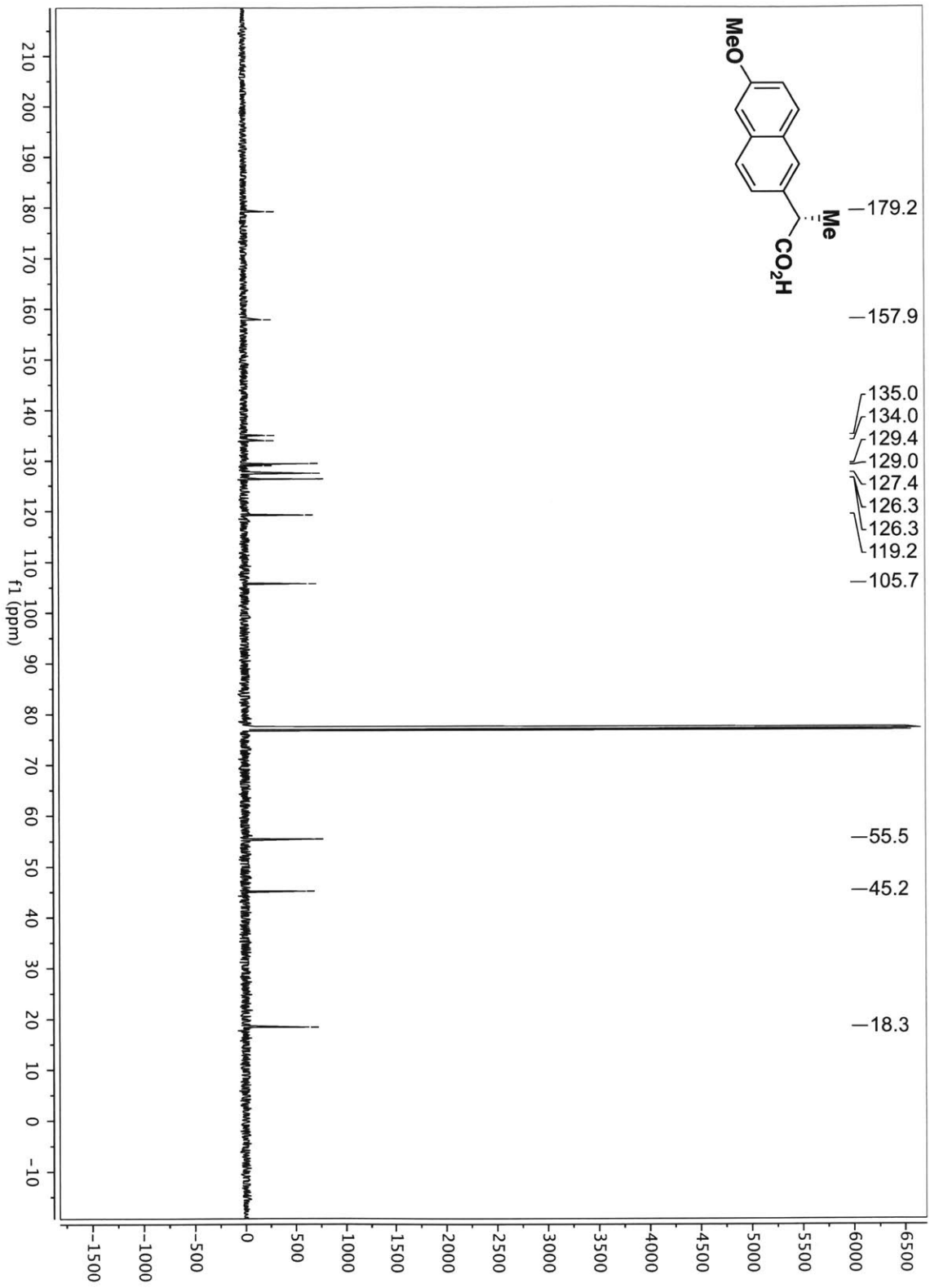

Figure S2. ^{13}C NMR for (*S*)-Naproxen.

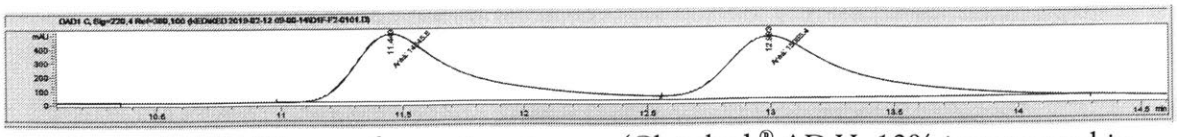

Figure S3. HPLC trace of racemic naproxen (Chiralpak® AD-H, 10% isopropanol in hexanes)

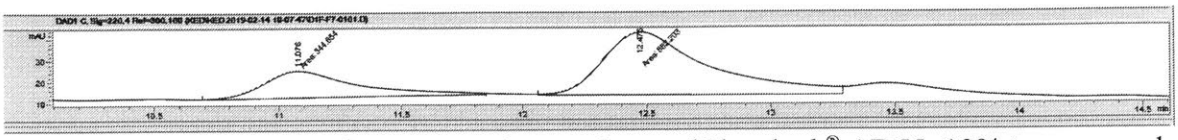

Figure S3. HPLC trace of naproxen after resolution (Chiralpak® AD-H, 10% isopropanol in hexanes), ee 65%.

References

1. Von Morze, H. *Process for the preparation of (d) 2-(d-methoxy-2-naphthyl) propionic acid and pharmaceutically acceptable salts thereof and new intermediates therefor.* 1983, EP0095901A1.
2. National Institute of Advanced Industrial Science and Technology (AIST). Spectral Database for Organic Compounds (SDBS); ^{1}H NMR; SDBS No.: 19020; RN 22204-53-1; https://sdbs.db.aist.go.jp/sdbs/cgi-bin/direct_frame_top.cgi (accessed February 15, 2019).